

Doctoral Dissertation

**Multiple Steerable Projector System
for Geometrically Correct Displays
in a Wide Environment**

Ikuhisa Mitsugami

February 20, 2007

Department of Information Processing
Graduate School of Information Science
Nara Institute of Science and Technology

A Doctoral Dissertation
submitted to Graduate School of Information Science,
Nara Institute of Science and Technology
in partial fulfillment of the requirements for the degree of
Doctor of ENGINEERING

Ikuhisa Mitsugami

Thesis Committee:

Professor Masatsugu Kidode	(Supervisor)
Professor Naokazu Yokoya	(Co-supervisor)
Associate Professor Shinsaku Hiura	(Member, Osaka University)
Associate Professor Yasuyuki Kono	(Member)

Multiple Steerable Projector System for Geometrically Correct Displays in a Wide Environment *

Ikuhisa Mitsugami

Abstract

This thesis describes a novel multiple steerable projector system that can display an image anywhere on surfaces in a wide environment. The system can not only display an undistorted image but also control the image's position and size precisely. In addition, by operating the multiple projectors simultaneously, the system can show an image larger or brighter than the capacity of a single projector by tiling or overlaying projected images. These properties enable the system to be utilized in a variety of applications: visual annotations on objects and places, human navigation, a flexible screen for lectures, remote instructions, color and texture simulations of non-textured surfaces, and many other augmented reality (AR) applications.

To realize such a projection system, it is necessary first to implement a steerable projector and calibrate it precisely. Calibration has been difficult and unstable, however, because conventional steerable projectors had much more complicated structures than fixed ones. In this thesis, a new structure is proposed, whose projection center corresponds precisely with its rotation center, so that the projection center does not move whichever direction it is oriented in. This unique structure reduces the parameters of the projector and enables its intrinsic calibration to be correct and stable. An extrinsic calibration method is also proposed, which is easy and effective as long as the image is projected onto planar

* Doctoral Dissertation, Department of Information Processing, Graduate School of Information Science, Nara Institute of Science and Technology, NAIST-IS-DD0361034, February 20, 2007.

surfaces in the real world. This method can realize display even at the boundaries of multiple planes; the image is shown in a similar way to a paper poster folded along the planes. The way is considered to be effective in various situations, such as advertisement, which is usually a 2D image.

When the multiple projectors are controlled simultaneously, two problems are revealed: (1) even a slight positional error of the projected image, which does not matter in the case of a single projector, causes misalignments of multiple projected images that can be perceived clearly when using multiple projectors; and (2) as the projectors usually do not have architectures for their synchronization it is impossible to display a moving image that is by tiling or overlaying precisely the multiple projected images. To overcome (1), a method is proposed that measures preliminarily the misalignments through every plane in the environment, and hence displays the image without the misalignment. For (2), a consideration and a new proposal for the synchronization of multiple projectors are also discussed.

Keywords:

augmented reality, steerable projector, calibration, geometric consistency, homography, undistortion, synchronized image projection

広範囲において幾何学的に正確な画像表示を実現する 複数台首振りプロジェクタシステム*

満上 育久

内容梗概

本論では、実環境中の任意位置に視覚情報を表示することが可能な複数台首振りプロジェクタシステムについて述べる。このシステムは、単に視覚情報を歪みなく表示するというだけでなく、その位置や寸法を正確に制御することが可能である。さらには、複数台を同時に利用することで、複数投影画像を並べて大きな画像を表示したり、重ね合わせて高輝度の画像を表示することも可能である。このような特徴を有する本システムは、実環境のオブジェクトや場所への注釈表示、ヒューマンナビゲーション、講義用のフレキシブルなスライド表示用スクリーン、遠隔操作指示、デザインシミュレーションやそれ以外の多くの AR アプリケーションに利用できる。

このようなプロジェクタシステムを実現するには、まず首振りプロジェクタのキャリブレーションを正確に行う必要がある。しかし従来、首振りプロジェクタは固定式プロジェクタと比較して非常に複雑な構造モデルを持つため、そのキャリブレーションは非常に精度が悪くかつ不安定であった。本論ではこの問題に対して、投影中心固定型、すなわち首振りを行ってもその投影中心位置が空間的に変動しないような構造を持つ首振りプロジェクタ機構を提案し、解決を図っている。この特殊な機構によって、構造モデルのパラメータ数が削減され、その内部・外部キャリブレーションが高精度かつ安定に行えるようになった。また、特に外部キャリブレーションについては、実環境中の複数の平面領域を投影対象とする場合に非常に簡便な作業で高精度な表示結果を得る手法を提案した。しかも、その手法によって、たとえ 2 平面の境界部に画像を表示しても画像が歪まず、紙のポスターがその境界部に沿って貼られているような表示を実現した。このような

* 奈良先端科学技術大学院大学 情報科学研究科 情報処理学専攻 博士論文, NAIST-IS-DD0361034, 2007年2月20日.

表示法は，広告などの2次元画像表示アプリケーションにおいて有効であると考えられる．

この首振りプロジェクタを複数台同時に利用する際には，さらに2つの問題が発生する．ひとつは，1台のプロジェクタによる表示では問題にならないような微小な画像表示位置誤差でも，複数台の投影画像を重ね合わせたり並べたりする際には，それらの画像間の相対的な位置ズレとして明確に観測されてしまうという問題，もうひとつは，通常プロジェクタは複数台の同期のための機構を持たないため，複数台による投影画像をズレなく重ね合わせたまま，その画像を連続的に移動させることは困難であるという問題である．本論では，まず前者については，投影を行う範囲に対して事前にズレ量マップを作成しておき，実利用時にそのマップを参照しズレを補正する手法を提案した．また後者については，プロジェクタにおける同期について検討し，連続移動する投影画像の重ね合わせに適した同期手法を提案した．

キーワード

拡張現実感，回転式プロジェクタ，キャリブレーション，幾何学的整合性，ホモグラフィ，歪み補正，同期画像投影

Contents

1. Introduction	1
1.1 Displaying in the Real World	1
1.1.1 Human Interfaces	1
1.1.2 Navigation Systems	3
1.1.3 Flexible Displays	3
1.1.4 Instruction Systems	4
1.1.5 Design simulation	6
1.2 Consideration about Devices	6
1.2.1 HMDs or Projectors	6
1.2.2 Worn by the User or Located in the Environment	7
1.3 Objectives	7
1.4 Related Work	8
1.5 Main Innovations	13
1.5.1 Structure of a Steerable Projector and Its Calibration	13
1.5.2 Projection Method	13
1.5.3 Precise Alignment of Multiple Projections	13
1.5.4 Synchronization of Multiple Steerable Projectors	14
1.6 Dissertation Outline	14
2. Conventional Steerable Projector Calibration	15
2.1 Calibration of a Fixed Projector	15
2.1.1 Duality between a Camera and a Projector	15
2.1.2 Calibration of a Camera	15
2.1.3 Calibration Method for a Projector	21
2.2 Non-FC-PT Projector Model	21
2.3 Calibration Methods of Non-FC-PT Projector	23
2.4 Calibration Experiments by Computer Simulation	24
2.5 Real Calibration and Its Problems	26
2.6 Causes of Bad Calibration of the Non-FC-PT projector	28
2.7 Concluding Remarks	30

3. An FC-PT Projector and Its Calibration	31
3.1 An FC-PT Projector	31
3.2 Fixing the Projection Center	31
3.3 FC-PT Projector Model	36
3.4 Intrinsic Calibration of an FC-PT Projector	37
3.5 Extrinsic Calibration of an FC-PT Projector	41
3.6 Concluding Remarks	43
4. Projecting Rectified Images onto the Real World Using an FC-PT Projector	45
4.1 Projection onto a Single Plane	45
4.2 Extension to Multiple Planes	47
4.2.1 Preparation for Multi-Planar Projection	47
4.2.2 Detection of Relations among Planes	48
4.2.3 Projection Method	50
4.3 Experiments	53
4.3.1 Experiments about Positional Accuracy	53
4.3.2 Effect of Rotatable Mechanism	55
4.3.3 Projection onto Multiple Planes	55
4.4 Concluding Remarks	57
5. Alignment of Multiple Projections	61
5.1 Causes of Misalignment and Strategy	61
5.2 Generation of Misalignment Map	61
5.3 Precise Alignment Using the Misalignment Map	64
5.4 Experimental Results	65
6. Synchronization of Multiple Projectors	71
6.1 Configuration for Controlling Multiple Projectors	71
6.2 Transmitted Data	72
6.3 Real Time Integration of Multiple Projectors	73
6.3.1 Problem of Integrating Multiple Projectors	73
6.3.2 Dynamic Memory	75
6.3.3 Applying Dynamic Memory to Multiple Steerable Projectors	76

6.4	Consideration about Synchronization	77
6.4.1	Two Definitions of Synchronization	77
6.4.2	Synchronization of the Multi-camera System	78
6.4.3	Synchronization of the Multi-projector System	79
6.5	Experiments	81
7.	Concluding Remarks	85
7.1	Thesis Summary	85
7.2	Applications	86
7.2.1	Application Fields	86
7.2.2	Implemented Example	87
7.3	Future Work	90
	Acknowledgements	93
	References	94

List of Figures

1	One example of wearable projector systems [KS03].	2
2	Bowl [KSK ⁺ 06].	2
3	WEAVY [KKS01].	3
4	Ubiquitous product finder [PKL ⁺ 03].	3
5	Projection onto a rectangular board [BRC03].	4
6	Escritoire [AR03].	4
7	KARMA [FM91, FMS93].	5
8	Remote instruction system [THI02].	5
9	Shader Lamps [RWLB01].	6
10	Validity of using multiple steerable projectors.	9
11	Autocalibration of multiple projectors [OD06].	10
12	Shadow elimination using two projectors [SCS01].	11
13	Steerable projector [Pin01].	12
14	Parameters included in the camera model.	16
15	Tsai's camera calibration method.	18
16	Zhang's calibration method.	19
17	Projector calibration based on Zhang's camera calibration method.	20
18	Model of the Non-FC-PT projector.	22
19	Simulation result of extrinsic calibration of a projection center.	25
20	Simulation result of a model parameter $ \mathbf{t}_{SP} $	27
21	Real experiments for calculating model parameters.	29
22	Structure of rotatable stage.	32
23	Rough estimation of projection center.	32
24	Precise fixing.	33
25	Simulation configuration for fixing the projection center.	34
26	Position of the projection center and movement of the projection.	34
27	Relation between the projection center position and the size of the projected area.	35
28	Model of an FC-PT projector.	37
29	The same point projection from different orientations.	38
30	Operation for optimization of the intrinsic parameters using a non-planar surface.	39

31	Confirmation of accuracy of the intrinsic calibration.	41
32	Regarding the FC-PT projector as a fixed projector.	42
33	Operation for extrinsic calibration of the FC-PT projector.	44
34	Projection onto a plane in the real environment.	46
35	Multiple planes in the real environment.	47
36	Two planes expanded onto one plane.	49
37	Flowchart of projection.	51
38	Projection onto the boundary of two planes.	52
39	Implemented FC-PT projector.	54
40	Experiments about positional accuracy of projections.	56
41	Projection by a fixed projector.	57
42	Projection to a wide area by a FC-PT projector.	58
43	Three planes in experimental environment.	59
44	Projection onto the planes and their boundary.	59
45	Configuration for generating the misalignment map.	62
46	Grid pattern projection at a sampling position.	63
47	Alignment by interpolation.	65
48	FC-PT projector.	66
49	Experimental environment.	67
50	Effect of the alignment method.	67
51	Larger image projection by tiling multiple projections.	69
52	Bright clear image obtained by overlaying multiple projections.	69
53	Configuration for multiple projectors.	72
54	Problems in using multiple projectors.	74
55	Dynamic memory.	75
56	Virtual synchronization of multiple projectors using dynamic memory architecture.	77
57	Discrete capture of a continuous scene.	79
58	Frame synchronization in the case of projectors.	80
59	Generating a continuous sequence by the discrete frames.	80
60	Moving image projection using two FC-PT projectors.	82
61	Misalignment when the image moves along a circle.	83
62	Maze puzzle application.	88

63	Bitmap data of Maze	88
64	Parts of Maze.	89
65	Control of difficulty.	89

List of Tables

1	Plane registration table.	48
2	Transformation parameters list	50
3	Specification list of the FC-PT projector prototype I.	54
4	Specification list of the FC-PT projector prototype II.	66

1. Introduction

1.1 Displaying in the Real World

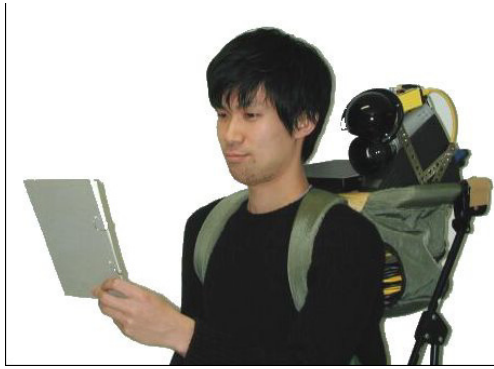
Visual information is one of the most important inputs of a human's intellect. The human fundamentally understands his/her surrounding environment by the information obtained by his/her eyes. This basic understanding, however, just concerns the physical content of the scene. The human in fact utilizes his/her imagination, memory and experience and links them to the scene so as to achieve intelligent comprehension. Therefore, if they are annotated in the scene the human can link them intuitively and comprehend better and more easily.

From such a motivation, there have been numerous studies about displaying visual information in the real world. Most of them use head-mounted displays (HMDs) or projectors to show the visual information. These studies are categorized into several groups according to their applications, some of which are listed below.

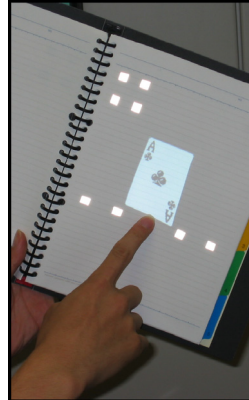
1.1.1 Human Interfaces

Displaying visual information is often used in studies about human interfaces because of the intuitiveness of its visual information annotations.

For example, in [KS03], Karitsuka *et al.* implemented a wearable projector-camera system that can measure the position and orientation of a planar surface, a notebook and a wall for example, so that an undistorted image can be displayed on the surface, as shown Figure 1. In [KSK⁺06], Kurata *et al.* also proposed another wearable system, as shown in Figure 2 (a), which is a kind of extension of [KS03] and can recognize two planes (a hand and a wall for example) simultaneously by a single projector so that its user can observe an image on a wall and, when he/she spreads his/her hand over the image, another image (an annotation of the wall's image for example) can be also observed on the hand, as shown in Figure 2 (b). There are also several examples of wearable systems [BFRV05, MOM⁺03] and systems located in the environment [Ber03, TBS03, LSYZ06]. These systems have the advantage that it is easier for their user to observe the displayed image than to observe HMD images, because the displayed image exists actually on a surface in the real world.

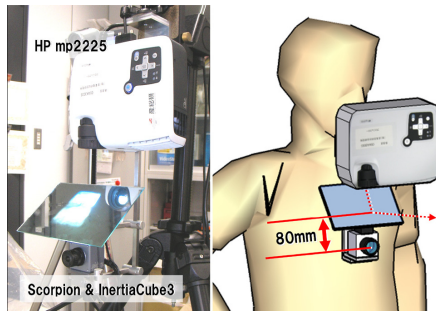


(a) System overview.



(b) Display result.

Figure 1. One example of wearable projector systems [KS03].



(a) System overview.



(b) Display results.

Figure 2. Bowl [KSK⁺06].



Figure 3. WEAVY [KKS01].

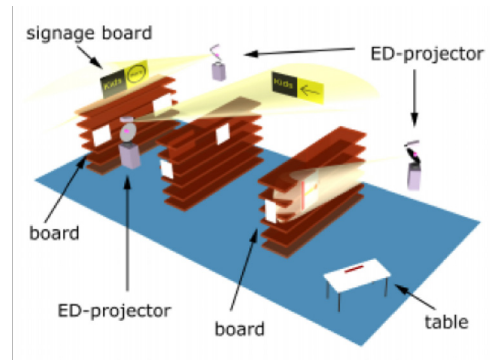


Figure 4. Ubiquitous product finder [PKL⁺03].

1.1.2 Navigation Systems

If a person who visits a museum or an academic building for example does not know the path in these buildings, he/she usually uses a map of the building. However, if he/she sees the navigation information in the scene, he/she can find the path easily and intuitively.

WEAVY [KKS01] is a wearable navigation system which shows text and map graphics in its user's sight to navigate the user in a building, as shown in Figure 3. Bell *et al.* proposed a similar system [BHF02]. In [PKL⁺03], the ubiquitous product finder was proposed. Using a steerable projector, the system showed navigation information for a user to find an object, as shown in Figure 4.

1.1.3 Flexible Displays

It is convenient if any surfaces in the environment can be used as display devices to watch TV programs or browse the web for example. It has flexibility not only about its position but also about its size because it is virtually displayed.

In [BRC03], Borkowski *et al.* proposed a method to show images on rectangular boards so that the boards could be used as thin display panels. Gupta *et al.* also implemented a similar system in [GJ05]. *Escritoire*, described in [AR03], was a virtual desktop system where multiple document images could be interactively



Figure 5. Projection onto a rectangular board [BRC03].



Figure 6. Escritoire [AR03].

moved and edited.

1.1.4 Instruction Systems

When using devices or making products, the worker learns procedures by documents or voice instruction from the operator. If the information about the parts of the objects and how to operate them is overlaid in the worker's sight, he/she can understand how to act intuitively. In addition, as the information is virtual, the remote operator can dynamically edit the instruction information in the worker's sight.

KARMA (Knowledge-based Augmented Reality for Maintenance Assistance) [FM91, FMS93] used HMD overlay graphics onto components of printers to instruct how to operate them for maintenance, as shown in Figure 7. Tojo *et al.* implemented a remote instruction system [THI02] as shown Figure 8. The remote operator can draw graphics for instruction virtually on objects on a worker's desk, so that the worker can understand easily how to move the objects. In [BS05], the system displayed text annotations by a projector on the objects on the desk.

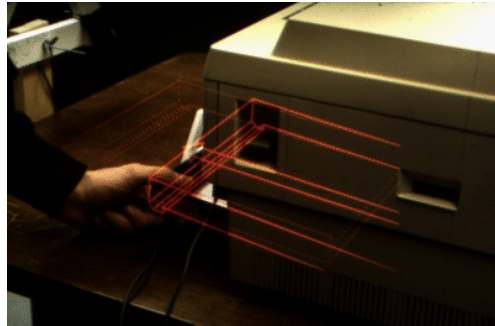
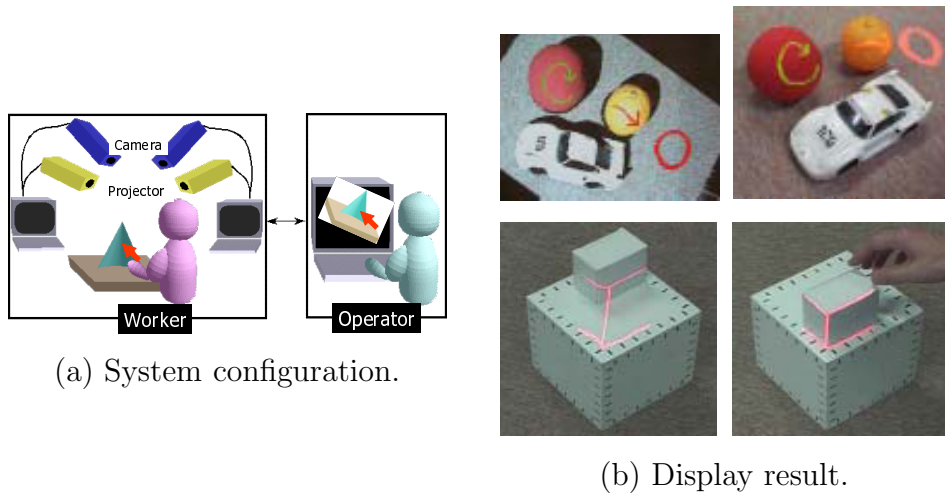


Figure 7. KARMA [FM91, FMS93].



(a) System configuration.

(b) Display result.

Figure 8. Remote instruction system [THI02].



(a) Virtual Reflectance.



(b) Virtual Illumination.

Figure 9. Shader Lamps [RWLB01].

1.1.5 Design simulation

By projecting images onto a clay model, a non-textured 3D object (a clay model of a car for example) can be colored/textured for design simulation. Alternatively, displaying images of windows or furnitures on walls and floors can be used as room design simulation.

Raskar *et al.* also implemented a system called Shader Lamps in [RWLB01]. As shown in Figure 9, clay models are colored or textured by multiple projectors surrounding them. By the projection, not only their texture but also the lighting condition are simulated. Mukaigawa *et al.* also implemented a similar system in [MNS01], where even the mutual reflectance of the clay models is considered.

1.2 Consideration about Devices

Overviewing the existing studies mentioned in Section 1.1, two comparisons are considered in the following sections.

1.2.1 HMDs or Projectors

The HMD shows the image in the user's sight. Therefore, the user can see the rectified image even when the user's viewpoint changes freely. In addition, the image is never occluded and its color and texture are independent from the en-

vironment. However, it has a risk: if the power supply suddenly stops, it turns off and shows nothing. In the case of the video see-through HMDs, especially, the whole user's field of vision becomes black. In addition, even when the power supply is stable, using HMDs for a long time fatigues the user, as reported in [ITSK05].

In contrast, the projector shows the image in the environment. The appearance of the image thus changes according to the user's viewpoint, and its color and texture are influenced by those of the projected surface, which means it is difficult to maintain consistency of color and texture. However, it has an important advantage that it is easier for the user to observe the displayed image than for images by the HMDs, because the displayed image exists actually on a surface in the real world. Another advantage of the projector is its safety: even when the power supply stops the user can still see the environment.

1.2.2 Worn by the User or Located in the Environment

The wearable device is convenient because it can show any graphics, anywhere. It is annoying, however, to always wear the device. This does not matter if the device is small enough for the user to forget that he/she is wearing it, but it will need a lot of time to realize such the small device. Another problem is that it is difficult to display the image precisely at a position where the system intends it to be shown, because the wearable device moves freely in the real world as the user's head moves so that precise measurement is difficult.

In the case of the located device, which means only the projector because the HMD is never situated in the environment, the image can be displayed only in an environment containing the device. However, it is much easier to achieve a positionally accurate display because the device does not change its position and so the relative positions of the device and the environment are fixed and can be measured stably.

1.3 Objectives

This thesis aims at the realization of a fundamental system that displays visual information in the environment so that the system can be used in many applica-

tions. To realize it, this thesis places importance on the positional accuracy and stability of the system so that it can be used in industrial and commercial scenes.

Although wearable devices including HMDs and projectors have often been studied, as mentioned in Section 1.1, and they are indeed interesting and convenient, they have rarely been used in industry or our daily lives. This may be because the existing approaches are not adequate in terms of the accuracy and stability. The size and weight of these wearable devices is also a cause of this impracticality. Considering the above, it is found that to work stably and precisely for use in many commercial applications, a system to show visual information in the real world should be constructed using projectors located not on the user's body but in the environment.

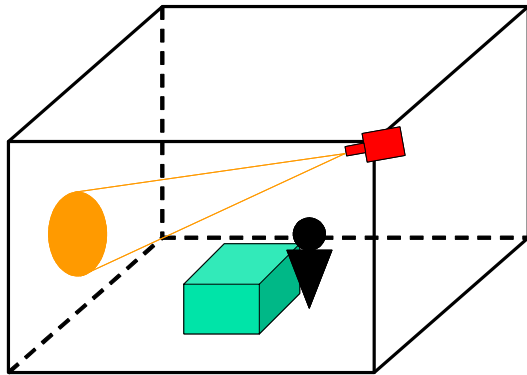
Figure 10 shows how to construct such a system. When there is a single fixed projector, its projectable area is very restricted as shown in (a). However, if the projector has a rotatable mechanism the projectable area is widely spread (b). In addition, if multiple steerable projectors are located with appropriate intervals, almost all the surfaces in the environment can be covered (c). By locating the multiple steerable projectors, cooperation between them can offer a larger or brighter image than the capacity of a single projector, by tiling or overlaying multiple projections (d). This study aims at the realization of such a multiple steerable projector system.

On constructing such a multiple steerable projector system, not only the geometric aspect mentioned above but also the photometric aspect should be considered. In fact, there have been many studies about the brightness or color compensation of multiple projections [NPG03, MJM⁺03, SC05, WSOS05, AOSS06]. This thesis, however, focuses on only the geometric aspect and describes the realization of a system to show visual information stably and precisely in the real world using multiple steerable projectors located in the environment.

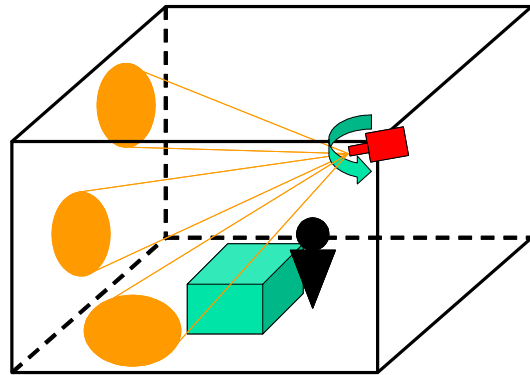
1.4 Related Work

There is much related work using projectors located in the environment. These studies are overviewed and categorized in this section.

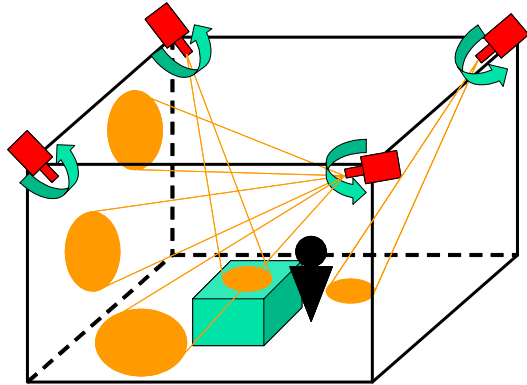
Most studies using multiple projectors are aimed at integrating multiple projections to generate a single display area. The main issue for the projector ar-



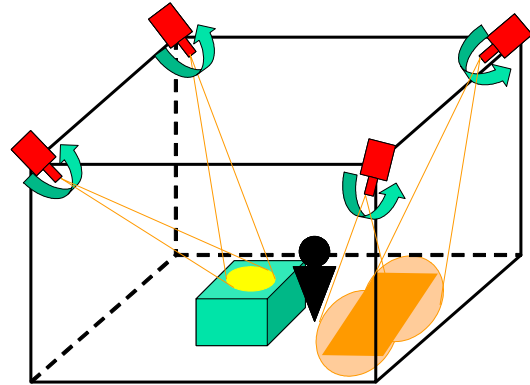
(a) Using a fixed projector.



(b) Using a steerable projector.

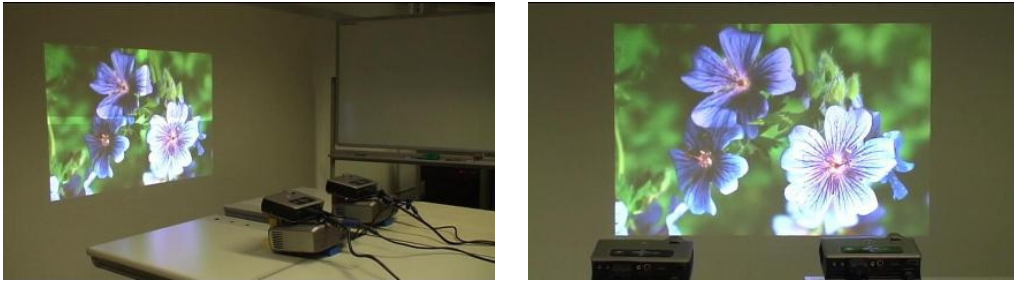


(c) Using multiple steerable projectors.



(d) Cooperation between multiple steerable projectors.

Figure 10. Validity of using multiple steerable projectors.



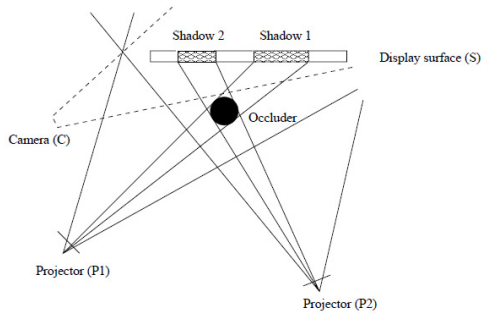
(a) System configuration.

(b) Projection result.

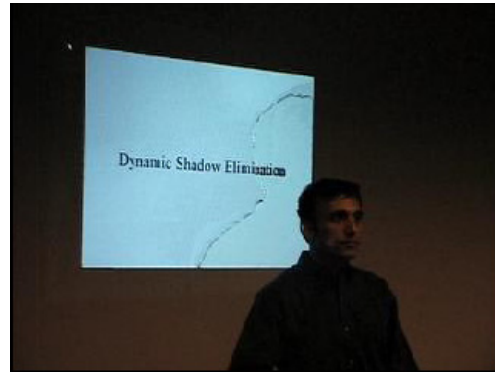
Figure 11. Autocalibration of multiple projectors [OD06].

ray is projector calibration methods, which include how to rectify every projection and tile or to overlay them without misalignments. [CCF⁺00, CSWC01, CSWL02, YGH⁺01, OD06, Her03, RGM⁺03, HS05] implemented projector arrays to generate a large display, and proposed calibration methods. Figure 11 shows an autocalibration by Okatani [OD05, OD06], where the user can locate multiple projectors freely; the system then recognizes relative positions and orientations and generates a rectified large display. Raskar *et al.* implemented calibration methods even for curved displays [RvBWR04]. On the other hand, Sukthankar *et al.* demonstrated another effect of using multiple projectors [SCS01, CRSS03, SFR⁺03, FSR05], where two projectors are used to compensate for shadows of a presenter that are generated by each other. As the shadows are detected and compensated in real time, observers can always see a shadow-free screen even though the presenter stands just in front of the screen, as shown in Figure 12. As these studies focused on the relative alignment of multiple projected images on a plane, their absolute positions and sizes are not considered.

There have also been several studies that focused on the absolute position of the projected image in the environment. [THI02, RWLB01, MNS01], mentioned in Section 1.1, are regarded as belonging to this category. These studies indicate that using multiple projectors is useful to eliminate unprojectable areas. However, they have a serious restriction in terms of the projectable area because the projectors are fixed.



(a) System configuration.

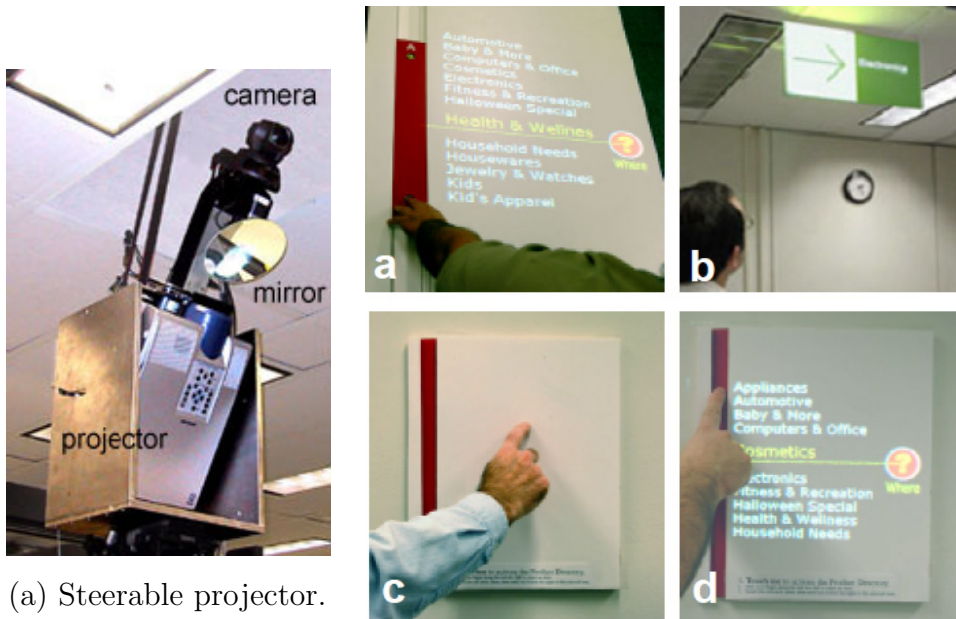


(b) Projection result.

Figure 12. Shadow elimination using two projectors [SCS01].

To overcome the restriction of the projectable area, an effective approach is to locate the projector on a rotatable mechanism. By using a steerable projector, the projectable area can be increased. In fact, there have been a few studies using such a steerable projector. For example, Pinhanez proposed a steerable projector [Pin01] which can be directed at multiple planes in the environment, select the corresponding image, and project it, as shown in Figure 13. Borkowski *et al.* proposed another steerable projector [BRC03] which can project rectified images onto planes in the environment in any orientation. Nakamura *et al.* proposed a similar system in [NN00, NH02] However, in these two studies the calibration of these steerable projectors was not very strict. As a result, they could not accomplish positionally precise image projection. Ashdown *et al.* addressed this issue [AS05]. They defined a strict steerable projector model and proposed a calculation procedure to derive all parameters of the model. However, this model has too many parameters to calculate them all correctly.

Overviewing these existing studies, it is found that both the rotatable mechanism and the use of multiple projectors are effective to increase the projectable area. However, none of them implemented both simultaneously: They chose each according to their applications. This is because calibration of steerable projectors is difficult and unstable, so that the alignment of multiple steerable projectors cannot be realized precisely. Note that if multiple steerable projectors are well-



(a) Steerable projector.

(b) Projection results.

Figure 13. Steerable projector [Pin01].

integrated, it can constitute a basic system for many AR applications.

1.5 Main Innovations

1.5.1 Structure of a Steerable Projector and Its Calibration

The existing steerable projectors [Pin01, BRC03, AFSR04] are implemented simply by locating the projector on a rotatable mechanism. Such implementations make the structure of these projectors complicated. As a result, it is very difficult to calibrate the steerable projectors precisely and stably. In this study, a new unique structure for a steerable projector and how to implement the structure are introduced to make its modelling less complex; the position of the projection center of the projector precisely corresponds to that of the rotation center of the rotatable mechanism, which means that the projection center never moves, whatever the projector's orientation. Thanks to this unique structure, its modelling is less complex than that of conventional ones, so that calibration becomes more precise and stable.

1.5.2 Projection Method

Once the steerable projector is calibrated precisely, the system can obtain the 3D structure of the surface environment and project a desired image on the surface. However, obtaining the 3D structure is tedious and takes a long time, so that the system may not become widely used. This thesis proposes an easy and stable method to obtain environmental structure information by setting the limitation that the projected surfaces consist of multiple planes.

1.5.3 Precise Alignment of Multiple Projections

When an image that is larger or brighter than the capacity of a single projector is needed, the multiple projectors have to collaborate with one another: tiling or overlaying multiple projections. If every steerable projector is precisely calibrated in the environment, tiling and overlaying are straightforward; we just input the coordinates of the projection images so that they become tiled or overlaid. In fact, however, every projection image has slight positional errors, which are ob-

served as relative misalignments when tiling and overlaying them. In this study, a misalignment map is prepared preliminarily to avoid misalignment during use.

1.5.4 Synchronization of Multiple Steerable Projectors

Even after implementation of the precise alignment of multiple projectors described in the previous section, misalignment still occurs when a moving image has to be projected from multiple projectors. This is because of (1) nonconstant delays in calculating the projection image and in network communication, and (2) unsynchronized projections by the multiple projectors. A new synchronization method for network-connected multiple projectors is proposed to realize the projection of well-aligned moving multiple images.

1.6 Dissertation Outline

This thesis describes the four main innovations in Section 1.5, in order. The first is the proposal of the structure of the steerable projector to realize a precise calibration, which is described in Chapter 3, before which the conventional steerable projector is considered in Chapter 2. In Chapter 4, a method to display a rectified image on multiple planes in the environment is explained. The next two chapters are about extension to multiple steerable projectors; the precise alignment method is presented in Chapter 5, and synchronization of the multiple steerable projectors in Chapter 6. The concluding remarks of this thesis are described in Chapter 7.

2. Conventional Steerable Projector Calibration

First, the calibration process of conventional steerable projectors is discussed to expose its disadvantages before considering the efficacy of FC-PT projectors. The conventional projectors are called “Non-FC-PT projectors,” in contrast with the FC-PT projectors.

In this chapter, a typical Non-FC-PT projector is defined and its calibration process is described. Although the steerable projector in [AS05] does not have exactly the same structure as the typical Non-FC-PT projector, the calibration process is almost the same.

2.1 Calibration of a Fixed Projector

2.1.1 Duality between a Camera and a Projector

Models of a camera and a projector are very similar to each other, although they have one essential difference about their light directions: while a camera receives light from the real world, a projector projects the light into the world. This characteristic is defined as “duality” and mentioned in some existing studies [SCG⁺05, NSI05, HSK06].

This “duality” has a specific narrowly-defined sense in [SCG⁺05], which proposed the dual photography in a projector and camera system. Exploiting Helmholtz reciprocity [Hel00, ZBK02] to interchange the lights and cameras in a scene, the system could generate pictures from the viewpoint of the projector, even though no camera was present at that location. Thus, the duality in [SCG⁺05] indicated that the projector could work as a camera.

In most other studies, however, “duality” is used in a broad sense, and means the structural similarity between a projector and a camera. In this thesis, it is also used in this broad sense.

2.1.2 Calibration of a Camera

Considering the duality as defined in Section 2.1.1, the calibration method for a projector should be executed based on that of a camera, which has been a major issue in computer vision since it is related to many vision problems such

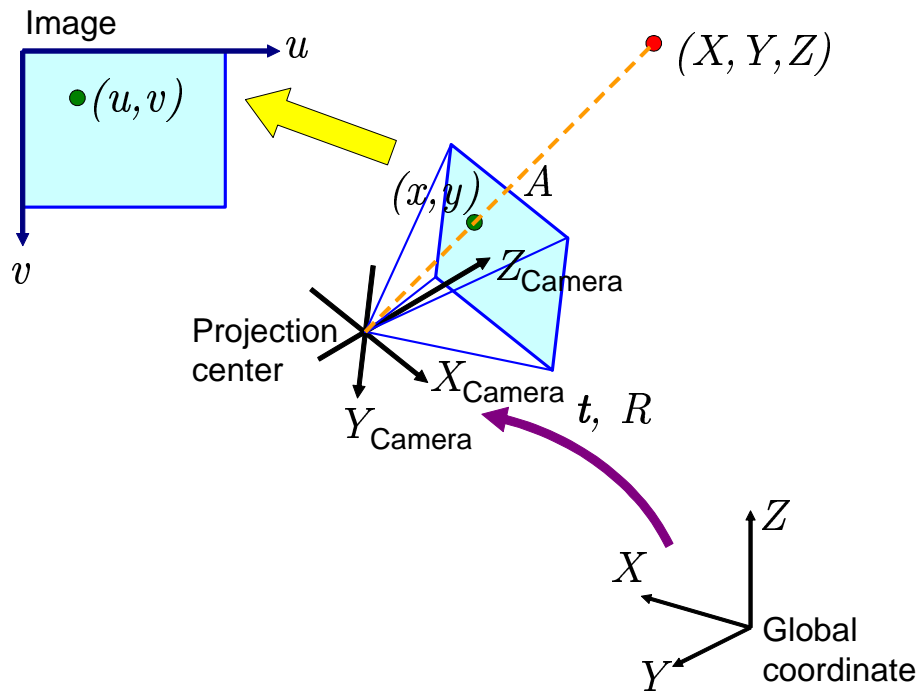


Figure 14. Parameters included in the camera model.

as stereovision, structure from motion, and robot navigation. In this section, therefore, existing studies about camera calibration are considered to find one suitable for a projector.

A model for the camera is first described before its calibration is considered. A 2D point is denoted by (u, v) , and a 3D point by (X, Y, Z) ; using the projective coordinate system, they are described $(u, v, 1)$ and $(X, Y, Z, 1)$ respectively. A camera is modeled by the usual pinhole: the relationship between a 3D point (X, Y, Z) and its image projection (u, v) is given by

$$s \begin{pmatrix} u \\ v \\ 1 \end{pmatrix} = A [R \ t] \begin{pmatrix} X \\ Y \\ Z \\ 1 \end{pmatrix}, \quad (1)$$

where s is an arbitrary scale factor, $[R \ t]$ is the rotation and translation relative

to a world coordinate system (called the extrinsic parameters), and A is the camera's intrinsic matrix. A is given by

$$A = \begin{pmatrix} f_u & \gamma & c_u \\ 0 & f_v & c_v \\ 0 & 0 & 1 \end{pmatrix}, \quad (2)$$

with (c_u, c_v) the coordinates of the principal point, f_u and f_v the scale factors in the image u and v axes, and γ the parameter describing the skewness of the two image axes. Introducing (x, y) such that

$$\begin{pmatrix} x \\ y \\ 1 \end{pmatrix} = A^{-1} \begin{pmatrix} u \\ v \\ 1 \end{pmatrix}, \quad (3)$$

and substituting it into Equation (1), the following equation is obtained:

$$s \begin{pmatrix} x \\ y \\ 1 \end{pmatrix} = [R \ \mathbf{t}] \begin{pmatrix} X \\ Y \\ Z \\ 1 \end{pmatrix}. \quad (4)$$

This equation indicates a camera that has unit focal length and whose xy plane is centered by the principal point, so that (x, y) is called the normalized image coordinate.

Lens distortion of a camera has not yet been considered. A camera usually exhibits significant lens distortion, especially radial distortion. The first two terms of radial distortion are generally considered. Other models that are more elaborate than this model are considered in [WCH92]. Roughly speaking, the distortion function is totally by the radial components, and especially dominated by the first term, according to existing studies [Tsa87b, WM94]. It has also been found that any more elaborate modeling not only would be negligibly better when compared with sensor quantization, but also would cause numerical instability [Tsa87b, WM94]. Let (x, y) be the ideal distortion-free pixel image coordinates, and (\hat{x}, \hat{y}) the corresponding real observed image coordinates. The ideal points are the projection of the model points according to the pinhole model.

$$\begin{aligned} \hat{x} &= x + x[k_1(x^2 + y^2) + k_2(x^2 + y^2)^2], \\ \hat{y} &= y + y[k_1(x^2 + y^2) + k_2(x^2 + y^2)^2], \end{aligned} \quad (5)$$

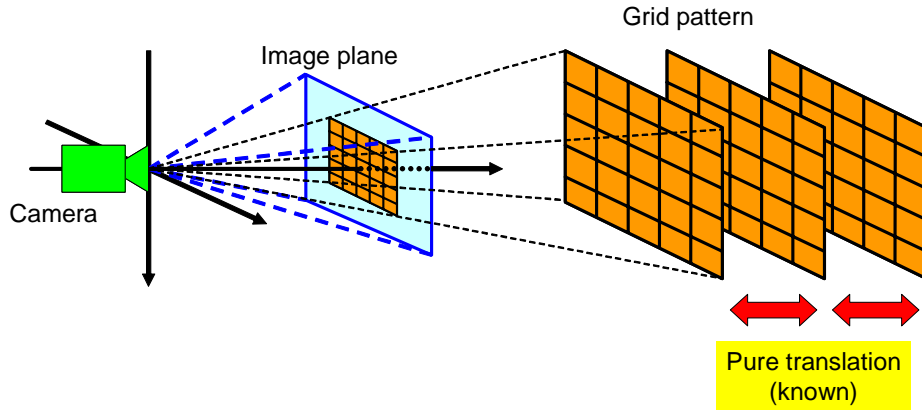


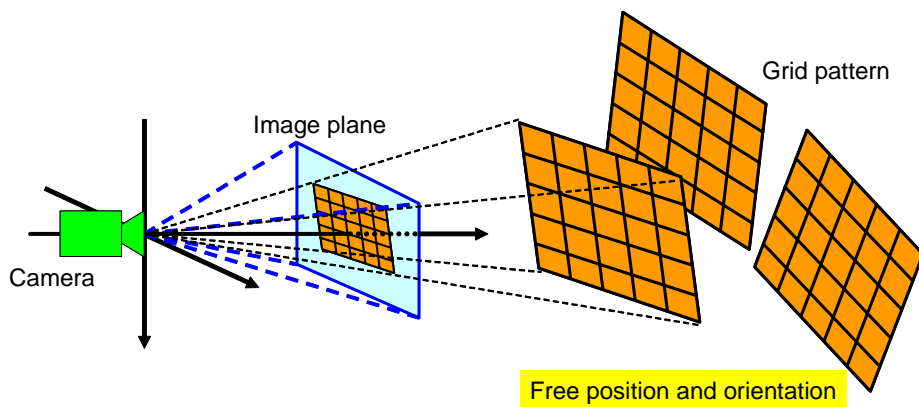
Figure 15. Tsai's camera calibration method.

where k_1 and k_2 are the coefficients of the radial distortion. The center of the radial distortion is the same as the principal point.

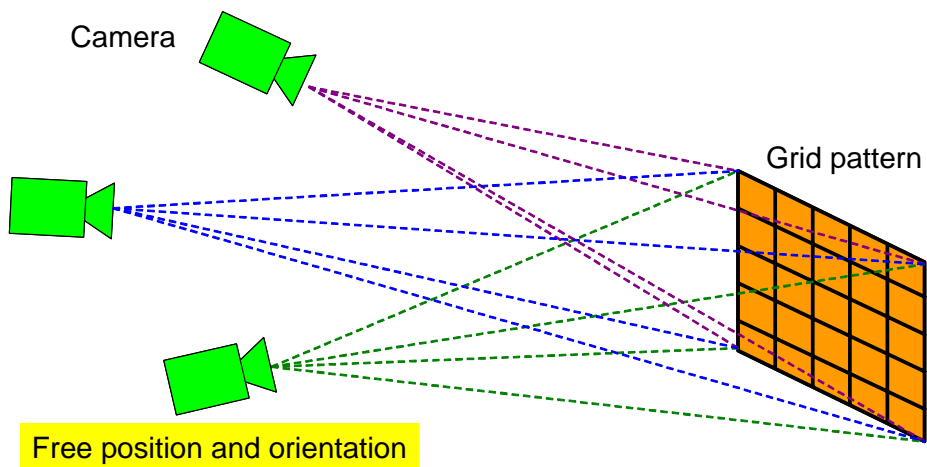
Summarizing the above, camera calibration means determining these parameters in this model, which are listed as follows:

- the intrinsic parameters, defined by A ,
- the extrinsic parameters containing the rotation matrix R and the translation vector \mathbf{t} ,
- the coefficient of the radial distortion k_1, k_2 .

One of the most widely used camera calibration techniques is the one proposed by Tsai [Tsa86, Tsa87a]. It obtains corresponding 3D point coordinates and 2D pixels in the image so as to estimate the position, orientation, and internal parameters of the camera using a two-stage technique to compute. When the geometry in space is known with good precision, calibration can be done very efficiently [Fau93]. In a real implementation, a planar grid pattern undergoing a precisely known translation is used, as shown in Figure 15. This approach is indeed the most famous and common for camera calibration. However, it has the restriction that the grid pattern needs to be moved without rotation so that it requires an expensive calibration apparatus and an elaborate setup.



(a) In the case that a camera is fixed.



(b) In the case that a pattern is fixed.

Figure 16. Zhang's calibration method.

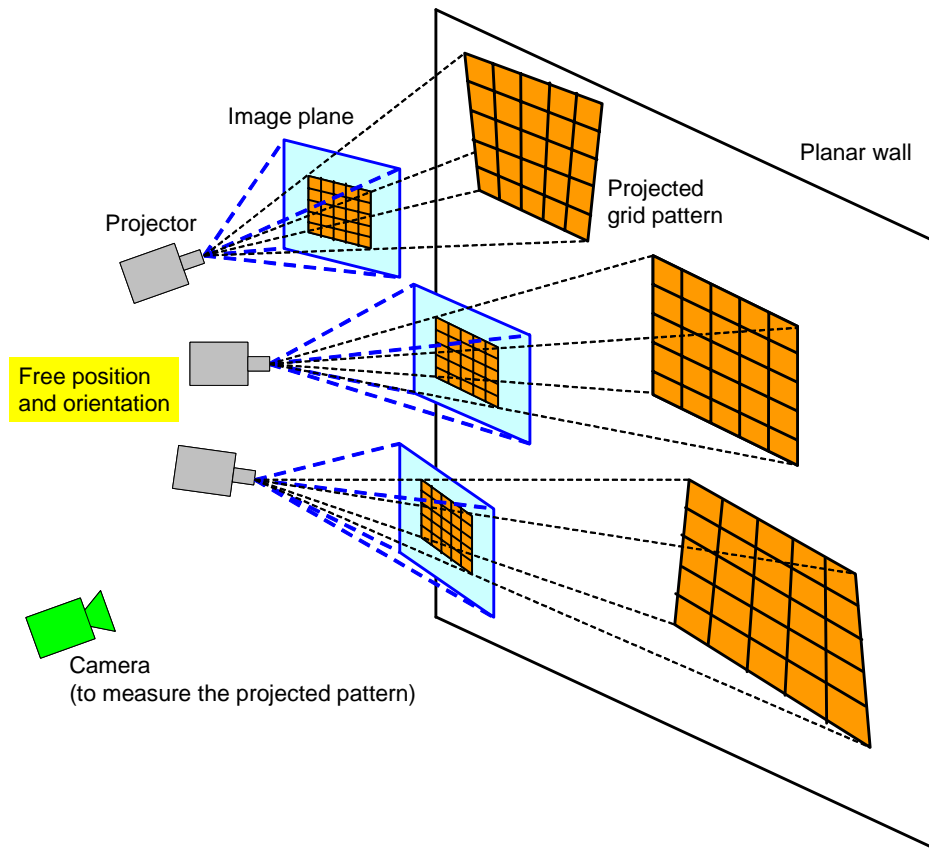


Figure 17. Projector calibration based on Zhang's camera calibration method.

Recently, a new technique was proposed in [Zha00], which only requires the camera to observe a planar pattern shown at a few (at least two) different orientations, as shown in Figure 16 (a). The pattern can be moved freely by hand because the motion does not need to be known and there is no restriction about the motion. This operation can also be done by fixing the pattern and moving the camera freely, as shown in Figure 16 (b). Therefore, compared with classical techniques, the new technique is considerably more flexible. Because of this flexibility, this method is widely used.

2.1.3 Calibration Method for a Projector

The calibrations of both a camera and a projector use the relations between the coordinate systems of the image plane and the plane in the real world (the grid pattern for example). To obtain these relations, known grid patterns are used. In the case of the camera, described in Section 2.1.2, a grid pattern whose metric intervals are known is used in the real world. This pattern is projected onto the image plane of the camera, and the projected pattern is measured in the pixel-wise image coordinate. On the other hand, in the case of the projector, a known pattern is prepared on the image plane; a pattern whose pixel-wise intervals are known is generated on the image plane, projected on the plane in the real world, and then the metric positions of the grids are measured¹.

As described in Section 2.1.2, Tsai’s method has the restriction that constant patterns in the real world have to be located in the known translations. This restriction is hard to achieve in the case of a projector, because the translations also causes scaling of the projected pattern. On the other hand, Zhang’s method has flexibility so that it can be applied even to the projector. In fact no modification is needed to make the method be applicable to the projector.

2.2 Non-FC-PT Projector Model

In this thesis, a model of the Non-FC-PT projector is defined as shown in Figure 18. Its rotation mechanism is designed so that the gimbal structure and the pan and tilt axes intersect with each other. Its initial orientation is defined, and the Non-FC-PT projector’s coordinate system is defined as that whose basic axes are its pan axis and tilt axis and the axis perpendicular to them. The position and orientation of the Non-FC-PT projector is defined as those of the coordinate system in the global coordinate system.

This Non-FC-PT projector model has 17 parameters to be estimated, which are grouped as follows:

- intrinsic parameters of its projector A (containing five parameters),

¹ This measurement is usually executed with a well-calibrated camera. However, it can be done in other ways; such as by rulers or surveying instruments.

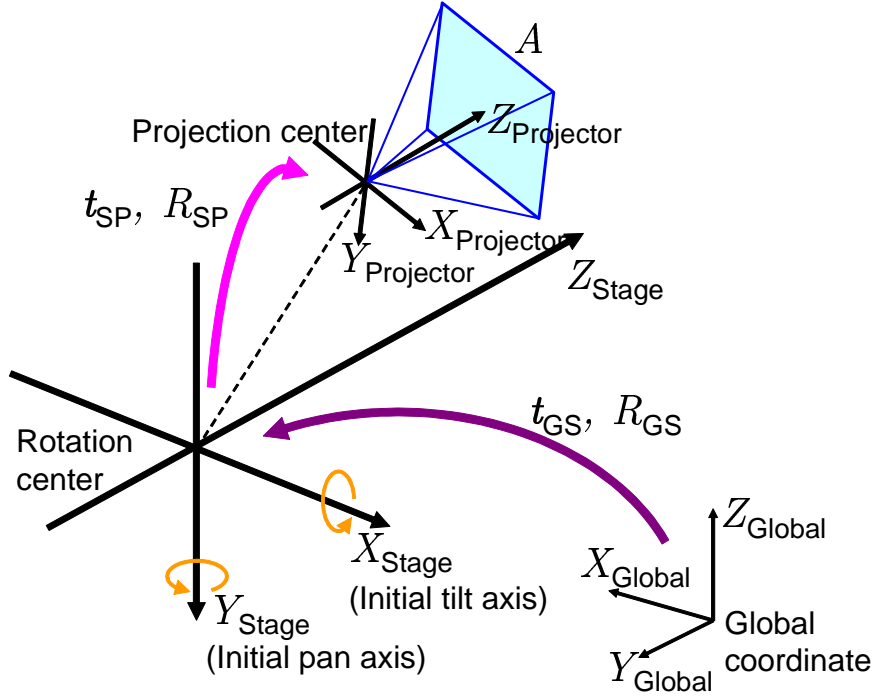


Figure 18. Model of the Non-FC-PT projector.

- the position \mathbf{t}_{SP} and orientation R_{SP} of its projector in the Non-FC-PT projector's coordinate (containing six parameters in total),
- the position \mathbf{t}_{GS} and orientation R_{GS} of the Non-FC-PT projector in the global coordinate (containing six parameters in total),

where $\mathbf{t}_{SP}, \mathbf{t}_{GS}$ are 3D vectors and R_{SP}, R_{GS} are rotation matrices. The lens distortion parameters are neglected, because conventional projectors are usually set up to display undistorted images and because the reduction in the number of parameters allows them to be estimated more precisely. In addition, the pan and tilt angles (α, β) are also parameters. They are, however, not to be estimated, but are input to operate the orientation of the projector.

2.3 Calibration Methods of Non-FC-PT Projector

The calibration method of the Non-FC-PT projector, which means the determination of the parameters listed in Section 2.2, is described in this section. The method is fundamentally the same as that in [AS05]. The differences between these methods are caused by the structural differences between the projectors.

In the method, various orientations and their corresponding positions are needed to determine the parameters. Therefore, calibration of the projector itself is necessary first. After calibration, the angles of the pan and tilt axes (α_i, β_i) and their corresponding positions \mathbf{p}_i and orientations V_i are measured, and then the remaining parameters $\mathbf{t}_{\text{SP}}, R_{\text{SP}}, \mathbf{t}_{\text{GS}}, R_{\text{GS}}$ can be estimated. On constructing the calibration, note that the angles of the axes (α_i, β_i) can be obtained correctly from the rotation stage, whereas \mathbf{p}_i and V_i are not very precise because they are obtained by extrinsic calibration of the projector. Therefore, these parameters should be calculated using a nonlinear optimization about errors of \mathbf{p}_i and V_i assuming that the angles (α_i, β_i) include no errors.

In the actual calculation process, an evaluated value e_{pos} , which concerns the position of the projection center and is defined below, is used for the optimization.

$$e_{\text{pos}} = \sum_i |(R_{\text{GS}}D_{(\alpha_i, \beta_i)}\mathbf{t}_{\text{SP}} + \mathbf{t}_{\text{GS}}) - \mathbf{p}_i|^2, \quad (6)$$

where $D_{(\alpha, \beta)}$ is a 3×3 rotation matrix that rotates α around the pan axis and then β around the tilt axis.

Another measured value e_{dir} , which concerns the directions of the projector, is also introduced. The orientation of the projector when the the two axes' angles are (α_i, β_i) is described as

$$R_{\text{GS}}D_{(\alpha_i, \beta_i)}R_{\text{SP}}. \quad (7)$$

The optimization should be done so that the orientation is equal to V_i for various angles (α_i, β_i) . When the estimated orientations are perfectly equal to the model, the following matrix V' would be the unit matrix:

$$V'_i = V_i^{-1}(R_{\text{GS}}D_{(\alpha_i, \beta_i)}R_{\text{SP}}). \quad (8)$$

Therefore, the evaluated value e_{dir} is defined as

$$e_{\text{dir}} = \sum_i |(v'_{11} - 1)(v'_{22} - 1)(v'_{33} - 1)|, \quad (9)$$

where v'_{ij} is a element of V' . The optimization minimizes the two values $e_{\text{pos}}, e_{\text{dir}}$ in Equations (6) and (9) so that the parameters $t_{\text{SP}}, R_{\text{SP}}, t_{\text{GS}}, R_{\text{GS}}$ are determined.

2.4 Calibration Experiments by Computer Simulation

The calibration process described in Section 2.3 is executed in simulation and real environments to validate its reliability.

Intrinsic and extrinsic calibration of the projector is important for this validation because the accuracy of the estimated positions and orientations strongly influences that of the model parameter estimation in the calibration process of 2.3. The camera calibration method in [Zha00] is applicable in this process. The pan and tilt axes of the projector are changed in various orientations and the given grid pattern is projected onto a plane in the real world, and the projected pattern is then measured. When using this process, the main source of estimation errors is the measurement error of the projected grid pattern. Therefore, the relation between the measurement error and the calibration error is investigated. The conditions of the simulation are as follows:

- Focal length of the projector is 23 mm. (This is almost the same as a real device.)
- Distance between the plane and the projector is 1600 mm.
- Projected grid points are $5 \times 5, 7 \times 7, 9 \times 9$.

The result is shown in Figure 19, where the horizontal axis denotes the standard deviation of the gaussian noise added to every grid point's position, and the vertical axis denotes the error of the estimated projection center's position. This graph indicates that the errors in the estimated positions of the projection center are about three to four times larger than the measurement errors of the projected points.

The next step focuses on estimation of the remaining parameters using the projection center positions in the various orientations. Another simulation experiment is performed to investigate the relation between the errors of the projection centers and those of the remaining parameters. The simulation conditions are as follows:

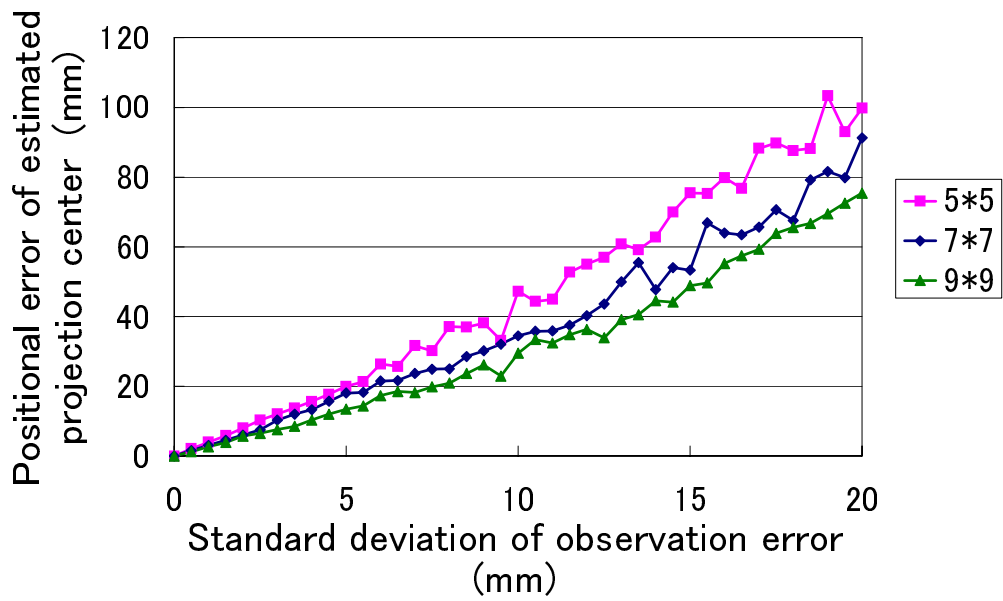


Figure 19. Simulation result of extrinsic calibration of a projection center.

- The pan and tilt angles are every 5° between $-30^\circ \sim 30^\circ$.
- The distance between the projection center and the rotation center is $0 \sim 200$ mm

Figure 20 shows the results. This graph shows the relation between the errors of the projection center positions and those of the length of estimated \mathbf{t}_{SP} , which means the distance between the projection and rotation centers. Only $|\mathbf{t}_{\text{SP}}|$ is highlighted here, although there are twelve parameters to be estimated, because $|\mathbf{t}_{\text{SP}}|$ is the most distinctive parameter of the steerable projector; it determines how the projection center moves according to the change of its orientation. The horizontal axis denotes the standard deviation of the projection center positions, and the vertical axis denotes the standard deviation of estimated $|\mathbf{t}_{\text{SP}}|$. This graph indicates that, as the distance between the projection and rotation center in the correct model becomes smaller, the estimation accuracy of $|\mathbf{t}_{\text{SP}}|$ become worse because the errors of the projection center positions gets relatively large. Conversely, the larger the distance between the two centers is, the smaller the errors of \mathbf{t}_{SP} are, which has, however, a minimum. The minimum is almost the same as the errors of the projection center positions.

According to these two simulation experiments, even in the case that the distance between the two centers is large, the estimated results have about three to four times larger errors than the measurement errors — in such a case the errors in the estimation are expected to be more accurate, because they are smaller than the movement of the projection center. The estimation errors can be also larger because of other causes of errors. This tendency is confirmed not only in the parameter \mathbf{t}_{SP} but also in other parameters of the Non-FC-PT projector model. It is concluded, therefore, that the calibration of the Non-FC-PT projector is generally unstable.

2.5 Real Calibration and Its Problems

While in Section 2.4 it is assumed that there are no causes of errors except the measurement errors, this section investigates how inaccurate the estimated parameters are in the case of using a real Non-FC-PT projector.

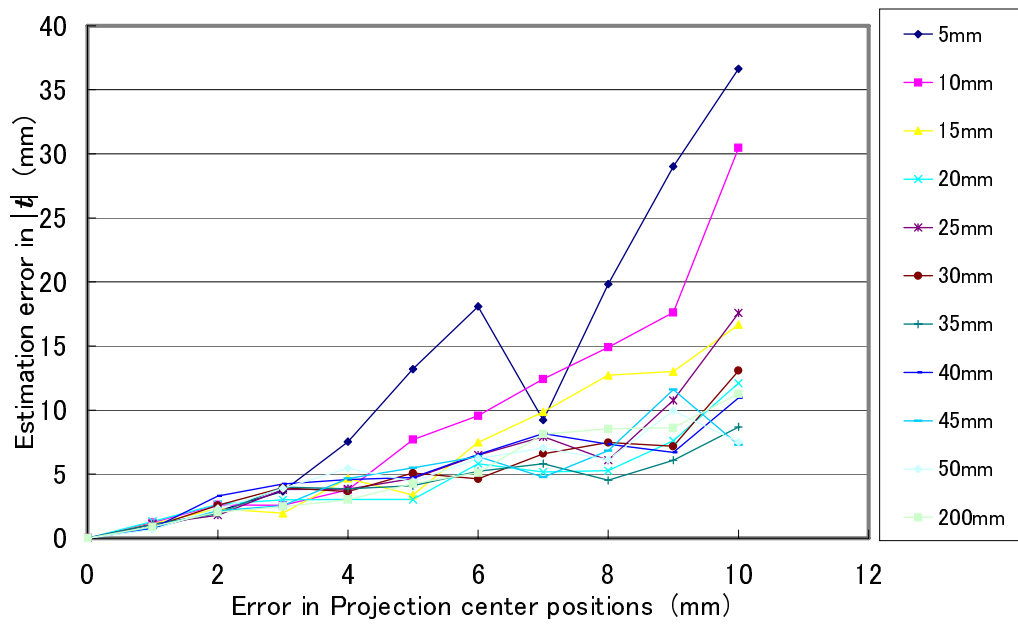


Figure 20. Simulation result of a model parameter $|t_{SP}|$.

In this investigation, the model parameters are estimated by the same calculation process as 2.3, in the two situations that the distances between the two centers are 0 mm and 50 mm. Figure 21 shows the results, where “+” denotes an estimated position of the projection center and “×” denotes a position based on the estimated model. In both cases, the estimated positions of the projection center contain about 20 mm errors, and so the calibration results is far from the true model.

2.6 Causes of Bad Calibration of the Non-FC-PT projector

Considering Sections 2.4 and 2.5, it was concluded that there are three main reasons for the bad estimation of the Non-FC-PT projectors other than measurement errors. These are as follows:

Cause 1. There are too many parameters in the Non-FC-PT projector model.

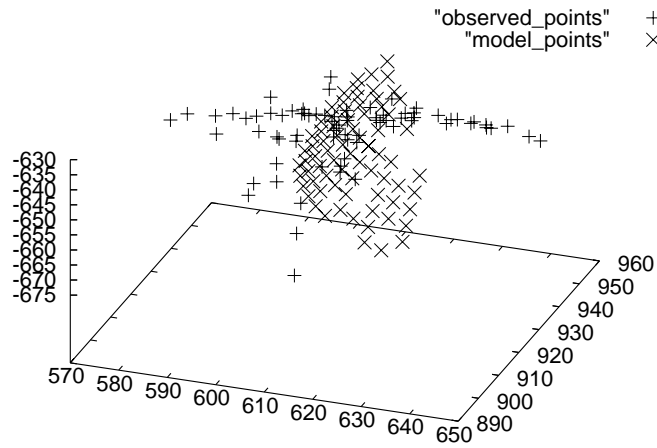
Considering Section 2.4, it was found that an essential problem of the Non-FC-PT projector calibration is its complicated structure; there are in total 17 parameters in the Non-FC-PT projector model defined in 2.2. The calibration process uses only the information about the estimated positions and orientations of the projector. It is considered that there are too many parameters to be estimated. An additional problem is that there is only a weak restriction that the projection center moves along a sphere centered around the rotation center, even though so many parameters have to be estimated. This weakness causes the instability of the calibration.

Cause 2. Assumption that the plane is perfectly flat.

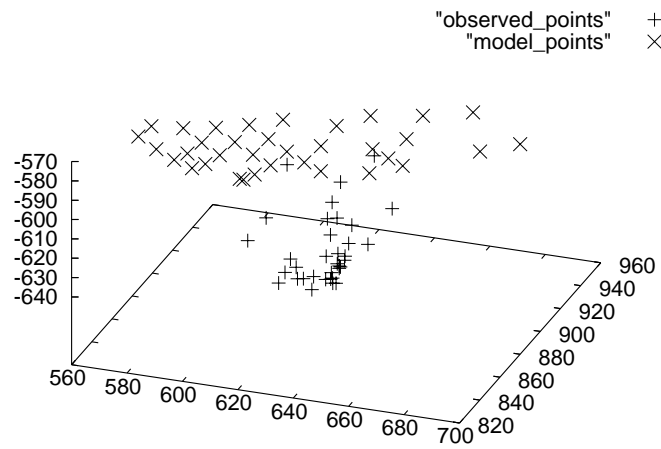
Although this calibration is based on the assumption that the plane used for the grid projection and measurement is perfectly flat, it is usually slightly curved or irregular.

Cause 3. The estimation of the projector’s position and orientation is inevitably unstable.

The extrinsic calibration of the projector based on [Zha00] depends on measurement of the projected grid patterns, which is just within the angle of



(a) The distance is 0 mm.



(b) The distance is 50 mm.

Figure 21. Real experiments for calculating model parameters.

view of the projector. As the angle is usually not so large, the estimation cannot work so well. This situation is similar to triangulation with a short baseline². This problem also affects **Cause 1**.

2.7 Concluding Remarks

In this chapter, the conventional steerable projector was considered. All the existing conventional projectors were classified as Non-FC-PT projectors. The typical model for the Non-FC-PT projector and its calibration method were described. Simulation and real experiments were then executed, and it was found that the calibration of the Non-FC-PT projector is inaccurate and unstable. The three causes of this inaccuracy and instability were listed, which can be overcome in the case of the FC-PT projector as described in Chapter 3.

² Conversely, however, when the angle is large the estimation may not work correctly because of **Cause 2**.

3. An FC-PT Projector and Its Calibration

3.1 An FC-PT Projector

Conventional steerable projectors, which are called Non-FC-PT projectors in this thesis, can be calibrated theoretically but the calibration is in fact incorrect and unstable for the reasons described in Section 2.6. In this thesis, a novel structure for a steerable projector, which is called the FC-PT projector, is proposed; it is designed so that the position of its projection center precisely corresponds with the rotation center. This means that its projection center position does not move, whatever its orientation. The method to implement the FC-PT projector and its advantages are described in Section 3.2. And the three causes of the bad calibration listed in Section 2.5 are overcome in Sections 3.3, 3.4 and 3.5 in order.

3.2 Fixing the Projection Center

This thesis proposes a new method without making the assumption of the perfect flatness of the plane used in Non-FC-PT projector calibration, described in Section 2.3, but using only the property that the light ray runs straight. This method adjusts the positions of the two centers to correspond precisely to each other. By applying the method, the FC-PT projector can be effectively implemented.

We prepare a rotatable stage that has a gimbal structure and electrically pans and tilts, as shown in Figure 22. The pan and tilt axes must cross each other, and the position of their intersection is fixed independently of the stage's orientation. To construct the FC-PT projector, its projection center must precisely correspond with this intersection. However, the complexity of obtaining the position of the projection center in space is such that we cannot directly fix the projection center precisely at the rotation center. Here, we apply a two-step method for constructing the FC-PT projector: rough estimation of the projection center's position, and precise fixing.

First, we roughly estimate the position of the projection center. A planar board is placed vertically and then horizontally in front of the projector as shown in Figure 23, and the boundary lines of the projected light are recorded. We then calculate the intersection of these lines, and treat the intersection as the roughly

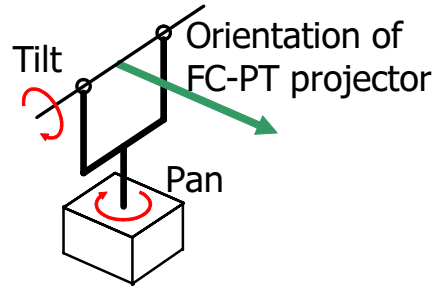


Figure 22. Structure of rotatable stage.

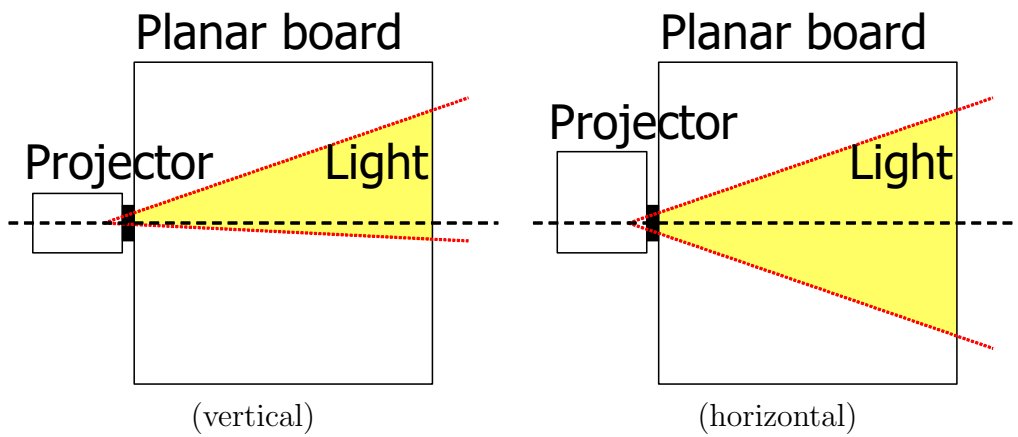


Figure 23. Rough estimation of projection center.

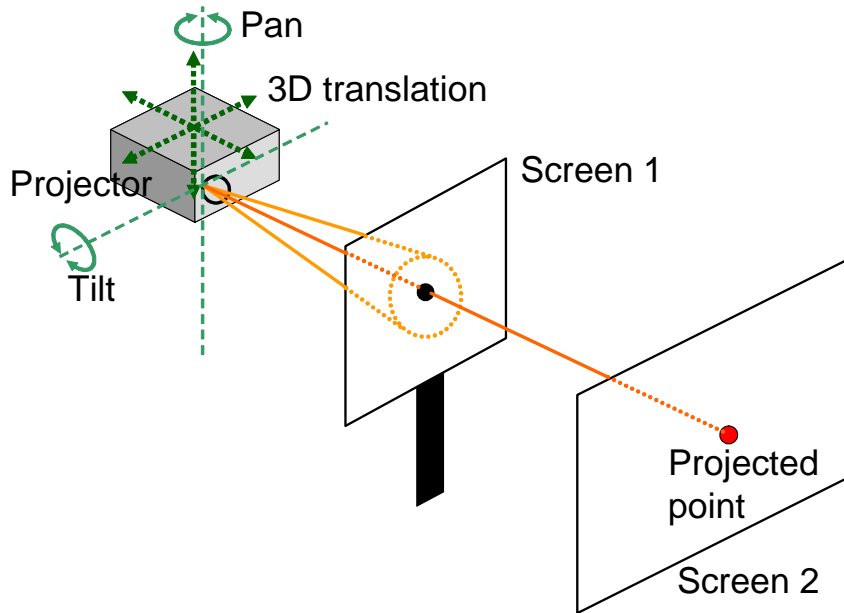


Figure 24. Precise fixing.

estimated position of the projection center.

Next, the projector is placed on the rotatable stage so that the roughly estimated position of the projection center corresponds with the rotation center, as shown in Figure 24. The projector can be three-dimensionally repositioned on the stage along the x , y and z axes. There are two screens in front of the projector, and the nearer one (screen 1) has a small hole. When the projector is turned on, only the light that goes through this hole reaches the further screen (screen 2). If the projection center is precisely at the rotation center, the projected point on screen 2 does not move even when the stage pans and tilts in any direction. This is because the light always originates from the same point. Inversely, the further the projection center is from the rotation center, the more the projected point moves. Therefore, the projector is continuously repositioned on the stage to search for the best position, where the projected point does not move at all.

Note that the movement of the projected points does not directly express the misalignment of the two centers. Simulation experiments were executed to investigate the relation between misalignment and projected point movement before the real implementation. The coordinate system is defined to be centered by the rotation center as shown in Figure 25, and there are two screens; the one

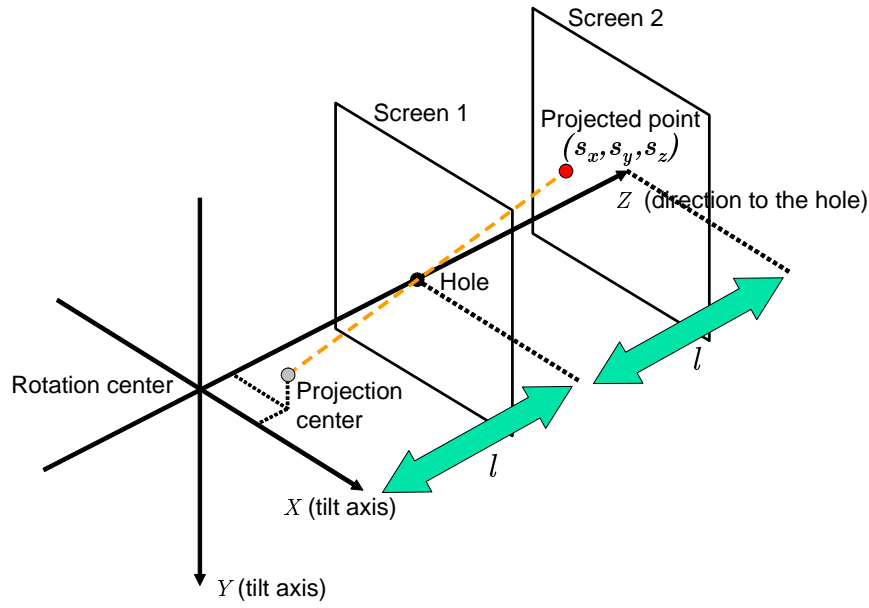
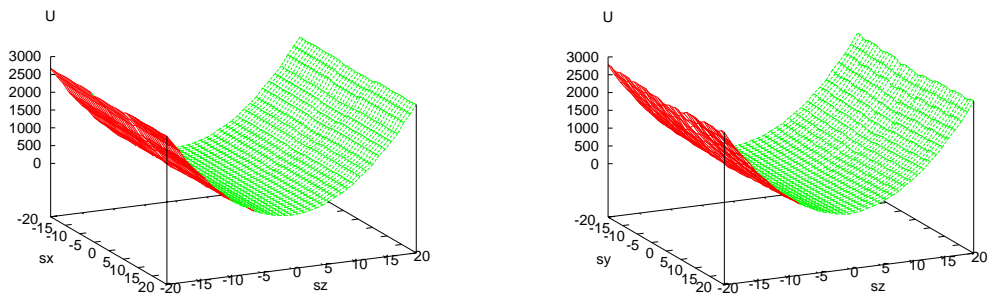
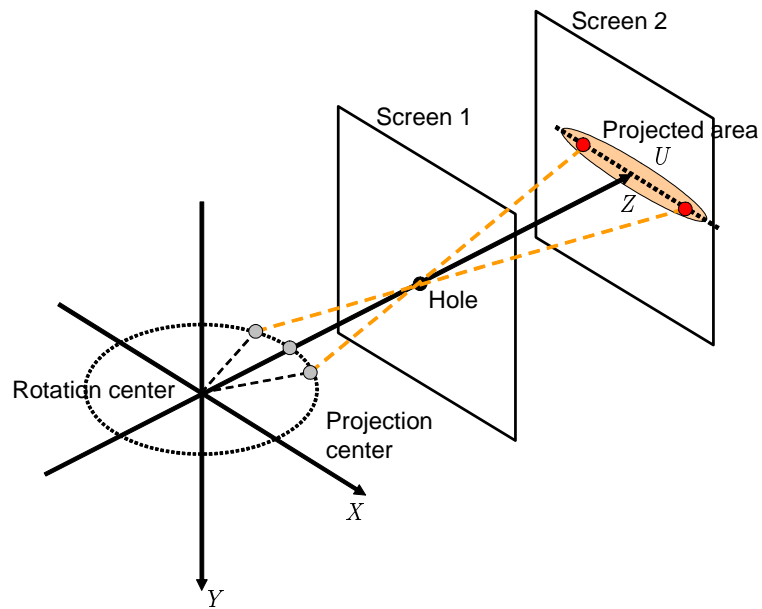


Figure 25. Simulation configuration for fixing the projection center.

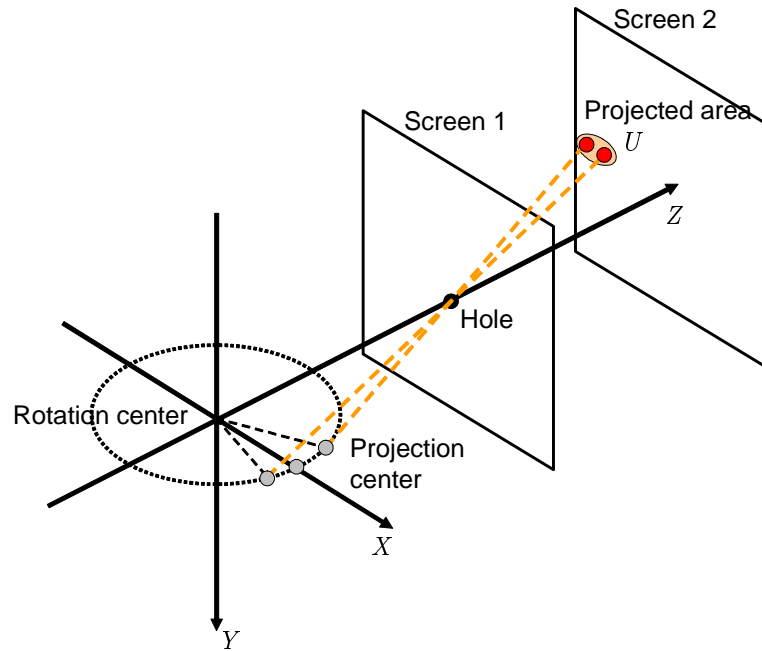


(a) Intersection of a plane $s_y = 0$. (b) Intersection of a plane $s_x = 0$.

Figure 26. Position of the projection center and movement of the projection.



(a) A case where the projected point moves widely.



(b) A case where the projected point is almost stationary.

Figure 27. Relation between the projection center position and the size of the projected area.

located at l in front of the projector has a hole and the projected beam running through the hole reaches the other screen located at $2l$. (s_x, s_y, s_z) denotes the position of the projection center and U denotes the area where the projected point moves when the pan and tilt angles are changed between $-15^\circ \sim 15^\circ$. Figure 26 shows the results. The variations of U along the X axis in (a) and the Y axis in (b) look almost flat, but in fact they are curved and in each graph there exists a minimum at $(0, 0, 0)$, which is the position of the rotation center. Note that the variations along the X or Y axes are much smaller than that along the Z axis. When the projection center is located along the Z axis the projected point widely moves so that U is large, as shown in Figure 27 (a). On the other hand, however, in the case where the projection center is located along the two other axes the projection center almost stops and then U is small, as shown in Figure 27 (b). In the real situation, this misalignment is much smaller than l , so that the projected point looks almost stationary.

From the simulation results, it is confirmed that the variation of U does not have multiple local minima but has only a single global minimum. Therefore, the desired alignment, where the two centers precisely correspond with each other, can be found by searching for the minimum. This minimum, however, may be difficult to find because the variation of U along the X and Y axes is very small and noise is added in the variation. To overcome this difficulty, curve fitting to the variation is used to stably find the minimum. In the implementation, the interval of sampling U is 1 mm and curve fitting is executed to find the minimum of the variation, so that the accuracy of fixing the projection center can be evaluated as 1 mm.

3.3 FC-PT Projector Model

Figure 28 shows the model of the FC-PT projector, which has the following parameters:

- the intrinsic parameter matrix of the projector B , and
- the position \mathbf{t}_{GS} and orientation R_{GS} of the FC-PT projector.

This model is different from that of the Non-FC-PT projector; it does not contain \mathbf{t}_{SP} and R_{SP} , which denote the position and orientation of the projector in the

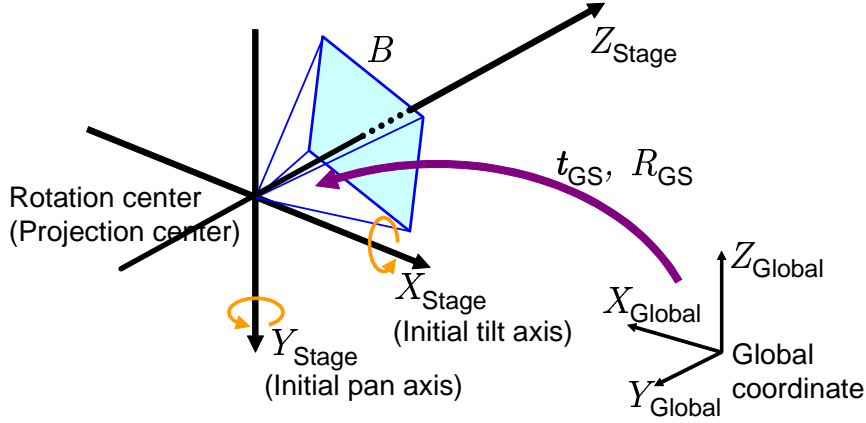


Figure 28. Model of an FC-PT projector.

FC-PT projector coordinate. This is because it is ensured in this model that $\mathbf{t}_{\text{SP}} = \mathbf{0}$, which means the projection and rotation centers precisely corresponds with each other, by the process described in Section 3.2. The orientation R_{SP} is multiplied by the projector's intrinsic matrix A to calculate B .

As described in this section, in the FC-PT projector model the parameters are reduced compared with those of the Non-FC-PT projector, so that **Cause 1** listed in Section 2.5 can be overcome by using the FC-PT projector.

3.4 Intrinsic Calibration of an FC-PT Projector

When the pan and tilt angles of the FC-PT projector are (α, β) , an arbitrary spatial point, which is defined as $(X_{\text{Stage}}, Y_{\text{Stage}}, Z_{\text{Stage}})^T$ in the stage coordinate system, corresponds with a 2D point (x, y) on the image plane of the projector according to the following equation:

$$\lambda \begin{pmatrix} x \\ y \\ 1 \end{pmatrix} = B(D_{(\alpha, \beta)} | \mathbf{0}) \begin{pmatrix} X_{\text{Stage}} \\ Y_{\text{Stage}} \\ Z_{\text{Stage}} \\ 1 \end{pmatrix} = BD_{(\alpha, \beta)} \begin{pmatrix} X_{\text{Stage}} \\ Y_{\text{Stage}} \\ Z_{\text{Stage}} \end{pmatrix}, \quad (10)$$

where λ is a proportional constant. Two 2D coordinates $(x_1, y_1), (x_2, y_2)$ are defined on the image planes of the projector at the two orientation $(\alpha, \beta) =$

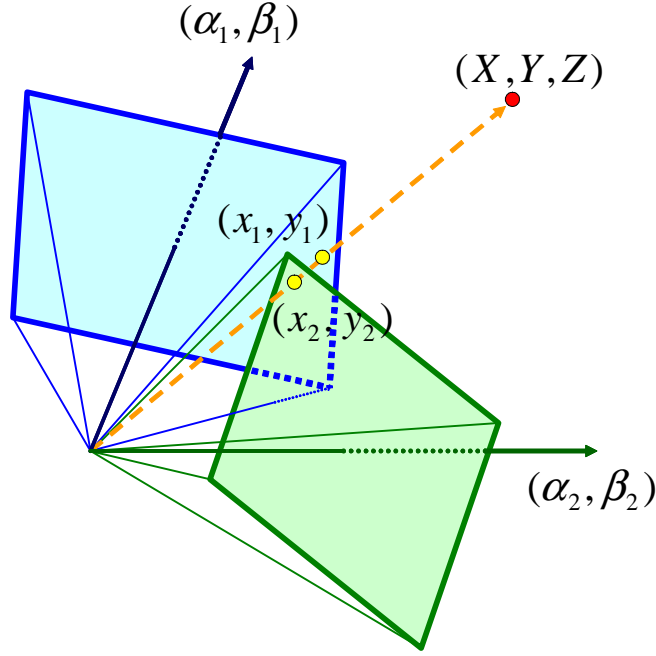


Figure 29. The same point projection from different orientations.

$(\alpha_1, \beta_1), (\alpha_2, \beta_2)$. When these are applied to Equation (10), the following equation is derived:

$$\lambda' \begin{pmatrix} x_2 \\ y_2 \\ 1 \end{pmatrix} = BD_{(\alpha_2, \beta_2)} D_{(\alpha_1, \beta_1)}^{-1} B^{-1} \begin{pmatrix} x_1 \\ y_1 \\ 1 \end{pmatrix}. \quad (11)$$

This equation gives the a unique property that an arbitrary spatial point (X, Y, Z) projected at (x_1, y_1) on the image plane in the orientation (α_1, β_1) is projected at (x_2, y_2) in the different orientation (α_2, β_2) as shown in Figure 29. This property is similar to that of the FV-PTZ camera in [WUM98]. In the calibration method of the FC-PT projector, this property is utilized to improve the method's accuracy.

First, at the initial orientation $(\alpha, \beta) = (0, 0)$, known multiple points $(x, y) = (x'_i, y'_i)$ ($i = 1, 2, 3, \dots$) on the image plane are projected onto surfaces in the real world as shown in Figure 30 (a). Note that the surfaces do not need to be flat. The FC-PT projector's orientation is then controlled so that the center

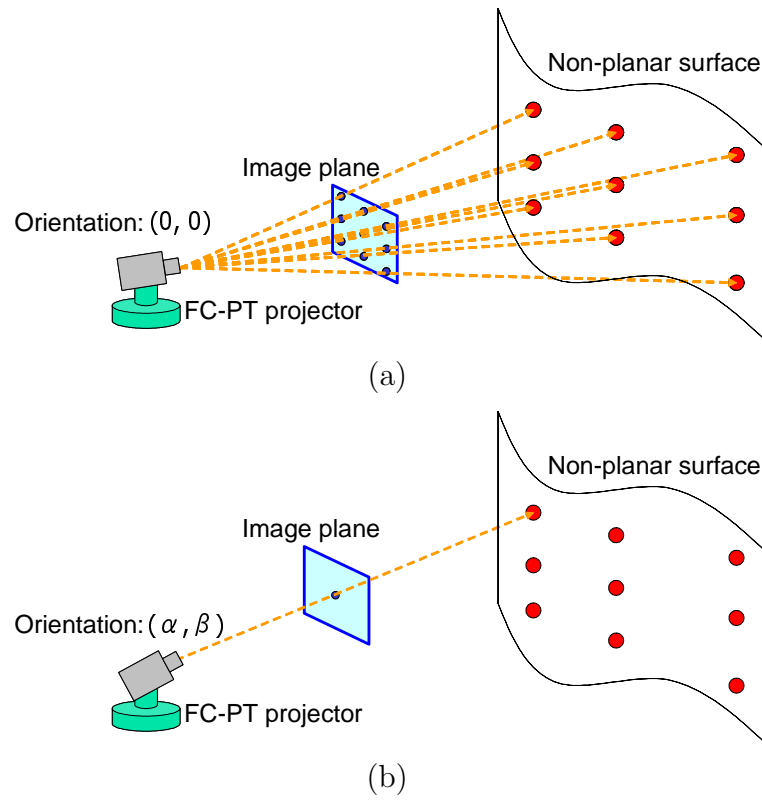


Figure 30. Operation for optimization of the intrinsic parameters using a non-planar surface.

point $(x, y) = (0, 0)$ projects the points projected at the initial points, and the orientations (α'_i, β'_i) corresponds with $(x, y) = (x'_i, y'_i)$, as shown in Figure 30 (b). When the FC-PT projector is precisely implemented, by Equation (11), (x'_i, y'_i) and (α'_i, β'_i) fulfill the following equation:

$$\lambda' \begin{pmatrix} 0 \\ 0 \\ 1 \end{pmatrix} = BD_{(\alpha'_i, \beta'_i)} B^{-1} \begin{pmatrix} x'_i \\ y'_i \\ 1 \end{pmatrix}. \quad (12)$$

As the orientation (α'_i, β'_i) is obtained precisely by the rotation stage, the intrinsic matrix B is likely to contain errors when the relation of this equation is not correctly fulfilled. Considering the above, an evaluated value e_{fc} defined by the following equation is introduced and used for nonlinear optimization, so that the intrinsic matrix B is precisely determined.

$$e_{fc} = \sum_i (\delta_{xi}^2 + \delta_{yi}^2), \quad (13)$$

where (δ_x, δ_y) is defined as

$$\lambda' \begin{pmatrix} \delta_{xi} \\ \delta_{yi} \\ 1 \end{pmatrix} = BD_{(\alpha'_i, \beta'_i)} B^{-1} \begin{pmatrix} x'_i \\ y'_i \\ 1 \end{pmatrix}. \quad (14)$$

In this study, the FC-PT projector is implemented so that the projector is located on the rotatable stage and directed roughly along the perpendicular axis of the pan and tilt axes, which means $R_{GS} \approx E$, and the intrinsic matrix A estimated by the method in [Zha00] is used as the initial B for the optimization.

In the case of the Non-FC-PT projector, as the variation of the projection center position with the change of its orientation is unknown, the calibration process has to include intrinsic and extrinsic calibration based on projection and observation of the grid patterns in [Zha00], which is not very stable. On the other hand, in the case of the FC-PT projector, the calibration process based on optimization does not depend on the unstable calibration method except when obtaining the initial value for the optimization. This means that it is not necessary to prepare a perfectly flat plane or to measure its 3D shape and position. In this calibration process, therefore, **Cause 2** listed in Section 2.5 is overcome.

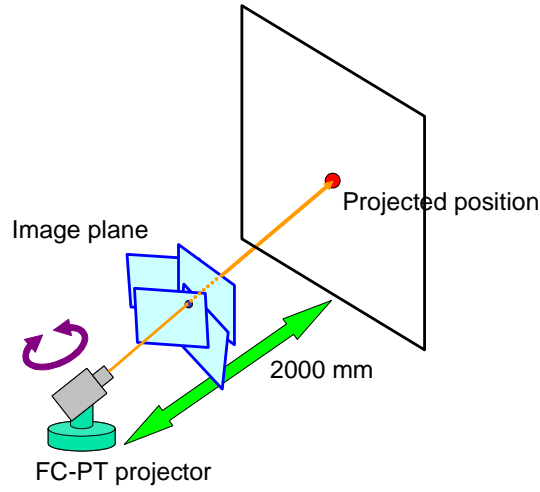


Figure 31. Confirmation of accuracy of the intrinsic calibration.

As an experiment, this intrinsic calibration was executed for an implemented FC-PT projector. To confirm the accuracy of the calibration, the calibrated FC-PT projector was controlled so as to project a fixed position in the environment while changing its orientation as shown in Figure 31. The projected position should be perfectly fixed if both the implementation of the FC-PT projector and its intrinsic calibration are done accurately. As a result, the projected point moves within two millimeters, which means the accuracy of the fixed point was less than two pixels of the projector. This accuracy is thought to be enough to regard that the implementation and the calibration were done well.

3.5 Extrinsic Calibration of an FC-PT Projector

After obtaining the precise intrinsic matrix by the method in Section 3.4, the relation described by Equation (11) is fulfilled, so that the coordinates at arbitrary orientation can be transformed to those of another orientation. This thesis introduces a plane that is parallel to the pan and tilt axes of the initial orientation and is at unit length from the rotation center. This plane is called the tangent plane. The coordinates of the image plane at any orientations are transformed to those of the tangent plane. Using Equation (10) and the definition of the tangent

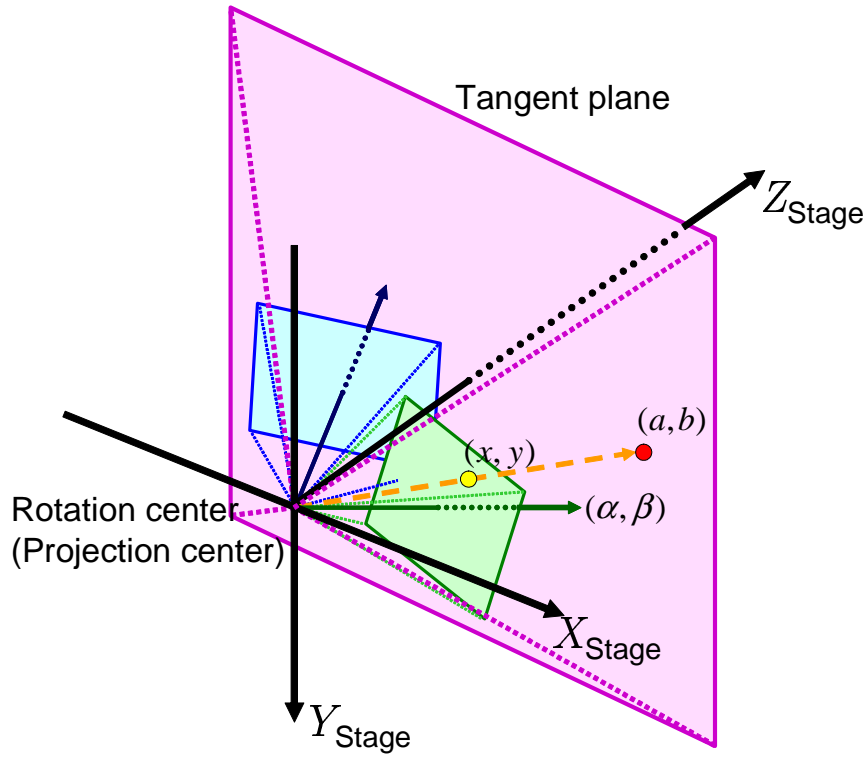


Figure 32. Regarding the FC-PT projector as a fixed projector.

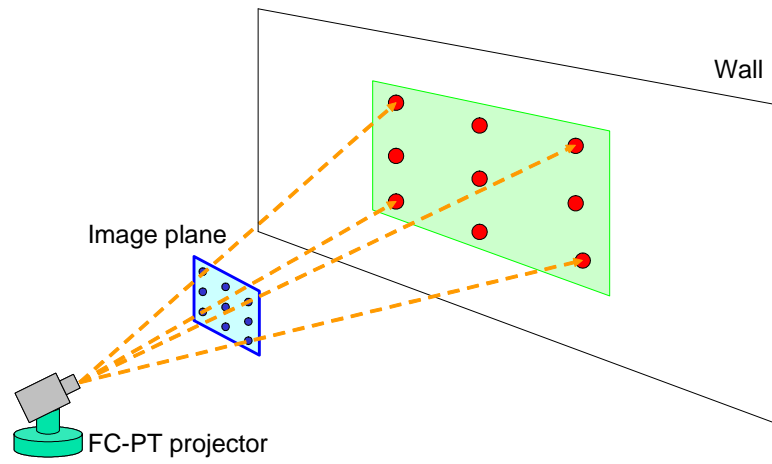
plane, an image plane coordinate (x, y) at an orientation (α, β) is transformed to (a, b) on the tangent plane by the following equation:

$$\begin{pmatrix} \lambda'' a \\ \lambda'' b \\ \lambda'' \end{pmatrix} = D_{(\alpha, \beta)}^{-1} B^{-1} \begin{pmatrix} x \\ y \\ 1 \end{pmatrix}. \quad (15)$$

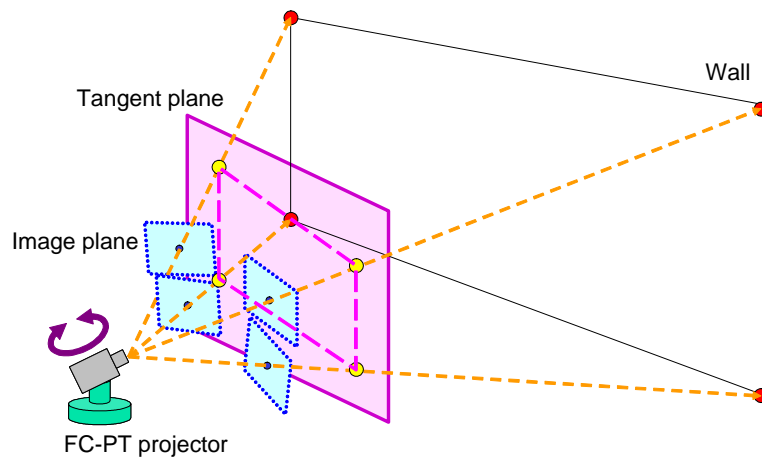
As the tangent plane is fixed independent of the orientation the projector, the FC-PT projector can be regarded as a fixed projector whose image plane corresponds with the tangent plane and whose orientation corresponds with that of the stage, as shown in Figure 32. While extrinsic calibrations of cameras and projectors usually calculate the relation between their image plane coordinates and the global coordinate, as shown in Figure 33 (a), in the case of the FC-PT projector the relation between the tangent plane is used instead of the image plane, as shown in Figure 33 (b). By using not the image plane but the tangent plane, a wider angle of information can be used in the extrinsic calibration than the angle of view of the fixed projector. This means, therefore, that **Cause 3** listed in 2.5 can be overcome in the FC-PT projector.

3.6 Concluding Remarks

In this chapter, the FC-PT projector, which is a new structure for a steerable projector, is proposed. Its implementation and calibration methods were described. By introducing the FC-PT projector, the three causes of the bad calibration that is inevitable in the case of other conventional steerable projectors are overcome.



(a)



(b)

Figure 33. Operation for extrinsic calibration of the FC-PT projector.

4. Projecting Rectified Images onto the Real World Using an FC-PT Projector

Once the intrinsic and extrinsic calibration have been executed for the steerable projector, the position and orientation at any pan and tilt angles are calculated correctly, so that it can be treated as a fixed projector. Since the FC-PT projector's calibration can be precise, it can be applied to the various conventional systems using fixed projectors [THI02, MNS01, RWLB01, GPNB04, RFC⁺02, SCS01, BFRV05].

In particular, when only planar areas in the environment (floors and walls for example) are used for projection, there is another way for extrinsic calibration of the FC-PT projector utilizing the tangent plane. This method can make extrinsic calibration easier and more precise.

4.1 Projection onto a Single Plane

As described in Section 3.5, by using the tangent plane instead of the image plane, a wider angle of information can be used in extrinsic calibration than the angle of view of the fixed projector, so that extrinsic calibration can be stable. When a planar area is used for the projection, extrinsic calibration should use information from a wide area. The relation between the plane in the environment and the tangent plane is defined by a 3×3 homography matrix [HZ00, Sat99], which can be determined four or more than four pairs of corresponding positions. In the case of walls or floors in the environment, their four corners are used for the calibration, for the following two reasons:

- **Stability.**

The calibration can use a wide angle of information, which is similar to triangulation by a long baseline, so that the calibration is expected to be accurate and stable.

- **Easy operation.**

In most indoor environments, the planes are walls, floors and ceilings. In such situations, they are all rectangles and their corners are easy to direct the projection at.

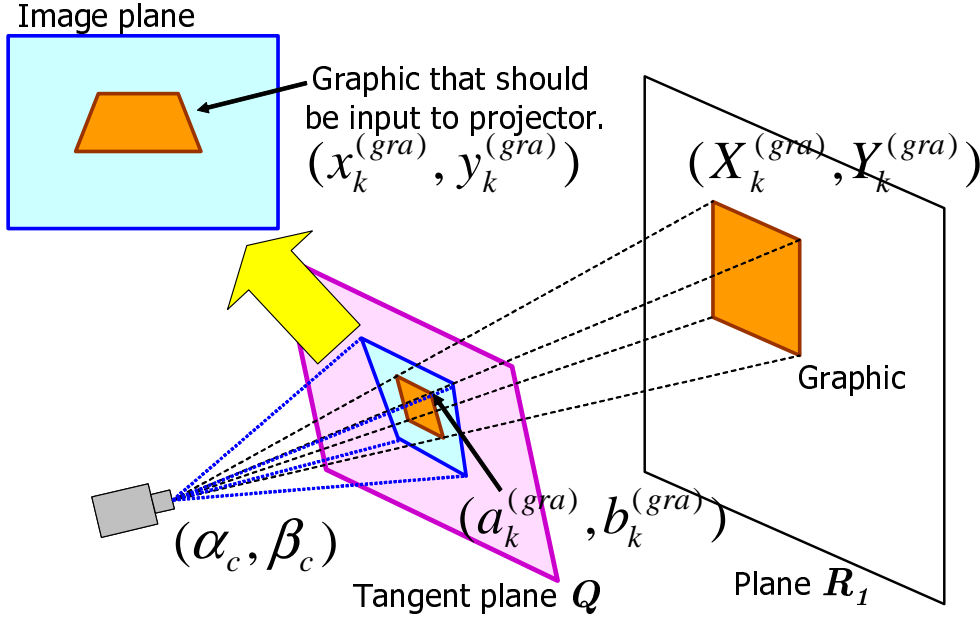


Figure 34. Projection onto a plane in the real environment.

In this section, the method used to display a graphic $(X_k^{(gra)}, Y_k^{(gra)})$ ($k = 1, \dots, 4$) on a single plane R_1 in the environment is described, given that the homography matrix H_{QR1} between the plane R_1 and the tangent plane Q is obtained, a status in which we can describe the plane as “registered.”

First, the graphic $(X_k^{(gra)}, Y_k^{(gra)})$ is projected onto R_1 by the homography H_{QR1} :

$$\begin{pmatrix} a_k^{(gra)} \\ b_k^{(gra)} \\ 1 \end{pmatrix} = H_{QR1}^{-1} \begin{pmatrix} X_k^{(gra)} \\ Y_k^{(gra)} \\ 1 \end{pmatrix}. \quad (16)$$

The gravity position $(a_c^{(gra)}, b_c^{(gra)})$ is then calculated, and from Equation (15) the pan and tilt angles (α_c, β_c) are determined as the orientation so as that the center position of the image plane is projected at the gravity position. Finally, the graphic on the image plane $(x_k^{(gra)}, y_k^{(gra)})$ is calculated by substituting (α_c, β_c) and $(a_k^{(gra)}, b_k^{(gra)})$ in Equation (15).

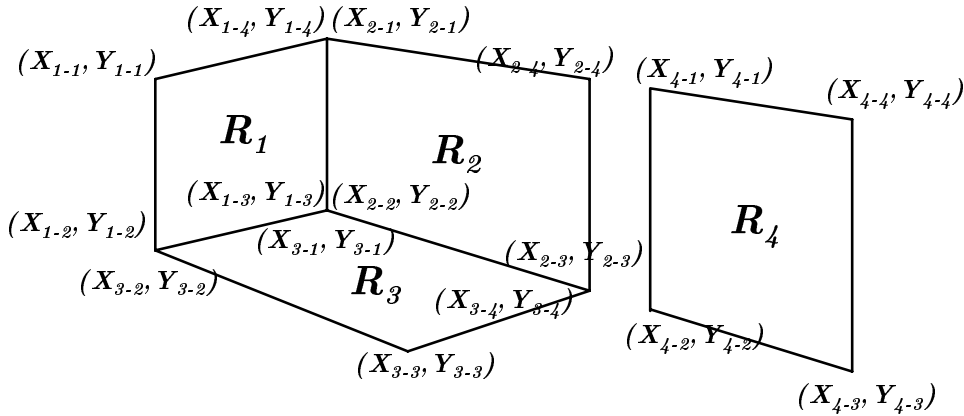


Figure 35. Multiple planes in the real environment.

4.2 Extension to Multiple Planes

There are many planes in the environment on which it may be desirable to be able to display graphics. The FC-PT projector is appropriate for such demands because the projection method for a plane described in Section 4.1 can easily be extended to that for multiple planes. In fact, as the plane registration can be done by measuring the direction of the four corners of the plane, we can register even multiple planes in the environment. However, in most cases, this is insufficient. Because the 2D coordinate system of each plane is defined independently, the projector system cannot recognize connections between the planes, and, as a result, it cannot precisely display graphics that lie across boundary lines of the planes. In this section, to overcome this problem, we describe a method for displaying graphics which gives the same effect as for paper posters folded and pasted across the boundary lines. A similar effect was implemented in [AS03], where the projector and the camera are fixed and there are only two planes connected to each other.

4.2.1 Preparation for Multi-Planar Projection

In the example shown in Figure 35, there are four planes in the environment, and some of them are interconnected. Each plane is described by its own 2D metric

Plane	(u, v)	(x, y)
R_1	(a_{1-1}, b_{1-1})	(X_{1-1}, Y_{1-1})
	(a_{1-2}, b_{1-2})	(X_{1-2}, Y_{1-2})
	(a_{1-3}, b_{1-3})	(X_{1-3}, Y_{1-3})
	(a_{1-4}, b_{1-4})	(X_{1-4}, Y_{1-4})
R_2	(a_{2-1}, b_{2-1})	(X_{2-1}, Y_{2-1})
	(a_{2-2}, b_{2-2})	(X_{2-2}, Y_{2-2})
	(a_{2-3}, b_{2-3})	(X_{2-3}, Y_{2-3})
	(a_{2-4}, b_{2-4})	(X_{2-4}, Y_{2-4})
R_3	(a_{3-1}, b_{3-1})	(X_{3-1}, Y_{3-1})
	(a_{3-2}, b_{3-2})	(X_{3-2}, Y_{3-2})

...

Table 1. Plane registration table.

coordinate system, which can be determined arbitrarily on the plane. In Figure 35, the coordinate system (X_1, Y_1) is used on plane R_1 and is independent of the other coordinate systems (X_l, Y_l) ($l = 2, 3, 4$). What we have to do is to measure the direction from the FC-PT projector to each corner of the planes, by rotating the projector manually. The directions are obtained as the orientation (α, β) , and they are transformed to (a, b) on the tangent plane by Equation (15). Table 1 shows the list of those coordinates, which is used to register the planes. We call this the “registration table.”

4.2.2 Detection of Relations among Planes

After registration in Section 4.2.1, the system recognizes the connections of the planes and calculates the relation between each pair of interconnected planes.

In Figure 35, (X_{1-4}, Y_{1-4}) and (X_{2-1}, Y_{2-1}) represent the same point in the environment so that their corresponding points (a_{1-4}, b_{1-4}) and (a_{2-1}, b_{2-1}) are the same; (a_{1-3}, b_{1-3}) and (a_{2-2}, b_{2-2}) are also the same. From these two points in the environment, the system can recognize that R_1 and R_2 are connected to each other. Using this logic, the system can detect any existing connection by focusing on each pair of planes and searching for (a, b) appearing more than once in the

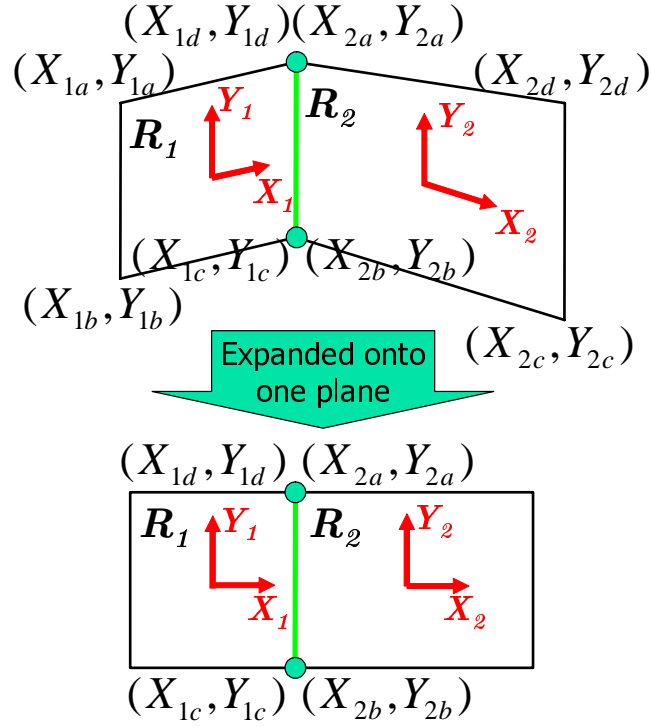


Figure 36. Two planes expanded onto one plane.

registered data of these planes. If two such points exist, the focused planes are connected to each other. By this process, the system makes a matrix as follows:

$$M = (m_{ij}) = \begin{pmatrix} 0 & 1 & 2 & - \\ 3 & 0 & 4 & - \\ 5 & 6 & 0 & - \\ - & - & - & 0 \end{pmatrix}, \quad (17)$$

where m_{ij} represents whether or not R_i and R_j are connected to each other. For each m_{ij} , “0” means that R_i and R_j are the same plane, and “-” means that there is no connection between R_i and R_j . Values larger than “0”, mean that the planes are connected. These values are assigned in order $(1, 2, 3, \dots)$, each of which denotes a unique ID of the pair. We call this matrix the “connection matrix.”

ID	parameters
1	$\theta_1 \quad t_{X1} \quad t_{Y1}$
2	$\theta_2 \quad t_{X2} \quad t_{Y2}$
3	$\theta_3 \quad t_{X3} \quad t_{Y3}$
...	...

Table 2. Transformation parameters list

Next, the system calculates the relations between the coordinates on the two planes. For each pair of two interconnected planes, by expanding these two planes into one plane, as shown in Figure 36, one coordinate is described as the 2D transformation of the other. Therefore, for example, focusing on R_1 and R_2 , a point (X_{2-n}, Y_{2-n}) on R_1 can be expressed by (X_{1-n}, Y_{1-n}) as follows:

$$\begin{pmatrix} X_{2-n} \\ Y_{2-n} \end{pmatrix} = \begin{pmatrix} \cos \theta & -\sin \alpha \\ \sin \theta & \cos \alpha \end{pmatrix} \begin{pmatrix} X_{1-n} \\ Y_{1-n} \end{pmatrix} + \begin{pmatrix} t_X \\ t_Y \end{pmatrix}. \quad (18)$$

Since every pair of connected planes has two common points, such as (X_{1-4}, Y_{1-4}) - (X_{2-1}, Y_{2-1}) and (X_{1-3}, Y_{1-3}) - (X_{2-2}, Y_{2-2}) in the case of the pair R_1 and R_2 , the transformation parameters (α, t_X, t_Y) can be calculated linearly by the equation below:

$$\begin{pmatrix} X_{2-1} \\ Y_{2-1} \\ X_{2-2} \\ Y_{2-2} \end{pmatrix} = \begin{pmatrix} X_{1-4} & -Y_{1-4} & 1 & 0 \\ Y_{1-4} & X_{1-4} & 0 & 1 \\ X_{1-3} & -Y_{1-3} & 1 & 0 \\ Y_{1-3} & X_{1-3} & 0 & 1 \end{pmatrix} \begin{pmatrix} \cos \theta \\ \sin \theta \\ t_X \\ t_Y \end{pmatrix}. \quad (19)$$

The system calculates the transformation parameters of all pairs of connected planes and saves them with their IDs as shown in Table 2. We call this list the “transformation parameters list.”

4.2.3 Projection Method

The flowchart for multi-planar projection is shown in Figure 37.

First, the system receives the orientation (α', β') of the FC-PT projector and describes the center direction on the tangent plane as (a_c, b_c) . The system then

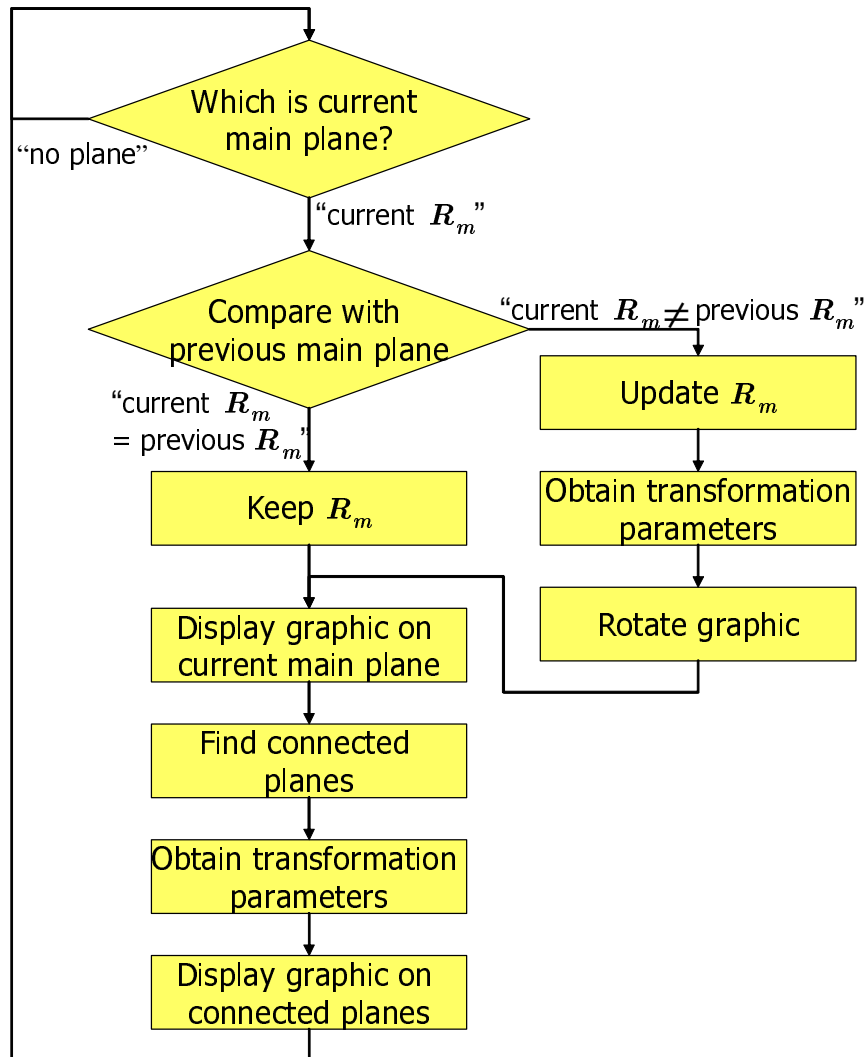


Figure 37. Flowchart of projection.

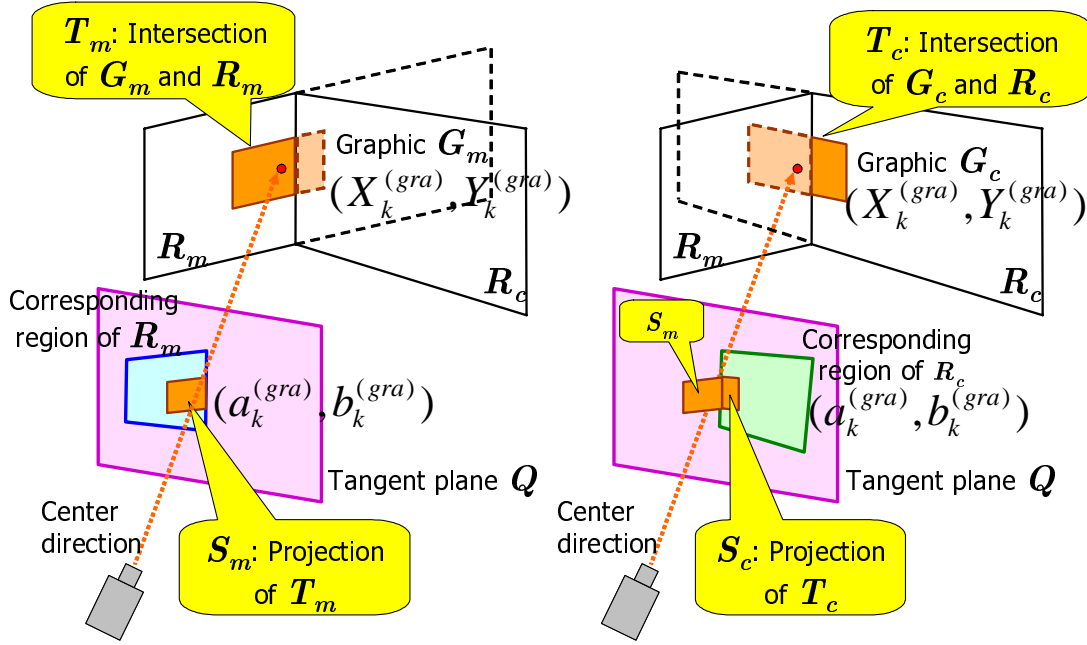


Figure 38. Projection onto the boundary of two planes.

consults the registration table (Table 1) to find which plane's region (a_c, b_c) belongs to, and treats this plane as the current main plane R_m .

Next, by the same process as in Section 4.1, the apices of the graphic $G_m : (X_k^{(gra),m}, Y_k^{(gra),m})$ on R_m are calculated from Equation (16). However, in the case of multi-planar projection, G_m cannot be directly projected onto Q . This is because we have to consider that every plane in the environment has its finite region and the graphics cannot be displayed outside that region. For example, as shown in Figure 38 (a), when the projector is directed to the boundary line of R_m the graphic cannot be completely included within R_m . Therefore, the intersection area T_m of G_m and R_m should be calculated, and be projected to $S_m : (a_k^{(gra),m}, b_k^{(gra),m})$ on Q .

As shown in Figure 38 (b), the system then searches for planes R_c connected to R_m by consulting the connection matrix (Equation (17)). From the connection matrix, the system can find not only planes connected to the main plane, but also the ID of the pair R_m - R_c . It then accesses the transformation parameters list

(Table 2) to obtain the appropriate parameters that transform the coordinates on R_m to those on R_c . Having done this, the system can describe the graphic $G_c(X_k^{(gra),c}, Y_k^{(gra),c})$ by the coordinates on R_c . In a similar way to R_m , the intersection area T_c of G_c and R_c is calculated, and is projected to $S_c : (a_k^{(gra),c}, b_k^{(gra),c})$ on Q . This process is executed for all the planes connected to R_m , and after the process S_m and all S_c are projected onto the image plane P' of the orientation (α', β') .

In addition to the process above, note that a countermeasure against a change of R_m is needed. As the graphic is defined by the coordinates on R_m , when the center direction goes across a boundary line, the orientation of the graphic is changed according to the difference between the coordinates of R_m and R_c , and the graphic cannot move continuously and smoothly. In this system, to overcome this problem, the previous R_m is always preserved, and by comparing the current R_m with the previous R_m the system detects the change of R_m and rotates the graphic appropriately. This additional process is also included in the flowchart shown in Figure 37, and, by this process, the graphic can be displayed continuously and smoothly.

4.3 Experiments

Figure 39 shows the FC-PT projector implemented in this study. This FC-PT projector consists of a small mobile projector V3-131 (PLUS VISION Corp.) and an electric rotatable stage. Their specifications are shown in Table 3. On the stage, stepping motors are used for positional accuracy and repeatability.

Using this projector, three experiments were executed. Note that in every experiment the planes in the environment were larger than the capacity of the projector so that rotation was needed.

4.3.1 Experiments about Positional Accuracy

The first experiment is about the positional accuracy of the projected images. Figure 40 (i) shows three planes in the environment. The FC-PT projector was located at about 1500 mm from the planes. The four corners of each plane were used to calculate the homography matrix between the plane and the tangent



Figure 39. Implemented FC-PT projector.

Projector (V3-131, PLUS VISION Corp.)	
Projection System	DLP
Contrast ratio	2000:1
Brightness	1000lm
Resolution	XGA (1024 × 768)
Weight	1.1kg
Rotatable stage	
Rotation range (pan)	-60 ~ 60 deg
Rotation range (tilt)	-30 ~ 30 deg
Accuracy (pan and tilt)	0.01 deg
Rotation speed	10 deg/s
Weight	15 kg

Table 3. Specification list of the FC-PT projector prototype I.

plane.

Grid points were located at every 200 mm on each plane. The FC-PT projector was controlled to display a crossing image as shown in Figure 40 (ii) at every grid point, and then its positional accuracy was measured. The maximum error is five millimeters and the average is about two millimeters, which corresponds with about two pixels of the projector.

4.3.2 Effect of Rotatable Mechanism

The rotation mechanism of the projector mainly aims at the expansion of its projectable area. The experiment in this section confirms the effectiveness of the expansion.

The whole of a large wall in the environment was used, and the FC-PT projector was located at 1500 mm from the wall. The extrinsic calibration used four corners of the plane.

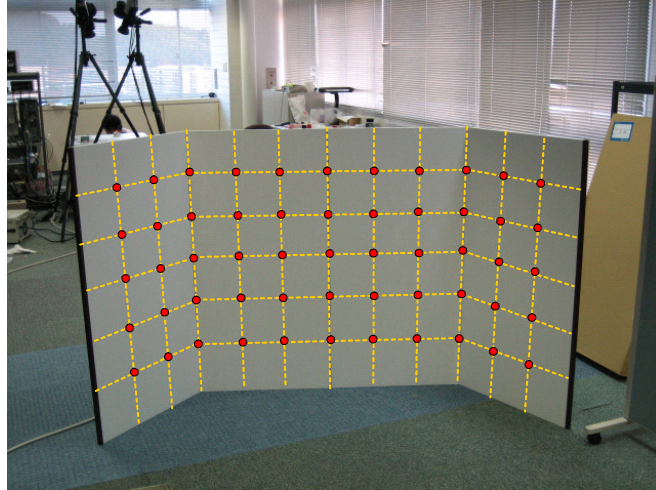
When the projector is fixed, its projectable area was restricted to the region shown in Figure 41 (A). Note that (B) was the input image into the FC-PT projector. In contrast, when rotation is allowed, its projectable area is expanded to the region shown in Figure 42 (B)~(D), which is 5×4 times larger than that of the fixed projector.

Although the region can be expanded more even more, in the actual use it is restricted to the region shown in (B)~(D). This is because the angle of the FC-PT projector gets larger and the projection distance gets longer in order to make the region more expanded, so that the projected image gets darker and the resolution of the image gets worse, as can be seen by comparing (a) with (b)~(d). The region shown in (B)~(D) was determined by considering these limitations.

Note that the focus was fixed throughout the experiments. As the projection system of the FC-PT projector is DLP, which has a long focal depth, the projected images did not defocus as long as projected in the region.

4.3.3 Projection onto Multiple Planes

The last experiment in this section is about projection to multiple planes in the environment. Three planes were located as shown in Figure 43 and the FC-PT projector was again located at about 1500 mm from the planes. Assuming that



(i) Three planes in the environment.



(ii) Projection to a grid position.

Figure 40. Experiments about positional accuracy of projections.

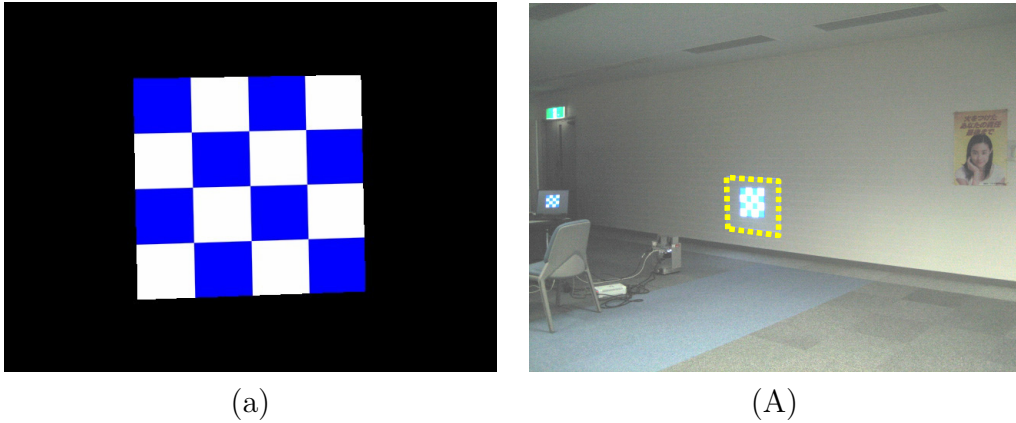


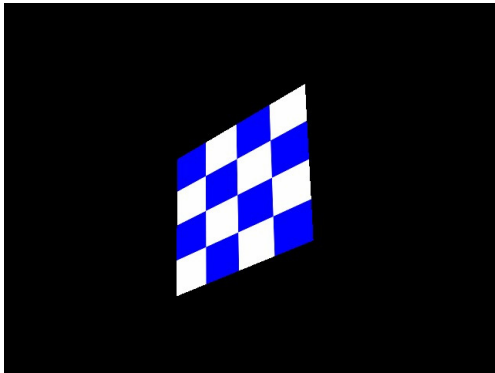
Figure 41. Projection by a fixed projector.

the FC-PT projector is used for a human navigation application, an arrow is displayed and controlled on the planes freely. Figure 44 shows the results.

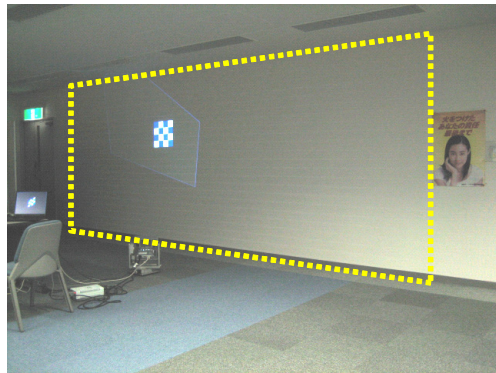
Thanks to the method described in Section 4.2, both the displays on every plane as shown in (E) and also the displays on the boundary of two planes as shown in (F) were realized. On the boundary, the image looked similar to that of a paper poster folded along the planes. In addition, as shown in (G), when a part of the image went out of the planes, an input image to the FC-PT projector was appropriately generated so as not to project the light out of the planes.

4.4 Concluding Remarks

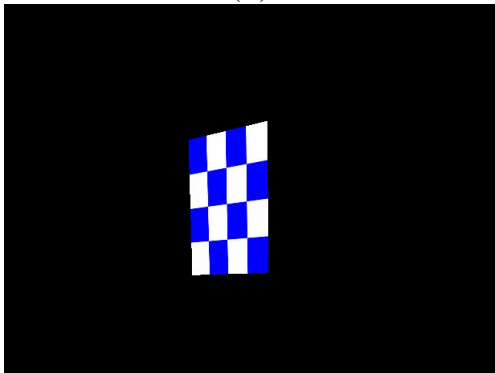
In this chapter, a method was developed to display a rectified image on planar surfaces in the environment using the FC-PT projector described in Chapter 3. Thanks to the method, all the user has to do is to locate the FC-PT projector in the environment, and direct it to the corners of the planes, whose 2D sizes have been measured. In addition, as the FC-PT projector can recognize automatically whether each plane is connected to others, it can display visual information that lies across the boundary line of two planes in a similar way to a paper poster folded along the planes.



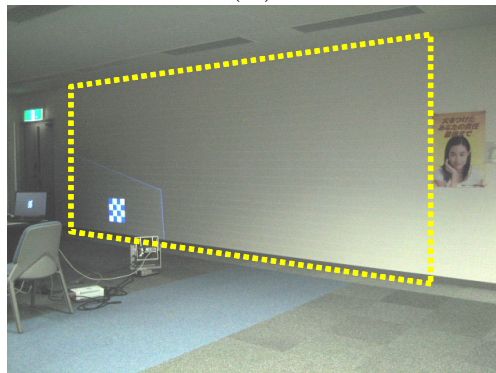
(b)



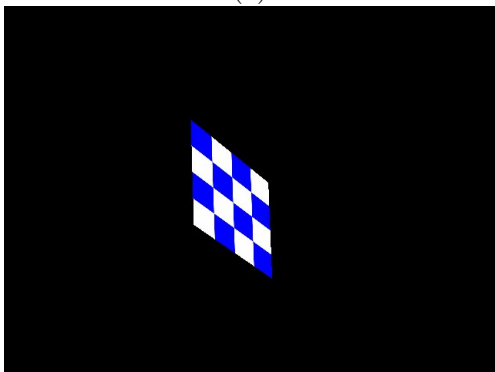
(B)



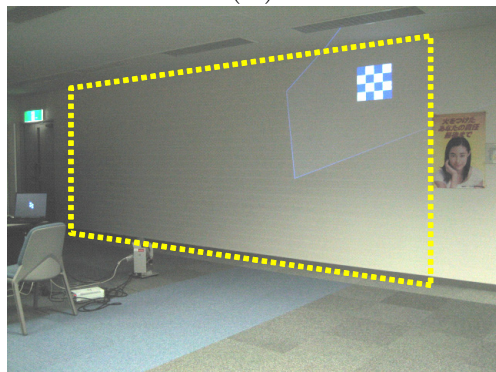
(c)



(C)



(d)



(D)

Figure 42. Projection to a wide area by a FC-PT projector.

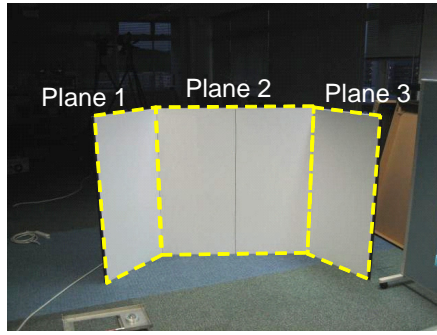
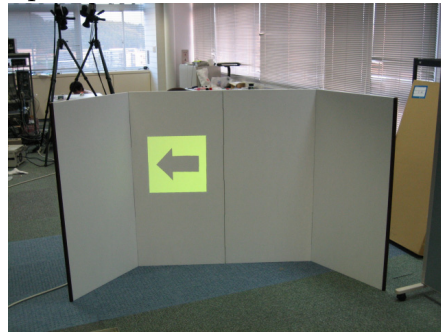


Figure 43. Three planes in experimental environment.



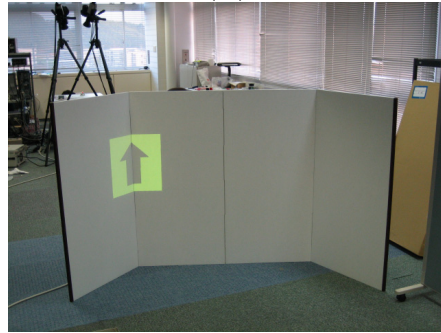
(e)



(E)



(f)



(F)



(g)



(G)

Figure 44. Projection onto the planes and their boundary.

5. Alignment of Multiple Projections

5.1 Causes of Misalignment and Strategy

There are several ways to achieve local alignment of multiple projections [OD06, YGH⁺01], and most of them use homography relations between the image planes and the plane in the real world, assuming its perfect flatness. In fact, when the planar region is not so large and can be regarded to be perfectly flat, such ways work precisely because a kind of optimization method can be applied based on the flatness. However, in the case of wide planes in the real world, flatness may not be fully achieved so that the optimization may yield a worse result. In these cases, a simpler way should be applied instead of such sophisticated approaches. To achieve this, the present section proposes a method that first samples misalignments on the plane and then estimates an alignment at any other position from the neighboring samples. Although these misalignments basically depend on both the image's position on the plane and the orientations of the projectors, as long as the intrinsic calibration of the FC-PT projector is executed precisely the misalignment depends on only the image's position. This approach, which does not consider the orientations, can thus be considered to be appropriate. A disadvantage of this method is that its application needs more time than that of the sophisticated one. However, this is not a serious issue because this time-consuming task has to be executed only once, just after the FC-PT projectors are located.

Note that in this method a pan-tilt-zoom camera is also used to detect local misalignment. The camera just needs a rough calibration; it just should be directed roughly to the position where the image is displayed in order to observe that area around the position.

5.2 Generation of Misalignment Map

The misalignment error of multiple projections depends on the position on the projected plane. Once the misalignment errors are preliminarily measured on the entire plane and saved as *a misalignment map*, a misalignment error at any position can be rectified by referring to the map. Since most planes in the real

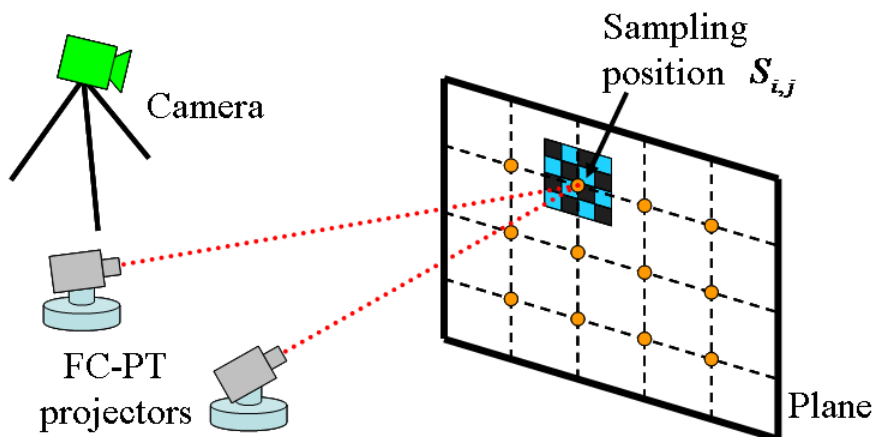


Figure 45. Configuration for generating the misalignment map.

environment are not perfectly flat (slightly curved, for example), the misalignment errors have to be measured very densely. However, as long as the area being focused on is only a localized area it can be regarded as being flat, so that the map has to retain the errors only at discrete positions and interpolation is effective for other positions. The discrete positions are spaced at a certain interval d , and are called sampling positions $\mathbf{S}_{i,j}$, and the misalignment error at $\mathbf{S}_{i,j}$ is defined as $\mathbf{v}_{i,j}$, where i, j are the indexes along the two dimensions of the plane. Figure 45 shows the overview of the configuration.

To robustly and precisely measure the misalignment $\mathbf{v}_{i,j}$ by a camera, a grid pattern each of whose interval is d and which contains 3×3 points is used. Such a grid pattern is projected at $\mathbf{S}_{i,j}$ so as that the center grid point corresponds with $\mathbf{S}_{i,j}$. Next, the projected grid patterns are observed by a pan-tilt-zoom camera. The orientation and zoom parameter of the camera is controlled according to the position of the projected image. As mentioned in 5.1, the camera just needs to be calibrated roughly.

Figure 46 (a) shows an example of the projected grid pattern. When using two projectors, by using different color channels for each projector, the two grid patterns can be detected simultaneously (Figure 46 (b),(c)), and then the grid points $\mathbf{p}_{i,j,k}$ and $\mathbf{q}_{i,j,k}$ in the camera image coordinate can be calculated (Figure 46 (d),(e)). When there are more projectors, this process is repeated for all the

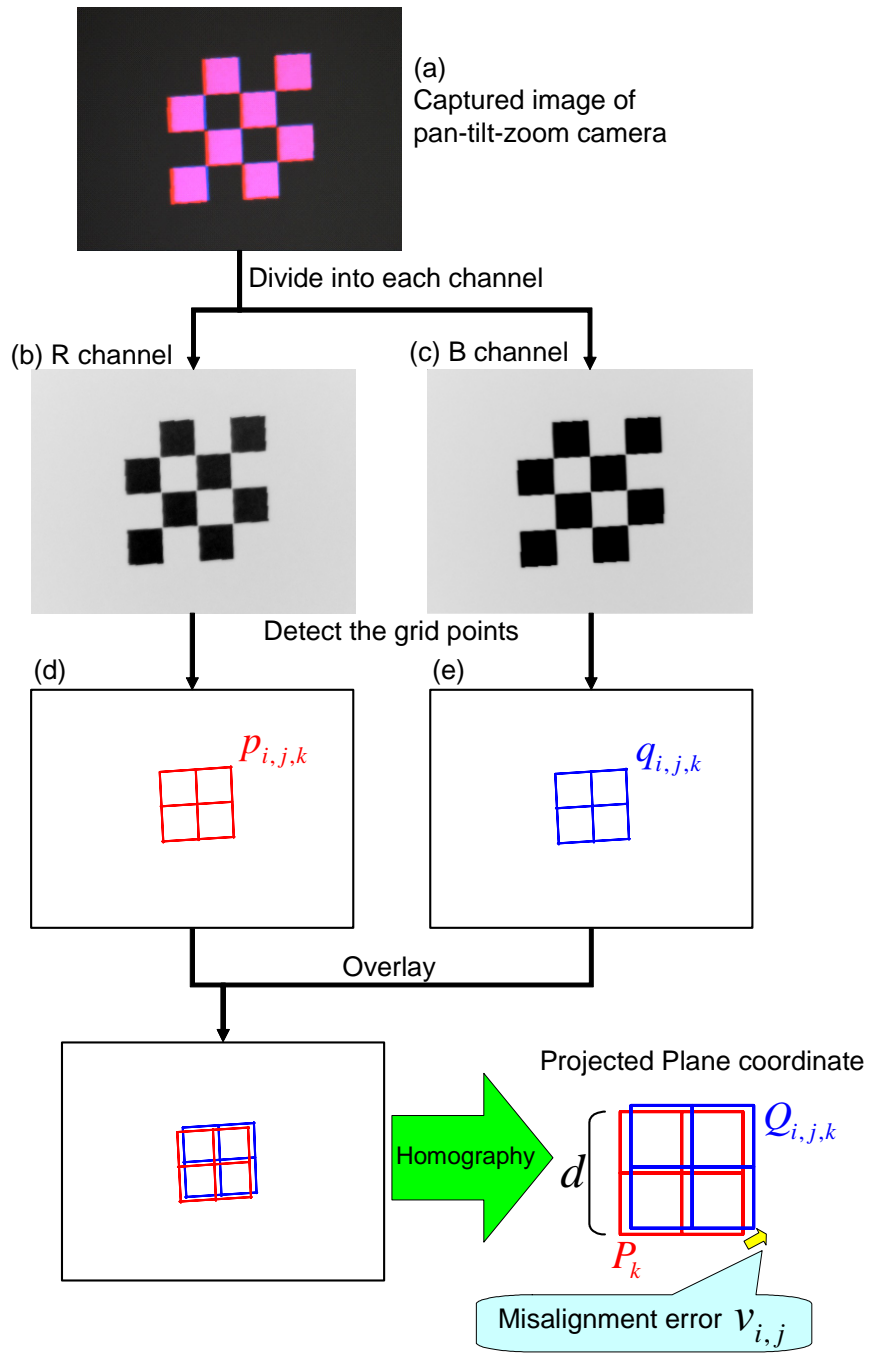


Figure 46. Grid pattern projection at a sampling position.

projectors while keeping the camera parameters.

Next, the misalignment between $\mathbf{p}_{i,j,k}$ and $\mathbf{q}_{i,j,k}$ in the camera image is transformed into that of the plane in the real environment. By the homography relation, $\mathbf{p}_{i,j,k}$ fulfills the following equation:

$$\begin{pmatrix} P_k^x \\ P_k^y \\ 1 \end{pmatrix} = H_{i,j} \begin{pmatrix} p_{i,j,k}^x \\ p_{i,j,k}^y \\ 1 \end{pmatrix}, \quad (20)$$

where $H_{i,j}$ is a 3×3 matrix, and \mathbf{P}_k are the metric grid point coordinate.

$$\begin{aligned} \mathbf{P}_1 &= (-d, -d), & \mathbf{P}_2 &= (0, -d), & \mathbf{P}_3 &= (d, -d), \\ \mathbf{P}_4 &= (-d, 0), & \mathbf{P}_5 &= (0, 0), & \mathbf{P}_6 &= (d, 0), \\ \mathbf{P}_7 &= (-d, d), & \mathbf{P}_8 &= (0, d), & \mathbf{P}_9 &= (d, d). \end{aligned} \quad (21)$$

As $\mathbf{p}_{i,j,k}$ are given from the observations by the camera, $H_{i,j}$ is calculated using Equations (20) and (21). Then, $\mathbf{Q}_{i,j,k}$, which are the grid points on the plane determined the other projector, are also calculated from $\mathbf{q}_{i,j,k}$.

$$\begin{pmatrix} Q_{i,j,k}^x \\ Q_{i,j,k}^y \\ 1 \end{pmatrix} = H_{i,j} \begin{pmatrix} q_{i,j,k}^x \\ q_{i,j,k}^y \\ 1 \end{pmatrix}. \quad (22)$$

Considering that the misalignment consists of translation, the misalignment $\mathbf{v}_{i,j}$ at the position $\mathbf{S}_{i,j}$ is obtained by the following equation:

$$\mathbf{v}_{i,j} = \frac{1}{9} \sum_k (\mathbf{Q}_{i,j,k} - \mathbf{P}_k). \quad (23)$$

Note that, using a pan-tilt-zoom camera, the process above can be executed automatically. This steerable camera only needs to be roughly calibrated to be adequately directed to the position of the projected pattern.

5.3 Precise Alignment Using the Misalignment Map

Once the misalignment map $\mathbf{v}_{i,j}$ is obtained, the translation for the alignment at any position (T^x, T^y) can be calculated by the following interpolation:

$$\begin{aligned} \mathbf{u} &= \frac{(d-l)(d-m)}{d^2} \mathbf{v}_{i,j} + \frac{l(d-m)}{d^2} \mathbf{v}_{i+1,j} \\ &+ \frac{(d-l)m}{d^2} \mathbf{v}_{i,j+1} + \frac{lm}{d^2} \mathbf{v}_{i+1,j+1}, \end{aligned} \quad (24)$$

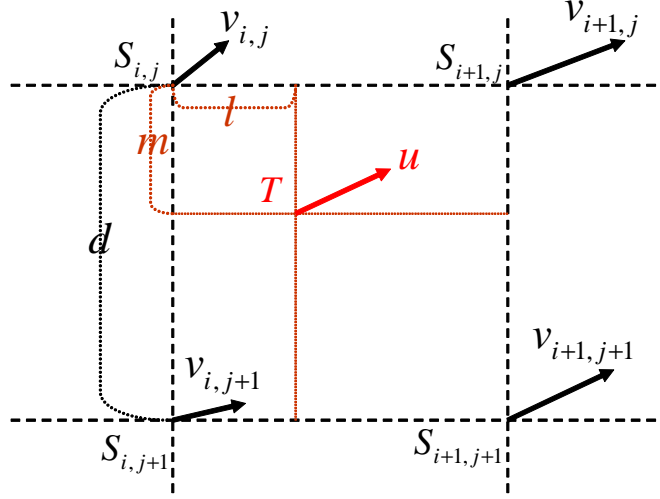


Figure 47. Alignment by interpolation.

where i, j are the maximum integer numbers that fulfill the following equation:

$$\begin{aligned} T^x &= S_{i,j}^x + l \quad (0 < l < d), \\ T^y &= S_{i,j}^y + m \quad (0 < m < d). \end{aligned} \quad (25)$$

This translation \mathbf{u} should be applied for one projector to cancel the misalignment.

5.4 Experimental Results

Figure 49 shows the experimental environment. Two FC-PT projectors and a pan-tilt-zoom camera were used. The specification of the FC-PT projector is shown in Tables 4. For the projected plane, we used a 1200 mm \times 2400 mm board that was slightly curved. The sampling interval d of the misalignment map was 200 mm.

To confirm the effectiveness of the proposed alignment method, the two projection results were compared with each other; one was obtained only by the FC-PT projector calibration and the other was rectified by the misalignment map. Note that the images from two projectors were overlaid in both results.

Projector (V3-131, PLUS VISION Corp.)	
Projection System	DLP
Contrast ratio	2000:1
Brightness	1000lm
Resolution	XGA (1024 × 768)
Weight	1.1kg
Rotatable stage	
Rotation range (pan)	-60 ~ 60 deg
Rotation range (tilt)	-30 ~ 30 deg
Accuracy (pan and tilt)	0.01 deg
Rotation speed	10 deg/s
Weight	10 kg

Table 4. Specification list of the FC-PT projector prototype II.

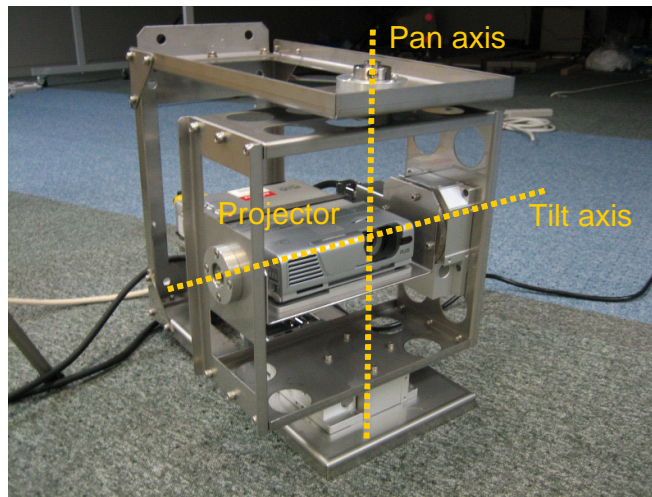


Figure 48. FC-PT projector.

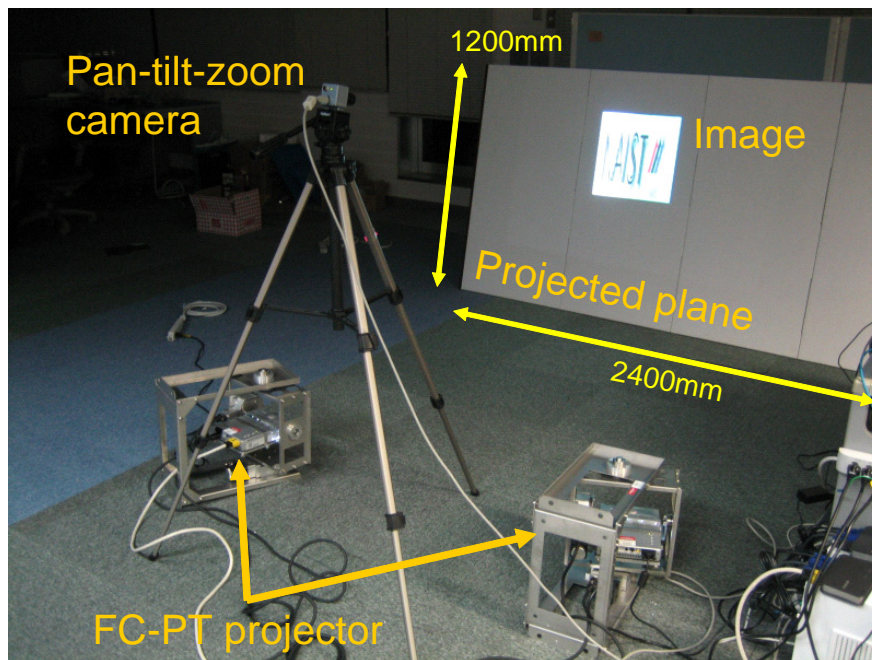
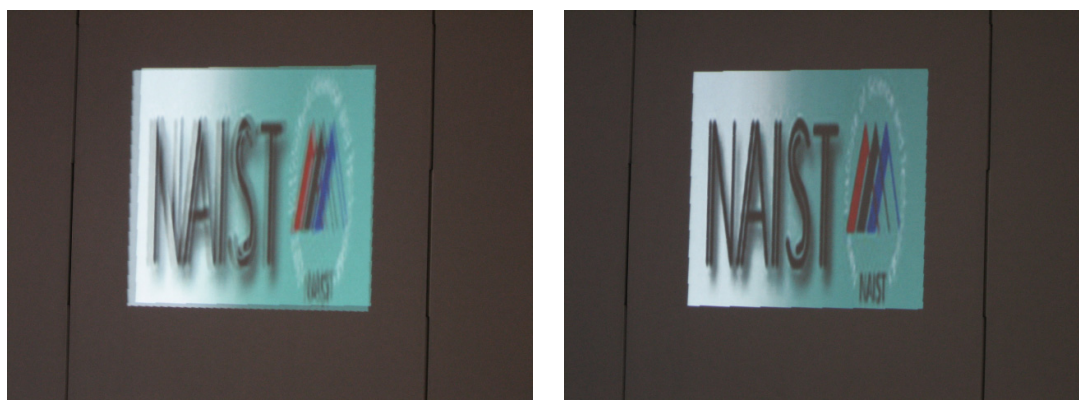


Figure 49. Experimental environment.



(a) Not aligned.

(b) Aligned.

Figure 50. Effect of the alignment method.

Although the misalignments were adequate large, whose maximum was 22 mm, they were much reduced to about one millimeter. Figure 50 shows an example of the result; (a) included 10 mm translation errors, which prevented us from observing the image naturally, while (b), rectified by the proposed method, looks natural.

The effects of tiling and overlaying multiple projections were also examined. Figure 51 shows a large image displayed by tiling two projections. The image had 1600 mm width while the maximum projection width of each projector was 1200 mm. Figure 52 shows an example of overlaying multiple projections. It was found that by overlaying them the image became bright and clear even when the brightness of each projector was not enough.

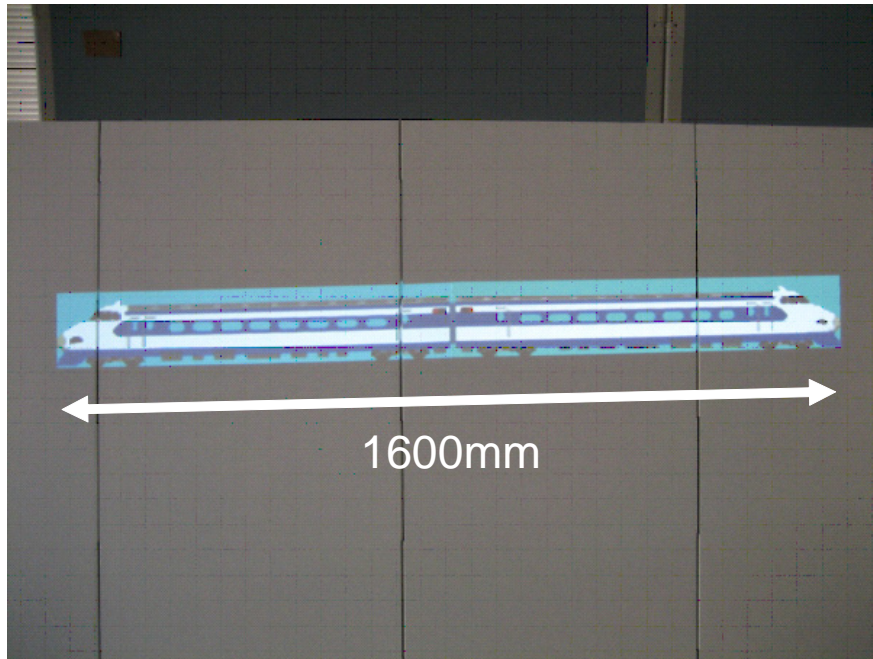
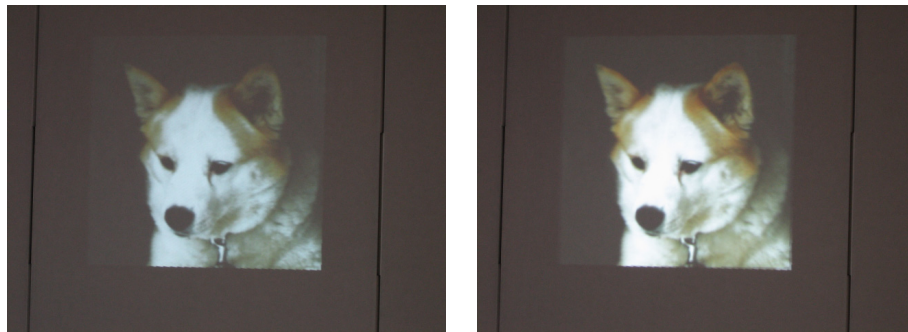


Figure 51. Larger image projection by tiling multiple projections.



(a) By one projector.

(b) By two projectors.

Figure 52. Bright clear image obtained by overlaying multiple projections.

6. Synchronization of Multiple Projectors

6.1 Configuration for Controlling Multiple Projectors

As long as the multiple steerable projectors are used independently, no architecture is needed to integrate them. However, it may be desirable that the multiple projectors collaborate to move the image widely in the environment, or to have the ability to display a larger or brighter image by tiling or overlaying the multiple projections.

To construct a system using multiple projectors, two kinds of architectures are considered; one consists of multiple projectors and a single computer that controls all the projectors, and the other uses multiple computers each of which controls a corresponding projector. The former can easily control the projectors, and this architecture can work well as long as there are only a few projectors, as mentioned in [YGH⁺01]. It is not good, however, for scalability; the calculation load of the computer increases in proportion to the number of projectors. In practice, in many applications, the number of projectors is decided according to the size and shape of the environment and they are usually located separately with adequate long intervals, around several meters in the environment for example, so that the scalability is very important requirement. For these reasons, the latter architecture is applied in this paper.

In this architecture, the multiple computers are connected to a network. To operate the projectors for the applications, there has to exist information about the image that is expected to be displayed, so that a computer for treating the information is also needed in the network³, as shown in Figure 53. This computer is called an “operator PC”, and the other computers for the controlling the projectors are called “receiver PCs.”

The information treated by the operator comes from various sources, which depend on the applications. In a human navigation system, for example, the information is the position of the human and so obtained by a sensing system such as a camera system in the environment. In another case, when the system is used simply as a virtual TV monitor for personal use, the information is input from some input devices.

³ The computer may be one of the computers being used for the projectors.

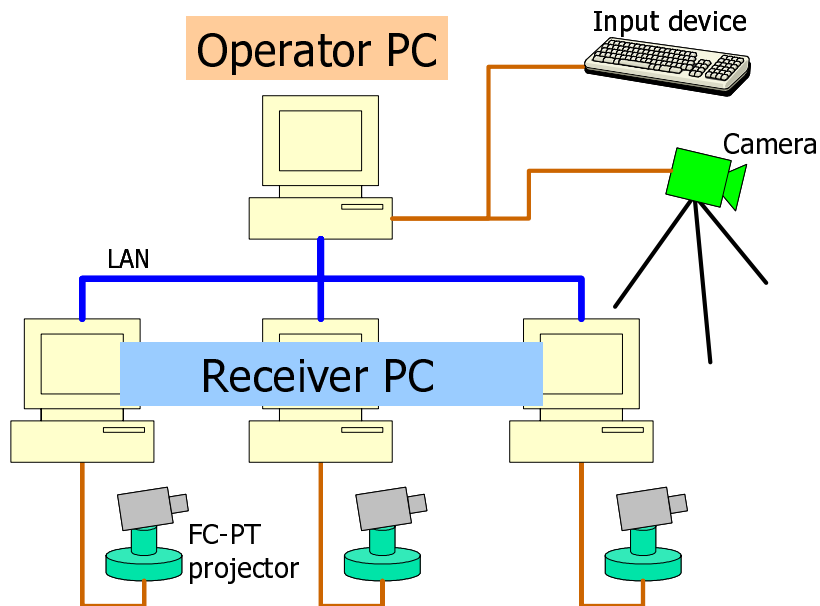


Figure 53. Configuration for multiple projectors.

The receivers get the information transmitted from the operator. Because the projectors may be located separately and at large distances from one another, the network transmission times from the operator to the receivers may be different according to the distances. Even when all the distances are similar to one another, their handling timing may be different from one another.

6.2 Transmitted Data

What information is communicated in the network should be considered. In the system proposed, every FC-PT projector is calibrated separately using global coordinates. Moreover, once the calibration is executed, every receiver can control the corresponding FC-PT projector independently only from variables about the image: its width, height and orientation in the environment, which are called *image parameters*. Therefore, the operator simply transmits the image parameters to all the receivers. Although in this configuration the operator does not manage a control state of each projector, it has the advantage of scalability; even when

the number of the projectors is changed, the transmitted data does not change at all.

6.3 Real Time Integration of Multiple Projectors

6.3.1 Problem of Integrating Multiple Projectors

As long as a position and size of an image are fixed, the system works well; every projected image is displayed at an adequately accurate position, and then the misalignment between the projected images is cancelled by the method in this paper. However, in the case of a moving image, it does not work adequately. Figure 54 shows problems in the case. In this figure, the horizontal axis denotes time and the vertical one denotes a value of one of the image parameters.

Problem 1 — Delay of data transmission: The variables of the displayed image are transmitted from the operator to the receivers through the network. This data transmission time and the handling timing may be different from one another.

Problem 2 — Delay of calculation: Having acquired the variables of the image, the receiver calculates the input image and orientation of the corresponding projector. These calculation times vary depending on the size of the input image and the CPU and GPU abilities of the receivers, so that they are usually different from one another.

Problem 3 — Asynchronization of multiple projectors: The projectors usually run asynchronously; every projector works based on its own clock and frame rate. Section 6.4 gives detailed discussion of this problem.

In constructing multiple camera systems similar problems have arisen in other studies. Matsuyama *et al.* considered these problems and proposed a new architecture in [MHW⁺00], which is called “dynamic memory.” This architecture overcame **Problem 1** and **Problem 3**. **Problem 2** was not considered because it is peculiar to projectors; in the camera system there is no calculation time for generating the projection image. This paper, therefore, modifies this dynamic memory architecture to take into account the delay of calculation.

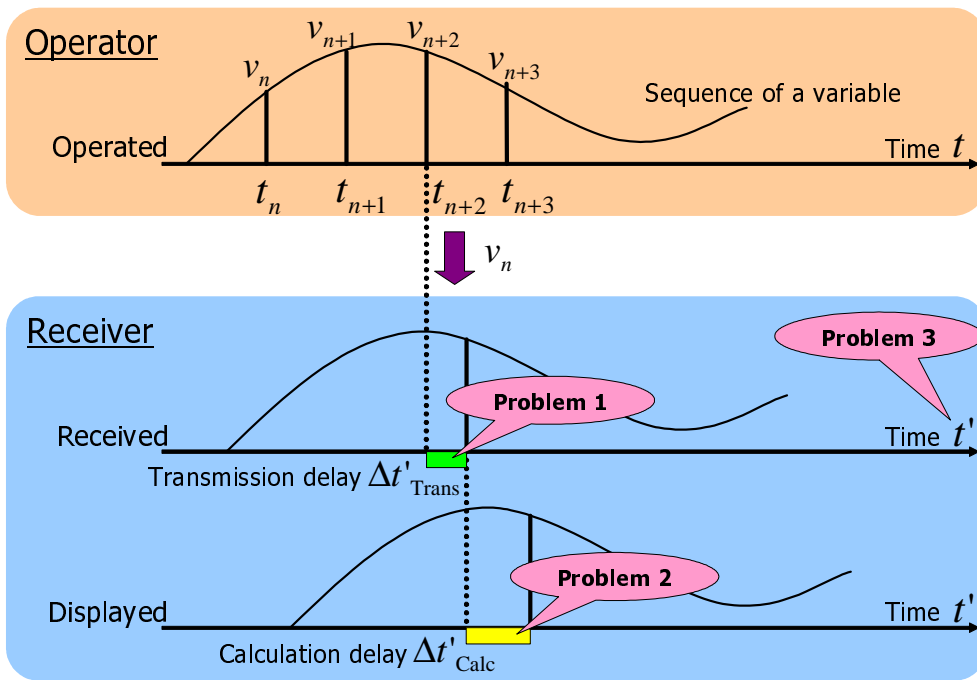


Figure 54. Problems in using multiple projectors.

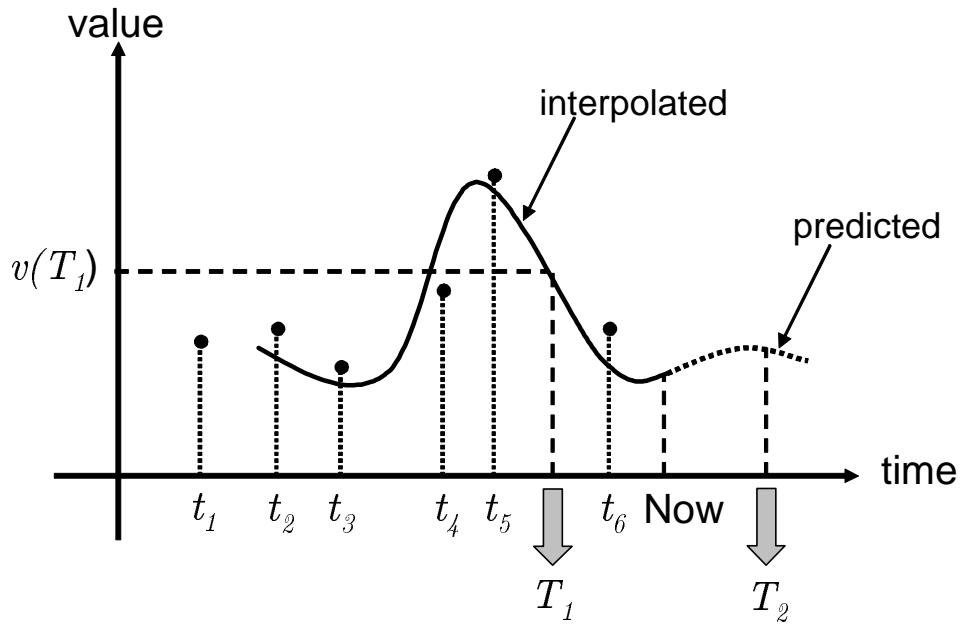


Figure 55. Dynamic memory.

6.3.2 Dynamic Memory

In [MHW⁺00] the dynamic memory architecture was proposed for dynamic integration of multiple steerable cameras, which were called AVAs (Active Vision Agents) and had three modules: (1) *visual perception*, (2) *action* and (3) *network communication*. In the dynamic memory architecture, multiple parallel processes of these above modules share what is called the dynamic memory. The read/write operations from/to the dynamic memory are defined as the following:

Write operation: When a process computes a value v for a variable at a certain moment t , it writes (v, t) into the dynamic memory. Since such computation is repeated according to the dynamics of the process, a discrete temporal sequence of values is recorded for each variable in the dynamic memory (a sequence of black dots in Figure 55). Note that since the speed of the computation varies depending on input data, the temporal interval between

a pair of consecutive value becomes irregular.

Read operation A read process runs in parallel to the write process and tries to read the value of the variable at a certain moment from the dynamic memory: for example, the value at T_1 in Figure 55. When no value was recorded at the specified moment, the dynamic memory interpolates it from its neighboring recorded discrete values. With this function, the reader process can read a value at any moment. In the case that the reader process runs fast and require data which are not yet written by the writer process (for example, the value at T_2 in Figure 55), the dynamic memory predicts an expected value in the future based on those data so far recorded and returns it to the reader process.

With the above described functions, each process can get any data at any moment. That is, the dynamic memory integrates parallel processes into a unified system. This asynchronous module interaction capability is highly effective for the implementation of a real time system.

In addition, the dynamic memory supports virtual synchronization between the multiple PCs. This virtual synchronization is achieved the following procedure. All PCs are first synchronized by NTP, and a timestamp L which indicates when the data should be processed is added to all transmitted data. Next, in the process of the network communication module, the write function writes not (v, t) but (v, L) . As the clocks of the PCs are synchronous, the time L for each PC indicates an identical time, so that the sequence of v for each PC is virtually synchronous. This function overcomes **Problem 1** and **Problem 3** in Section 6.3.1.

6.3.3 Applying Dynamic Memory to Multiple Steerable Projectors

In the multiple projector system, there are also three modules, where the *action* and *network communication* modules are the same as those in the camera system but the *visual perception* module is replaced by an *image calculation* module. The dynamic memory architecture essentially allows them to run asynchronously and thus realizes virtual synchronization between the multiple projectors. However, a modification is necessary to fit fully this architecture to the multiple projector

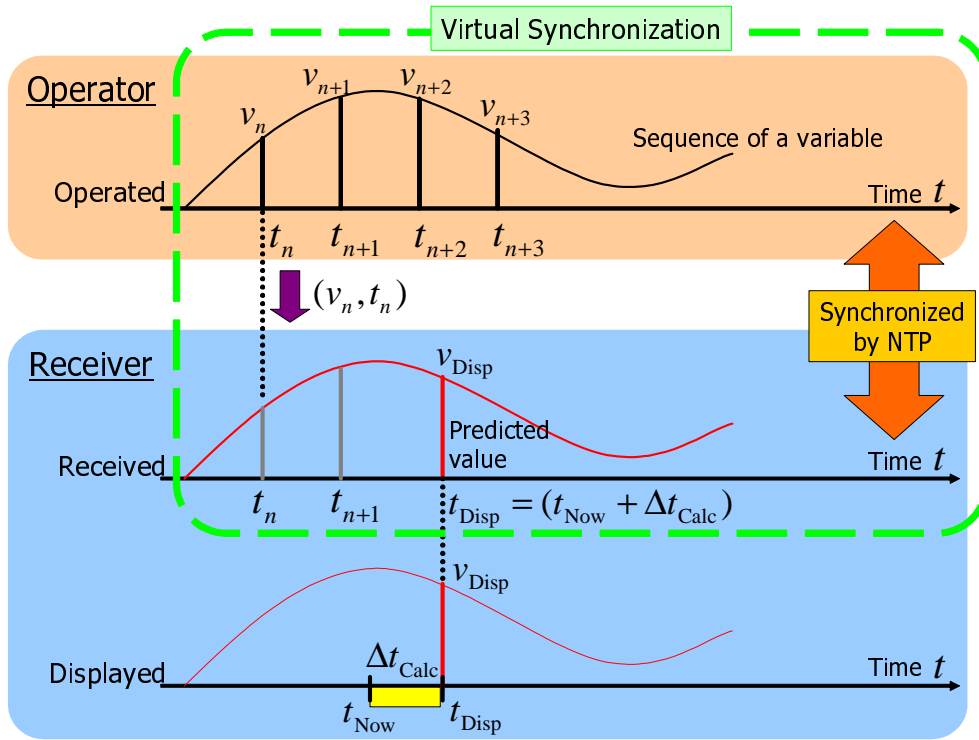


Figure 56. Virtual synchronization of multiple projectors using dynamic memory architecture.

system; in the image calculation module, when the image calculation of the next frame of the projector begins at t_{Now} , the corresponding image parameters should not be those at t_{Now} but those at $t_{\text{Disp}} = t_{\text{Now}} + \Delta t_{\text{Calc}}$, as shown in Figure 56. Δt_{Calc} is determined by the previous frame, and the image parameters at t_{Disp} can be obtained by the read operation of the dynamic memory.

6.4 Consideration about Synchronization

6.4.1 Two Definitions of Synchronization

The word “synchronization” for cameras and projectors has the following two meanings:

- **Synchronization of frames:**

This means making multiple cameras capture images at the same moment. In most camera systems, this definition is used. In the case of projectors, however, it means making multiple projectors project images at the same time.

- **Virtual synchronization of continuous sequences:**

This does not consider timing of capturing or projecting, but means making sequences of variables for them run in unison.

Keeping the above in mind, this section discusses the importance of the synchronization of frames in multi-camera and multi-projector systems.

6.4.2 Synchronization of the Multi-camera System

Multiple cameras are often used to obtain 3D shapes in the real world using the stereo vision or the volume intersection method. In these situations, it is very important that images of the multiple cameras at every capture have to be captured at the same time. If this is not achieved, moving objects cannot be measured precisely.

The capture rate of every camera should be increased to record more detailed changes of the scene, but a higher priority should be put on realizing the frame synchronization, as mentioned above; even if the rate gets a little lower because of waiting times for capture by the cameras, frame synchronization should be maintained.

This argument can be supported by the explanation below from another viewpoint. The images captured by the camera are discrete, as shown in Figure 57; the scene is divided into multiple still images. The camera is, therefore, regarded as a device that samples discrete values (corresponding to still images) from a continuous sequence (corresponding to the scene). To record the continuous sequence more precisely, the rate of sampling should be higher. However, according to the Nyquist-Shannon sampling theorem, twice the maximum frequency in the sequence is enough as the capture rate to recover the sequence perfectly; the rate does not need to be higher than that.

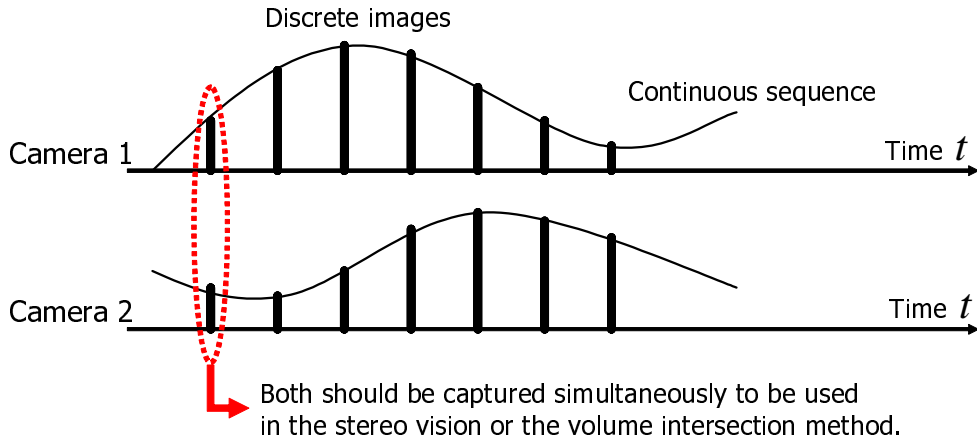


Figure 57. Discrete capture of a continuous scene.

6.4.3 Synchronization of the Multi-projector System

In contrast with cameras, projectors can be regarded as devices that transform discrete images to a continuous scene in the real world. However, this transformation cannot be fulfilled perfectly because the projector projects a still image discretely and keeps it in its frame interval as shown in Figure 58. Although the sequence of the discrete images looks similar to the desired continuous sequence as shown in Figure 59 when the rate gets higher, it can never coincide perfectly with the continuous one. This means that in the case of the projector there is no sufficient rate; the rate should be increased as much as possible.

Considering above, increasing frame rate of a projector is more important than for a camera, and when integrating multiple projectors a higher priority should be put on accomplishing the as high frame rate as possible; the frame synchronization, which is more important in the case of cameras, is less important. This paper, therefore, does not consider frame synchronization of multiple projectors but implements asynchronous projection, where every projector projects at its maximum frame rate.

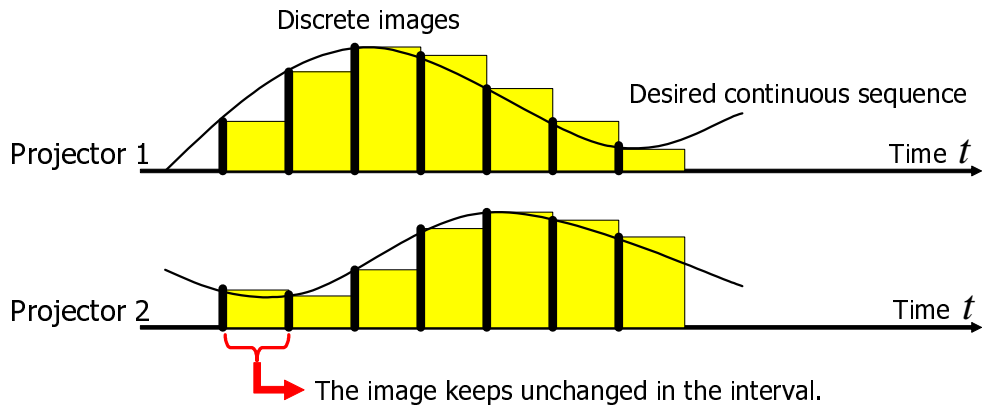


Figure 58. Frame synchronization in the case of projectors.

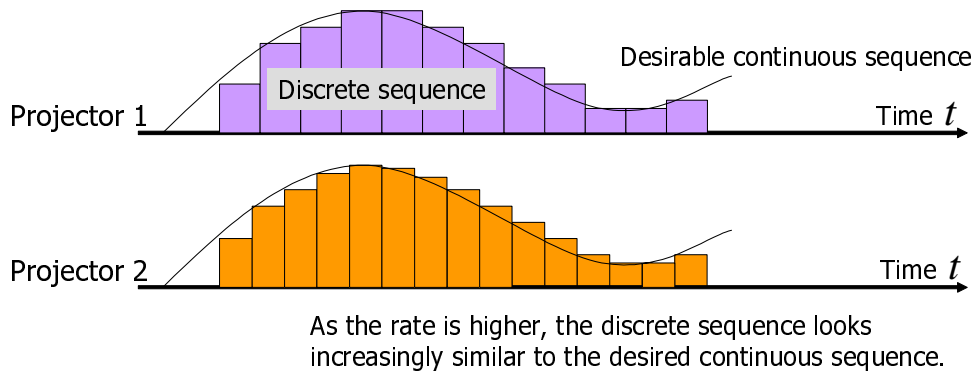


Figure 59. Generating a continuous sequence by the discrete frames.

6.5 Experiments

Projection experiments were executed using two FC-PT projectors. The experimental environment is the same as in Section 5.4. The alignment method was applied the projected plane, and the sampling interval d of the misalignment map was 200 mm.

Note that in the implementation the projector’s orientation is controlled by the stop-and-go method because of the limitation of the rotation stage, whereas in [MHW⁺00] orientation was smoothly and precisely controlled by the PID method.

Figure 60 shows the results, where an image of a car is displayed by overlaying two projections at the same position. Two quadrangles around the car indicate the projectable area of the projectors. It was observed that the two projections remained well-aligned while the car image moved on the wall in a circle. Sometimes the misalignment was observed and it only occurred when each projector began or stopped its rotation. The cause of the misalignment is failure of the stage orientation estimation; when beginning or stopping the rotation, the variables change suddenly. If the PID method is adopted so that the stage moves smoothly, misalignment can be much reduced.

Experiments for quantitative evaluation were also executed. Chessboard patterns were projected instead of the car image at the same position from the two FC-PT projectors and were tracked by a zoom camera to measure their misalignments. Figure 61 show the result in the case of circular paths on the wall. In the graph, the horizontal axis is time and the vertical axis is the misalignment. Although several peaks caused by the stage orientation estimation failure are observed in these graphs, it is confirmed that the system worked well; the misalignments stayed around one millimeters except these peaks.

It was also confirmed that the frame rate of each projector is adequately high: 60 fps, which is the maximum rate of the device. Such a high rate was achievable because the system was implemented so as to put a higher priority not on fulfilling frame synchronization but on increasing the high frame rate. It was observed that the movement of the image looked very smooth due to this high rate.

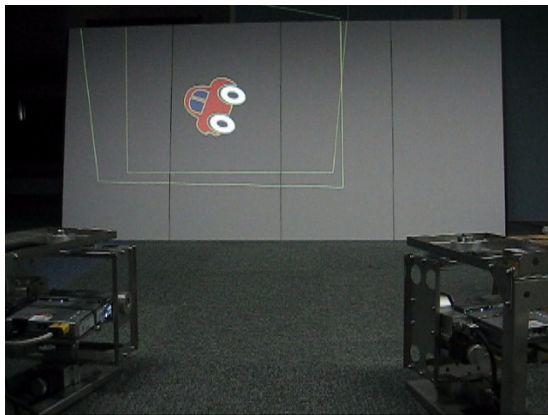
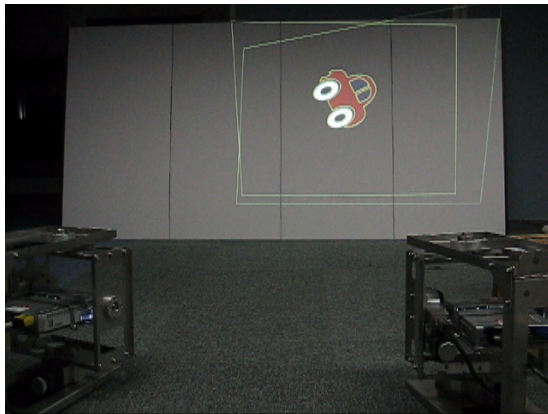
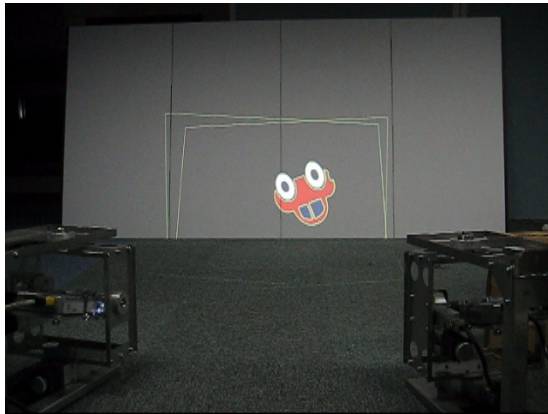


Figure 60. Moving image projection using two FC-PT projectors.

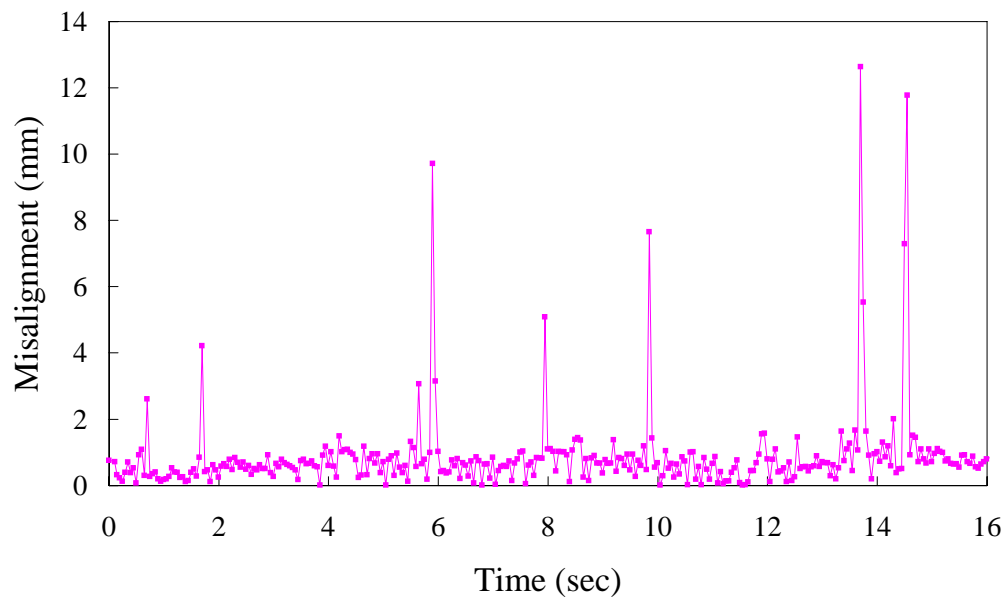


Figure 61. Misalignment when the image moves along a circle.

7. Concluding Remarks

7.1 Thesis Summary

This thesis has presented a novel multiple steerable projector system that can display an image anywhere on various surfaces in a wide environment. The system can not only display an undistorted image but also control the image's position and size precisely. In addition, by operating multiple projectors simultaneously, it can show a larger or brighter image than the capacity of a single projector by tiling or overlaying projected images. These properties enable the system to be utilized in a variety of applications: visual annotations for objects and places, human navigation, a flexible screen for lectures, remote instructions, color and texture simulations of non-textured surfaces, and many other AR applications.

1. Structure of a Steerable Projector and Its Calibration

To realize such a projection system, it is necessary to implement a steerable projector and calibrate it precisely. This calibration has been, however, difficult and unstable because conventional steerable projectors have much more complicated structures than fixed ones. Existing steerable projectors [Pin01, BRC03, AFSR04], in fact, had complicated models so that their calibrations were inaccurate or unstable. In this thesis, a new structure has been proposed, whose projection center precisely corresponds with its rotation center, so that the projection center does not move whichever direction it is controlled toward. This unique structure reduces the parameters of the projector and enables its intrinsic and extrinsic calibration to be correct and stable.

2. Displaying rectified images on the real world

To project a desired image on a surface in the environment, knowledge of the 3D structure of the environment is required. However, obtaining this information is usually tedious and takes a long time, so that the system has not become widely used. This thesis proposes an easy and stable method to obtain environmental structure information by setting the limitation that the projected surfaces consist of multiple planes. The thesis also describes how to realize display not only on every plane but also at the boundaries

of multiple planes; the image is shown in a similar way to a paper poster folded along the planes.

3. **Precise Alignment of Multiple Projections**

To display a larger image or a brighter image than the capacity of a single projector allows, cooperation between multiple projectors is effective; the larger image by tiling and the brighter image by overlaying multiple projections. If every steerable projector is precisely calibrated in the environment, tiling and overlaying are very easy. In fact, however, every projection image has slight positional errors, so that we observe the errors as relative misalignments when tiling and overlaying them. This thesis describes a method to overcome this problem; the misalignment map is prepared preliminarily to avoid misalignment during use.

4. **Synchronization of Multiple Steerable Projectors**

Even after implementing precise alignment of multiple projectors, misalignment still occurs when a moving image is projected from multiple projectors. This is because of (1) nonconstant delays in calculating the projection image and in network communication, and (2) unsynchronized projections of the multiple projectors. In this thesis, the synchronization of the multiple steerable projector has been considered, and a new synchronization method for network-connected multiple projectors is proposed to realize the successful projection of well-aligned moving multiple images.

7.2 Applications

7.2.1 Application Fields

The proposed system can be used in many applications for personal, business, academic, manufacturing, welfare, entertainment uses and so on. Some of them are listed as follows:

Human navigation: In a museum or an academic building, for example, a projected image such as an arrow navigates a visitor. As there are multiple projectors and every projector can rotate, the image can be moved so that

it follows the visitor's walk, and an active projector selected according to his/her position.

Intelligent lecture room: Multiple projectors can generate a virtual white-board or screen, which can move according to the position of the teacher/presenter. Its size and brightness can be also manipulated; when we need a large screen the multiple projections are tiled, and when the room is bright with sunshine, the multiple projections are overlaid onto the same position to generate a brighter image.

Remote instruction: In a building site or a factory, a remote operator can specify the place that a worker should move to, or the surface of a 3D object that should be manufactured, by showing visual information. The worker can easily thus understand what to do next.

Design simulation: By projecting images onto a clay model, a non-textured 3D object (a clay model of a car, for example) can be colored/textured for design simulation. Displaying images of windows or furniture on walls and floors can also be used in room design simulation.

7.2.2 Implemented Example

As one of the applications for entertainment, a maze puzzle system was implemented. In this system, the user can see and control a character on the wall in the environment and can always see a small part of the maze around the character, as shown in Figure 62.

The maze is defined by bitmap data, as shown in Figure 63, that is assigned to 3 walls, in this example, shown in Figure 64. Using this data and the position of the character, the system can generate a partial image of the maze and display it precisely on the walls. As shown in Figure 64, it is sufficient for the user to have the illusion that the maze is drawn fixed on the walls, and only a part is lighted while the other part is hidden. This effect can be achieved because of the precision of the FC-PT projector.

This system is interesting because the user can use a wide area in his/her room, much wider than the projectable area of the projector. It is also interesting from

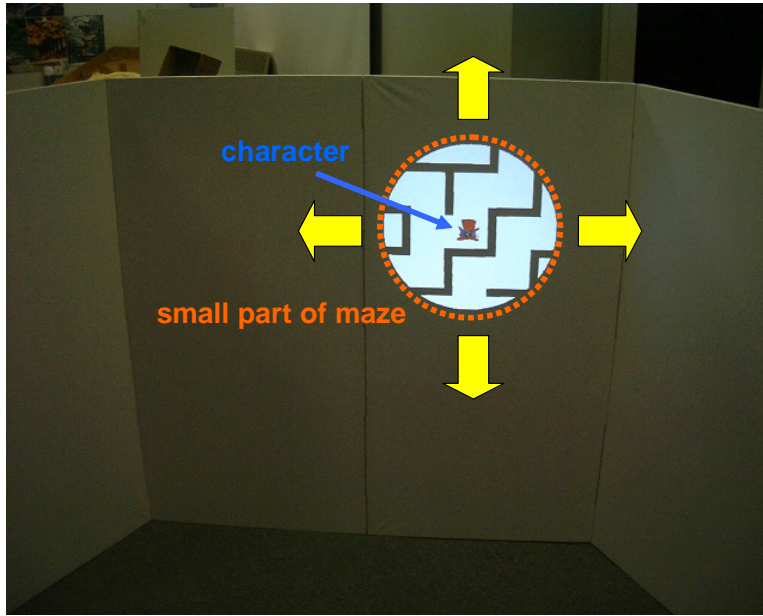


Figure 62. Maze puzzle application.

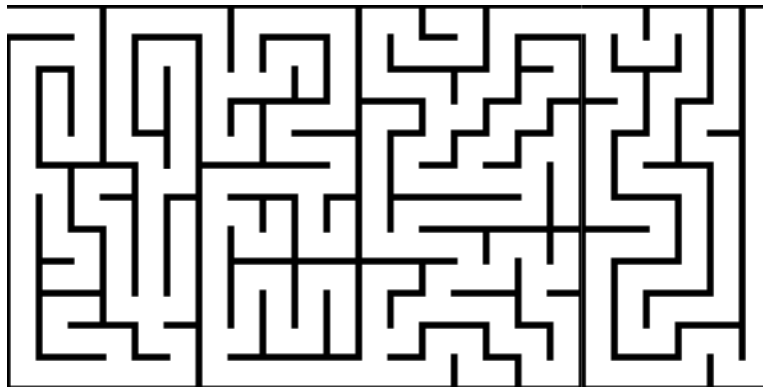
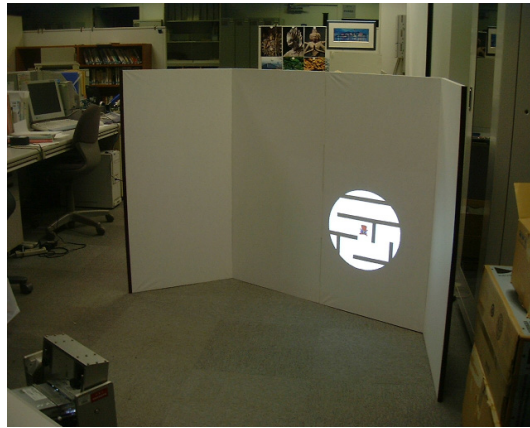


Figure 63. Bitmap data of Maze



(a)

(b)



(c)

Figure 64. Parts of Maze.

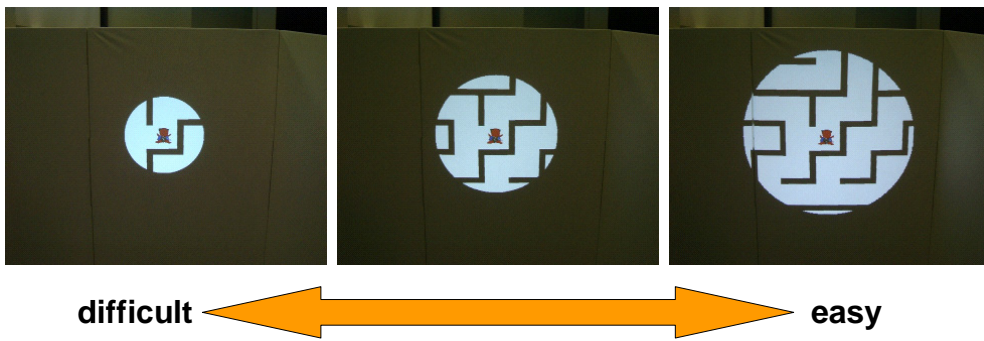


Figure 65. Control of difficulty.

the aspect of the amusement of the puzzle, because seeing not the whole maze but only a small part of it should make the puzzle more difficult and more exciting. This system also has a function that the size of the displayed area can be changed to control the difficulty, as shown in Figure 65.

7.3 Future Work

This thesis has described basic technologies for multiple steerable projector systems, focusing mainly on the geometric aspects of the steerable projector and the integration of multiple projectors. To realize a widely-used, stable, versatile system, other issues should also be considered. In the following, some aspects that are not mentioned in the thesis are briefly summarized.

1. **3D shape measurement**

Many existing studies using projectors were about 3D shape measurement [SI85, JKG03, Cha03, WHWT03, VVSC05, FB05, FK05, PCCS06]. Exploiting the characteristic of the FC-PT projector that it can be virtually regarded as a fixed projector whose image plane corresponds with the tangent plane as described in Section 3.5, these studies can easily be extended for FC-PT projectors, so that a new 3D measurement system for wider area than the existing ones can be achieved.

2. **Projection onto non-planar surfaces in the environment**

As long as the image is projected only onto planar surfaces in the environment, the extrinsic calibration and rectified image projection described in Chapter 4 work well from the viewpoints of both accuracy and ease of setup. There are, however, many non-planar surfaces in the environment. 3D shape measurement mentioned above can be used to obtain these non-planar surfaces, and existing methods for texture mapping in the computer graphics field is applicable to show images onto the surfaces correctly.

3. **Projection onto moving objects**

This thesis has described a method to display moving 2D images by tiling or overlaying multiple projections without misalignments. This is effective

because it can show a larger and brighter image than the capacity of a single projector. Projection from multiple projectors is thought to be more effective when projecting onto moving 3D objects; by projecting from different positions, the surfaces of the 3D object can be kept fully covered without any occluded regions. However, in fact, all existing studies such as [RWLB01, THI02] for 3D object projection have been applied only to fixed objects. By extending the proposed integration method of multiple steerable projectors, a novel method for moving 3D objects will be studied.

4. **Photometric calibration**

There are no places without textures. The color and brightness of a projected image is observed differently according to the color, material and texture of the surface. Brightness also changes according to the relative positions and orientations of the projector and the surface. Therefore, to show a constant image on any position in the environment, the color and brightness of the projection have to be dynamically controlled. There have been several studies about the photometric calibration of multiple fixed projectors [NPGB03, MJM⁺03, SC05, WSOS05, AOSS06, BMY05, Uli03, WCL03], but all of them are about static images. These existing studies, therefore, should be extended to be applicable to images whose position and content dynamically change.

5. **Considering architecture according to the environment**

In Chapter 6, a method for real time integration of multiple projectors was described, but only a simple situation was considered, in which all the projectors were located in the same space and shared unique global coordinate system. In real applications, the situation may be more complicated; for example, the environment may contain multiple rooms and the projectors may be located in these rooms. In such a situation, all the projectors cannot have the same unique coordinate. The projectors should be divided into groups according to which room every projector exists in, and then the architecture acquires hierarchical structure. Therefore, the architecture for multiple projectors has to be more flexible in order to accommodate such a hierarchical structure.

6. Implementation of applications

The proposed methods of this thesis are fundamental, so that they can be applied to various kinds of situations. To confirm this versatility, the applications examples described in Section 7.2 have to be implemented. In particular, when a specific kind of AR system is implemented, the user's viewpoint may also be required. This position can be achieved with some existing methods such as [NKY05].

Acknowledgements

First of all, I would like to express my deepest thanks to Professor Masatsugu Kidode at Nara Institute of Science and Technology. He has taught me how to think and how to act as a researcher and an engineer. He has also given me the great environment and many opportunities, which are now very helpful for me.

I would also like to thank the members of my thesis committee, Prof. Naokazu Yokoya and Associate Prof. Yasuyuki Kono at Nara Institute of Science and Technology, and Associate Prof. Shinsaku Hiura at Osaka University. Prof. Yokoya has given me the comments in my presentations to make my study more consistent. Associate Prof. Kono worked for keeping our laboratory to be comfortable to study there. Associate Prof. Hiura was so kind and intelligent to give me the smart comments in every conference and meeting.

I wish to express my special appreciation to Assistant Prof. Norimichi Ukita. He introduced me to the world of Computer Vision and has given me a lot of comments, advice, opportunities to give presentations and to meet other researchers. He has supported me in any aspect of my doctoral course. This thesis could never exist without him.

I would also like to thank Prof. Ian Smith at Graduate School of Biological Sciences in Nara Institute of Science and Technology. He was always kind to check all of my manuscripts in English and give me a lot of advice.

I wish to thank all the students of the Artificial Intelligence Laboratory in Nara Institute of Science and Technology. They gave me the good environment and kept me happy to be there.

I also wish to thank Ms. Yuki Tatsumi, Ms. Noriko Yamao and Ms. Hiromi Mochizuki. They assisted me in performing office jobs.

I would like to thank my family and my friends, who supported me for a long time in my doctoral course.

Finally, this work was supported by the PRESTO program of JST and a Grant-in-Aid for Scientific Research (No.15700157).

References

- [AFSR04] Mark Ashdown, Matthew Flagg, Rahul Sukthankar, and James M. Rehg. A flexible projector-camera system for multi-planar displays. In *Proc. IEEE Computer Society Conference on Computer Vision and Pattern Recognition (CVPR2004)*, volume 02, pages 165–172, Los Alamitos, CA, USA, 2004. IEEE Computer Society.
- [AOSS06] Mark Ashdown, Takahiro Okabe, Imari Sato, and Yoichi Sato. Robust content-dependent photometric projector compensation. In *International Workshop on Projector-Camera Systems (ProCams2006)*. IEEE Computer Society Press, 2006.
- [AR03] Mark Ashdown and Peter Robinson. Experiences implementing and using personal projected displays. In *International Workshop on Projector-Camera Systems (ProCams2003)*. IEEE Computer Society Press, 2003.
- [AS03] Mark Ashdown and Rahul Sukthankar. Robust calibration of camera-projector system for multi-planar displays. Technical Report HPL-2003-24, HP Labs, 2003.
- [AS05] Mark Ashdown and Yoichi Sato. Steerable projector calibration. In *International Workshop on Projector-Camera Systems (ProCams2005)*. IEEE Computer Society Press, 2005.
- [Ber03] Francois Berard. The magic table: Computer-vision based augmentation of a whiteboard for creative meetings. In *International Workshop on Projector-Camera Systems (ProCams2003)*. IEEE Computer Society Press, 2003.
- [BFRV05] Paul Beardsley, Clifton Forlines, Ramesh Raskar, and Jeroen VanBaar. Handheld projectors for mixing physical and digital textures. In *International Workshop on Projector-Camera Systems (ProCams2005)*. IEEE Computer Society Press, 2005.

- [BHF02] Blaine Bell, Tobias Hollerer, and Steven Feiner. An annotated situation-awareness aid for augmented reality. In *Proc. the 15th annual ACM symposium on User interface software and technology (UIST '02)*, pages 213–216, Oct 2002. Paris, France.
- [BMY05] Michael Brown, Aditi Majumder, and Ruigang Yang. Camera-based calibration techniques for seamless multiprojector displays. *IEEE Transactions on Visualization and Computer Graphics*, 11(2):193–206, 2005.
- [BRC03] Stanislaw Borkowski, Olivier Riff, and James L. Crowley. Projecting rectified images in an augmented environment. In *International Workshop on Projector-Camera Systems (ProCams2003)*. IEEE Computer Society Press, 2003.
- [BS05] Andreas Butz and Christian Schmitz. Annotating real world objects using a steerable projector-camera unit. In *International Workshop on Projector-Camera Systems (ProCams2005)*. IEEE Computer Society Press, 2005.
- [CCF⁺00] Yuqun Chen, Douglas W. Clark, Adam Finkelstein, Timothy C. Housel, and Kai Li. Automatic alignment of high-resolution multiprojector display using an un-calibrated camera. In *Proc. the conference on Visualization '00 (VIS '00)*, pages 125–130, 2000.
- [Cha03] Nelson L. Chang. Efficient dense correspondences using temporally encoded light patterns. In *International Workshop on Projector-Camera Systems (ProCams2003)*. IEEE Computer Society Press, 2003.
- [Col06] Francois Coldefy. Remote gesturing visualization system for distant collaboration. In *International Workshop on Projector-Camera Systems (ProCams2006)*. IEEE Computer Society Press, 2006.
- [CRSS03] Tat-Jen Cham, Jim Rehg, Rahul Sukthankar, and Gita Sukthankar. Shadow elimination and occluder light suppression for

- multi-projector displays. In *Proc. IEEE Computer Society Conference on Computer Vision and Pattern Recognition (CVPR2003)*, June 2003.
- [CSWC01] Han Chen, Rahul Sukthankar, Grant Wallace, and Tat-Jen Cham. Calibrating scalable multi-projector displays using camera homography trees. In *Proc. IEEE Computer Society Conference on Computer Vision and Pattern Recognition (CVPR2001)*, 2001.
- [CSWL02] Han Chen, Rahul Sukthankar, Grant Wallace, and Kai Li. Scalable alignment of large-format multi-projector displays using camera homography trees. In *Proc. the conference on Visualization '02 (VIS '02)*, pages 339–346, Washington, DC, USA, 2002. IEEE Computer Society.
- [dAHH99] Lourdes de Agapito, Eric Hayman, and Richard I. Hartley. Linear self-calibration of a rotating and zooming camera. In *Proc. IEEE Computer Society Conference on Computer Vision and Pattern Recognition (CVPR1999)*, volume 01, page 1015, Los Alamitos, CA, USA, 1999. IEEE Computer Society.
- [DGB03] James Davis and Hector Gonzalez-Banos. Enhanced shape recovery with shuttered pulses of light. In *International Workshop on Projector-Camera Systems (ProCams2003)*. IEEE Computer Society Press, 2003.
- [Fau93] Oliver Faugeras. *Three-Dimensional Computer Vision: a Geometric Viewpoint*. MIT Press, 1993.
- [FB05] Philip Fong and Florian Buron. Sensing deforming and moving objects with commercial off the shelf hardware. In *International Workshop on Projector-Camera Systems (ProCams2005)*. IEEE Computer Society Press, 2005.
- [FCL06] Jan-Michael Frahm, Greg Coombe, and Anselmo Lastra. Calibration of a surface light field capture system. In *International Work-*

- shop on Projector-Camera Systems (ProCams2006)*. IEEE Computer Society Press, 2006.
- [Fia05] Mark Fiala. Automatic projector calibration using self-identifying patterns. In *International Workshop on Projector-Camera Systems (ProCams2005)*. IEEE Computer Society Press, 2005.
- [FK05] Ryo Furukawa and Hiroshi Kawasaki. Dense 3d reconstruction with an uncalibrated stereo system using coded structured light. In *International Workshop on Projector-Camera Systems (ProCams2005)*. IEEE Computer Society Press, 2005.
- [FM91] Steven K. Feiner and Kathleen R. McKeown. Automating the generation of coordinated multimedia explanations. *Computer*, 24(10):33–41, 1991.
- [FMS93] Steven K. Feiner, Blair Macintyre, and Doree Seligmann. Knowledge-based augmented reality. *Communications of the ACM*, 36(7):53–62, 1993.
- [FSR05] Matthew Flagg, Jay Summet, and James M. Rehg. Improving the speed of virtual rear projection: A gpu-centric architecture. In *International Workshop on Projector-Camera Systems (ProCams2005)*. IEEE Computer Society Press, 2005.
- [FZ05] Christian Frueh and Avidesh Zakhor. Capturing 2.5d depth and texture of time-varying scenes using structured infrared light. In *International Workshop on Projector-Camera Systems (ProCams2005)*. IEEE Computer Society Press, 2005.
- [GG06] Andreas Griesser and Luc Van Gool. Automatic interactive calibration of multi-projector-camera systems. In *International Workshop on Projector-Camera Systems (ProCams2006)*. IEEE Computer Society Press, 2006.
- [GJ05] Shilpi Gupta and Christopher Jaynes. Active pursuit tracking in a projector-camera system with application to augmented real-

- ity. In *International Workshop on Projector-Camera Systems (ProCams2005)*. IEEE Computer Society Press, 2005.
- [GPNB04] Michael D. Grossberg, Harish Peri, Shree K. Nayar, and Peter N. Belhumeur. Making one object look like another: Controlling appearance using a projector-camera system. In *Proc. IEEE Computer Society Conference on Computer Vision and Pattern Recognition (CVPR2004)*, volume 1, pages 452–459, 2004.
- [GSP⁺05] Jinghua Ge, Dan Sandin, Tom Peterka, Todd Margolis, and Tom DeFanti. Camera based automatic calibration for the varrier system. In *International Workshop on Projector-Camera Systems (ProCams2005)*. IEEE Computer Society Press, 2005.
- [HCS⁺06] Michael Harville, Bruce Culbertson, Irwin Sobel, Dan Gelb, Andrew Fitzhugh, and Donald Tanguay. Practical methods for geometric and photometric correction of tiled projector displays on curved surfaces. In *International Workshop on Projector-Camera Systems (ProCams2006)*. IEEE Computer Society Press, 2006.
- [HDBJ06] Chris Hermans, Maarten Dumont, Philippe Bekaert, and Eric Joris. Januslights: A camera-projection system for telematic omnipresence with correct eye gaze. In *International Workshop on Projector-Camera Systems (ProCams2006)*. IEEE Computer Society Press, 2006.
- [Hel00] Hermann Von Helmholtz. *Helmholtz’s Treatise on Physiological Optics*, volume 1. Thoemmes Press, 2000.
- [Her03] Mark Hereld. Local methods for measuring tiled display alignment. In *International Workshop on Projector-Camera Systems (ProCams2003)*. IEEE Computer Society Press, 2003.
- [HMM00] Shinsaku Hiura, Kentaro Murase, and Takashi Matsuyama. Real time object tracking using dynamic memory. *Transactions of Information Processing Society of Japan*, 41(11):3082–3091, Nov 2000.

- [HS05] Mark Hereld and Rick L. Stevens. Pixel-aligned warping for multi-projector tiled display. In *International Workshop on Projector-Camera Systems (ProCams2005)*. IEEE Computer Society Press, 2005.
- [HSK06] Shinsaku Hiura, Kosuke Sato, and Ichiro Kanaya. Germination of the active lighting : An introduction and brief history of our research. In *International Workshop on Projector-Camera Systems (ProCams2006)*. IEEE Computer Society Press, 2006.
- [HZ00] R. Hartley and A. Zisserman. *Multiple View Geometry in Computer Vision*, chapter 12. Cambridge University Press, 2000.
- [ITSK05] Hiroyuki Izumi, Hidenori Togami, Noriaki Sato, and Masaharu Kumashiro. Psychophysiological effects of the monocular head mounted display. In *23rd Meeting of Kyushu Branch of Japan Ergonomics Society*, 2005. (written in Japanese).
- [JKG03] Tobias Jaeggli, Thomas P. Koninckx, and Luc Van Gool. Online 3d acquisition and model integration. In *International Workshop on Projector-Camera Systems (ProCams2003)*. IEEE Computer Society Press, 2003.
- [JR03] Christopher Jaynes and Divya Ramakrishnan. Super-resolution composition in multi-projector displays. In *International Workshop on Projector-Camera Systems (ProCams2003)*. IEEE Computer Society Press, 2003.
- [KKS01] Masakatsu Kouroggi, Takeshi Kurata, and Katsuhiko Sakaue. A panorama-based method of personal positioning and orientation and its real-time applications for wearable computers. In *Proc. International Symposium on Wearable Computers (ISWC2001)*, page 107, Los Alamitos, CA, USA, 2001. IEEE Computer Society.
- [KPYT05] Cheolhwon Kim, Jiyoung Park, Juneho Yi, and Matthew Turk. Structured light based depth edge detection for object shape re-

- covery. In *International Workshop on Projector-Camera Systems (ProCams2005)*. IEEE Computer Society Press, 2005.
- [KS03] Toshikazu Karitsuka and Kosuke Sato. A wearable mixed reality with an on-board projector. In *Proc. the The 2nd IEEE and ACM International Symposium on Mixed and Augmented Reality (ISMAR '03)*, page 321, Washington, DC, USA, 2003. IEEE Computer Society.
- [KSK⁺06] Takeshi Kurata, Nobuchika Sakata, Masakatsu Kouroggi, Takashi Okuma, and Yuichi Ohta. Toward the realization of interaction using nearby and far projection surfaces with the bowl procam. In *CVIM*, volume 2006-CVIM0156-1, pages 1–8, Nov 2006. (written in Japanese).
- [LSYZ06] Miao Liao, Mingxuan Sun, Ruigang Yang, and Zhengyou Zhang. Robust and accurate visual echo cancelation in a full-duplex projector-camera system. In *International Workshop on Projector-Camera Systems (ProCams2006)*. IEEE Computer Society Press, 2006.
- [LTZ06] Weihong Li, Hao Tang, and Zhigang Zhu. Vision-based projection-handwriting integration in classroom. In *International Workshop on Projector-Camera Systems (ProCams2006)*. IEEE Computer Society Press, 2006.
- [MB05] Richard May and Bob Baddeley. Hi-space: A projector-camera interaction system. In *International Workshop on Projector-Camera Systems (ProCams2005)*. IEEE Computer Society Press, 2005.
- [MG06] David Molyneaux and Hans-Werner Gellersen. Cooperatively augmenting smart objects with projector-camera systems. In *International Workshop on Projector-Camera Systems (ProCams2006)*. IEEE Computer Society Press, 2006.
- [MHW⁺00] T. Matsuyama, S. Hiura, T. Wada, K. Murase, and A. Yoshioka. Dynamic memory: Architecture for real time integration of visual

- perception, camera action, and network communication. In *Proc. IEEE Computer Society Conference on Computer Vision and Pattern Recognition (CVPR2000)*, volume 02, page 2728, Los Alamitos, CA, USA, 2000. IEEE Computer Society.
- [MJM⁺03] Aditi Majumder, David Jones, Matthew McCrory, Michael E. Papka, and Rick Stevens. Using a camera to capture and correct spatial photometric variation in multi-projector displays. In *International Workshop on Projector-Camera Systems (ProCams2003)*. IEEE Computer Society Press, 2003.
- [MKO06] Yasuhiro Mukaigawa, Takayuki Kakinuma, and Yuichi Ohta. A fast compensation method of inter-reflection for pattern projection onto a non-planar surface. In *International Workshop on Projector-Camera Systems (ProCams2006)*. IEEE Computer Society Press, 2006.
- [MNS01] Yasuhiro Mukaigawa, Masashi Nishiyama, and Takeshi Shakunaga. Creation of virtual photometric environment by photometric pattern projection onto screen object. *Transaction of The Institute of Electronics, Information and Communication Engineers*, J84-D-II(7):1448–1455, Jul 2001. (written in Japanese).
- [MOM⁺03] Masaki Maeda, Takefumi Ogawa, Takashi Machida, Kiyoshi Kiyokawa, and Haruo Takemura. Indoor localization and navigation using ir markers for augmented reality. In *Adjunct Proc. 10th International Conference on Human-Computer Interaction (HCI International 2003)*, pages 283–284, Jun 2003.
- [NH02] Nobutatsu Nakamura and Ryuichi Hiraie. Active projector: Image correction for moving image over uneven screens. In *Proc. FIT2002*, pages 423–424, Sep 2002. (written in Japanese).
- [NKHI02] Atsushi Nakazawa, Hirokazu Kato, Shinsaku Hiura, and Seiji Inokuchi. Tracking multiple people using distributed vision systems. In *Proc. IEEE International Conference on Robotics and Automation*, volume 3, pages 2974–2981, 2002.

- [NKY05] Yusuke Nakazato, Masayuki Kanbara, and Naokazu Yokoya. Wearable augmented reality system using invisible visual markers and an ir camera. In *Proc. the Ninth IEEE International Symposium on Wearable Computers (ISWC'05)*, pages 198–199, Washington, DC, USA, 2005. IEEE Computer Society.
- [NN00] Nobutatsu Nakamura and Toshiyasu Nakao. Active projector system. In *Proc. Human Interface Symposium 2000*, pages 113–116, 2000. (written in Japanese).
- [NPGB03] Shree K. Nayar, Harish Peri, Michael D. Grossberg, and Peter N. Belhumeur. A projection system with radiometric compensation for screen imperfections. In *International Workshop on Projector-Camera Systems (ProCams2003)*. IEEE Computer Society Press, 2003.
- [NSI05] Hideaki Nii, Maki Sugimoto, and Masahiko Inami. Smart light ultra high speed projector for spatial multiplexing optical transmission. In *International Workshop on Projector-Camera Systems (ProCams2005)*. IEEE Computer Society Press, 2005.
- [OD05] Takayuki Okatani and Koichiro Deguchi. Autocalibration of a projector-camera system. *IEEE Transactions on Pattern Analysis and Machine Intelligence*, 27(12):1845–1855, Dec. 2005.
- [OD06] Takayuki Okatani and Koichiro Deguchi. Autocalibration of an ad hoc construction of multi-projector displays. In *International Workshop on Projector-Camera Systems (ProCams2006)*. IEEE Computer Society Press, 2006.
- [PCCS06] Jordi Pages, Christophe Collewet, Francois Chaumette, and Joaquim Salvi. A camera-projector system for robot positioning by visual servoing. In *International Workshop on Projector-Camera Systems (ProCams2006)*. IEEE Computer Society Press, 2006.
- [Pin01] Claudio S. Pinhanez. The everywhere displays projector: A device to create ubiquitous graphical interfaces. In *Proc. the 3rd interna-*

- tional conference on Ubiquitous Computing (UbiComp '01)*, pages 315–331, London, UK, 2001. Springer-Verlag.
- [PKL⁺03] Claudio Pinhanez, Rick Kjeldsen, Anthony Levas, Gopal Pingali, Mark Podlaseck, and Noi Sukaviriya. Applications of steerable projector-camera systems. In *International Workshop on Projector-Camera Systems (ProCams2003)*. IEEE Computer Society Press, 2003.
- [RBJ05] Martin Kaltenbrunner Ross Bencina and Sergi Jorda. Improved topological fiducial tracking in the reactivation system. In *International Workshop on Projector-Camera Systems (ProCams2005)*. IEEE Computer Society Press, 2005.
- [RBY⁺99] Ramesh Raskar, Michael S. Brown, Ruigang Yang, Wei-Chao Chen, Greg Welch, Herman Towles, Brent Seales, and Henry Fuchs. Multi-projector displays using camera-based registration. In *VIS '99: Proceedings of the conference on Visualization '99*, pages 161–168, Los Alamitos, CA, USA, 1999. IEEE Computer Society Press.
- [RFC⁺02] James M. Rehg, Matthew Flagg, Tat-Jen Cham, Rahul Sukthankar, and Gita Sukthankar. Projected light displays using visual feedback. In *Proc. International Conference on Control, Automation, Robotics, and Vision*, volume II, pages 926–932, 2002.
- [RGM⁺03] Andrew Raij, Gennette Gill, Aditi Majumder, Herman Towles, and Henry Fuchs. Pixelflex2: A comprehensive, automatic, casually-aligned multi-projector display. In *International Workshop on Projector-Camera Systems (ProCams2003)*. IEEE Computer Society Press, 2003.
- [RvBB⁺03] Ramesh Raskar, Jeroen van Baar, Paul Beardsley, Thomas Willwacher, Srinivas Rao, and Clifton Forlines. ilamps: geometrically aware and self-configuring projectors. *ACM Trans. Graph.*, 22(3):809–818, 2003.

- [RvBWR04] Ramesh Raskar, Jeroen van Baar, Thomas Willwacher, and Srinivas Rao. Quadric transfer for immersive curved screen displays. In *Proc. EUROGRAPHICS 2004*, pages 451–460, 2004.
- [RWC⁺98] Ramesh Raskar, Greg Welch, Matt Cutts, Adam Lake, and Lev Steven. The office of the future: A unified approach to image-based modeling and spatially immersive displays. In *ACM SIGGRAPH98*, 1998.
- [RWLB01] Ramesh Raskar, Greg Welch, Kok-Lim Low, and Deepak Bandyopadhyay. Shader lamps: Animating real objects with image based illumination. In *Proc. 12th Eurographics Workshop on Rendering Workshop*, pages 89–102, 2001.
- [Sat99] Jun Sato. *Computer vision : geometry of vision*, chapter 3. CORONA PUBLISHING CO.,LTD., 1999. (written in Japanese).
- [SAY06] Jun Shimamura, Hiroyuki Arai, and Takayuki Yasuno. Multiple plane detection for flexible projection. In *International Workshop on Projector-Camera Systems (ProCams2006)*. IEEE Computer Society Press, 2006.
- [SBM06] Pinaki Sinha, Ezekiel Bhasker, and Aditi Majumder. Mobile displays via distributed networked projector-camera pairs. In *International Workshop on Projector-Camera Systems (ProCams2006)*. IEEE Computer Society Press, 2006.
- [SC05] Peng Song and Tat-Jen Cham. A theory for photometric self-calibration of multiple overlapping projectors and cameras. In *International Workshop on Projector-Camera Systems (ProCams2005)*. IEEE Computer Society Press, 2005.
- [SC06] Hyunjung Shim and Tsuhan Chen. Adaptive environment map for relighting: Using cameras and projected light. In *International Workshop on Projector-Camera Systems (ProCams2006)*. IEEE Computer Society Press, 2006.

- [SCG⁺05] Pradeep Sen, Billy Chen, Gaurav Garg, Stephen R. Marschner, Mark Horowitz, and Marc Levoy Hendrik P. A. Lensch. Dual photography. In *Proceedings of ACM SIGGRAPH 2005*, 2005.
- [SCS01] Rahul Sukthankar, Tat-Jen Cham, and Gita Sukthankar. Dynamic shadow elimination for multi-projector displays. In *Proc. IEEE Conference on Computer Vision and Pattern Recognition*, volume II, pages 151–157, 2001.
- [SFR⁺03] Jay Summet, Matthew Flagg, James M. Rehg, Gregory M. Corso, and Gregory D. Abowd. Increasing the usability of virtual rear projection displays. In *International Workshop on Projector-Camera Systems (ProCams2003)*. IEEE Computer Society Press, 2003.
- [SI85] Kosuke Sato and Seiji Inokuchi. Three-dimensional surface measurement by space encoding range imaging. *Journal of Robotic Systems*, 2(1):27–39, 1985.
- [SJ06] Nathaniel Sanders and Christopher Jaynes. A camera-based energy relaxation framework to minimize color artifacts in a projected display. In *International Workshop on Projector-Camera Systems (ProCams2006)*. IEEE Computer Society Press, 2006.
- [SNG03] Rahul Swaminathan, Shree K. Nayar, and Michael D. Grossberg. Framework for designing catadioptric projection and imaging systems. In *International Workshop on Projector-Camera Systems (ProCams2003)*. IEEE Computer Society Press, 2003.
- [TBS03] Naoya Takao, Simon Baker, and Jianbo Shi. Steady-state feedback analysis of tele-graffiti. In *International Workshop on Projector-Camera Systems (ProCams2003)*. IEEE Computer Society Press, 2003.
- [THI02] Kenji Tojo, Shinsaku Hiura, and Seiji Inokuchi. 3-d tele-direction interface using video projector. *Journal of the Virtual Reality Society of Japan*, 7:169–176, 2002. (written in Japanese).

- [Tsa86] Roger Y. Tsai. An efficient and accurate camera calibration technique for 3d machine vision. In *Proceedings of IEEE Conference on Computer Vision and Pattern Recognition*, pages 364–374, Miami Beach, FL, 1986.
- [Tsa87a] Roger Y. Tsai. Metrology using off-the-shelf tv cameras and lenses. *IEEE Journal of Robotics and Automation*, 3(4):323–344, Aug 1987.
- [Tsa87b] Roger Y. Tsai. A versatile camera calibration technique for high-accuracy 3d machine vision metrology using off-the-shelf tv cameras and lenses. *Robotics and Automation, IEEE Journal of [legacy, pre - 1988]*, 3(4):323–344, Aug 1987.
- [TWH03] Yu-Pao Tsai, Yian-Nien Wu, and Yi-Ping Hung. Generating a multiresolution display by integrating multiple projectors. In *International Workshop on Projector-Camera Systems (ProCams2003)*. IEEE Computer Society Press, 2003.
- [Uli03] Robert Ulichney. Method for increasing apparent amplitude resolution, and correcting luminance nonuniformity in projected displays. In *International Workshop on Projector-Camera Systems (ProCams2003)*. IEEE Computer Society Press, 2003.
- [VVSC05] Marcelo Bernardes Vieira, Luiz Velho, Asla Sa, and Paulo Cezar Carvalho. A camera-projector system for real-time 3d video. In *International Workshop on Projector-Camera Systems (ProCams2005)*. IEEE Computer Society Press, 2005.
- [WCH92] Juyang Weng, Paul Cohen, and Marc Herniou. Camera calibration with distortion models and accuracy evaluation. *Pattern Analysis and Machine Intelligence, IEEE Transactions on*, 14(10):965–980, Oct. 1992.
- [WCL03] Grant Wallace, Han Chen, and Kai Li. Deskalign: Automatically aligning a tiled windows desktop. In *International Workshop on Projector-Camera Systems (ProCams2003)*. IEEE Computer Society Press, 2003.

- [WHWT03] Guanghui Wang, Zhanyi Hu, Fuchao Wu, and Hung-Tat Tsui. Projector-camera based system for fast object modeling. In *International Workshop on Projector-Camera Systems (ProCams2003)*. IEEE Computer Society Press, 2003.
- [WM94] Guo-Qing Wei and Song De Ma. Implicit and explicit camera calibration: theory and experiments. *Pattern Analysis and Machine Intelligence, IEEE Transactions on*, 16(5):469–480, May 1994.
- [WMD06] Alexander Wu, Siddharth Madan, and Kristin Dana. Projector-camera structured light using photometric ratios. In *International Workshop on Projector-Camera Systems (ProCams2006)*. IEEE Computer Society Press, 2006.
- [WSOS05] Dong Wang, Imari Sato, Takahiro Okabe, and Yoichi Sato. Radiometric compensation in a projector-camera system based on the properties of human vision system. In *International Workshop on Projector-Camera Systems (ProCams2005)*. IEEE Computer Society Press, 2005.
- [WUM98] Toshikazu Wada, Norimichi Ukita, and Takashi Matsuyama. Fixed-viewpoint pan-tilt-zoom camera and its applications. *Transaction of The Institute of Electronics, Information and Communication Engineers*, J81-DII(6):1182–1193, 1998. (written in Japanese).
- [YGH⁺01] Ruigang Yang, David Gotz, Justin Hensley, Herman Towles, and Michael S. Brown. Pixelflex: a reconfigurable multi-projector display system. In *VIS '01: Proceedings of the conference on Visualization '01*, pages 167–174, Washington, DC, USA, 2001. IEEE Computer Society.
- [ZBK02] Todd E. Zickler, Peter N. Belhumeur, and David J. Kriegman. Helmholtz stereopsis: Exploiting reciprocity for surface reconstruction. *Int. J. Comput. Vision*, 49(2-3):215–227, 2002.
- [Zha00] Zhengyou Zhang. A flexible new technique for camera calibration.

IEEE Transactions on Pattern Analysis and Machine Intelligence,
22(11):1330–1334, 2000.

Publications List

Journal

1. Ikuhisa Mitsugami, Norimichi Ukita, Masatsugu Kidode, “Fixed-Center Pan-Tilt Projector and Its Calibration Method,” Transaction of The Institute of Electronics, Information and Communication Engineers, Vol.J90-D, No.11, Nov. 2007.

International Conferences

1. Ikuhisa Mitsugami, Norimichi Ukita, Masatsugu Kidode, “Displaying a Moving Image By Multiple Steerable Projectors,” Proc. IEEE International Workshop on Projector-Camera Systems (Procams2007), – in conjunction with CVPR2007, Jun, 2007.
2. Ikuhisa Mitsugami, Norimichi Ukita, Masatsugu Kidode, “Multi-Planar Projection by Fixed-Center Pan-Tilt Projectors,” Proc. IEEE International Workshop on Projector-Camera Systems (Procams2005), – in conjunction with CVPR2005, pp.108, Jun, 2005.
3. Ikuhisa Mitsugami, Norimichi Ukita, Masatsugu Kidode, “Fixed-Center Pan-Tilt Projector and Its Calibration Methods”, IAPR Conference on Machine Vision Applications (MVA2005), pp.492–497, May, 2005.

Domestic Symposia/Meetings/etc.

1. Ikuhisa Mitsugami, Norimichi Ukita, Masatsugu Kidode, “Displaying a Moving Image By Multiple Steerable Projectors,” IPSJ SIG Technical Reports, 2006-CVIM-156, pp41–48, Nov, 2006.
2. Ikuhisa Mitsugami, Norimichi Ukita, Masatsugu Kidode, “Rectifying Positional Errors in Projected Images from Multiple Steerable Projectors,” Proc. Meeting on Image Recognition and Understanding 2006 (MIRU2006), pp.436-441, Jul, 2006.

3. Ikuhisa Mitsugami, Norimichi Ukita, Masatsugu Kidode, "Multi-Planar Projection by Fixed-Center Pan-Tilt Projectors," Proc. Meeting on Image Recognition and Understanding 2005 (MIRU2005), pp.1590-1597, Jul, 2005.
4. Ikuhisa Mitsugami, Norimichi Ukita, Masatsugu Kidode, "Fixed Projection Center Pan-Tilt Projector and Its Calibration Methods," Proc. Meeting on Image Recognition and Understanding 2004 (MIRU2004), vol.1, pp.57-62, Jul, 2004.

Patents

1. Ikuhisa Mitsugami, Norimichi Ukita, Masatsugu Kidode, "PROJECTION DEVICE, CONTROL, METHOD FOR PROJECTION DEVICE, COMPOSITE PROJECTION SYSTEM, CONTROL PROGRAM FOR PROJECTION DEVICE, AND RECORDING MEDIUM HAVING PROJECTION DEVICE CONTROL PROGRAM RECORDED THEREIN," PCT/JP2005/11652, 2005.6.24.
2. Ikuhisa Mitsugami, Norimichi Ukita, Masatsugu Kidode, "PROJECTION DEVICE, CONTROL, METHOD FOR PROJECTION DEVICE, COMPOSITE PROJECTION SYSTEM, CONTROL PROGRAM FOR PROJECTION DEVICE, AND RECORDING MEDIUM HAVING PROJECTION DEVICE CONTROL PROGRAM RECORDED THEREIN," No.4002983, 2007.8.31.